Sustainable Engineering, Click Chemistry and Catalysis: Modification, Fabrication and Application of Cellulosic Materials

Abdolrahim Abbaszad Rafi

Supervisor: Prof. Armando Cordova

Faculty of Science, Technology and Media (NMT)

Thesis for Doctoral degree in Chemistry

Mid Sweden University

Sundsvall, 2025-01-23

Akademisk avhandling som med tillstånd av Mittuniversitetet i Sundsvall framläggs till offentlig granskning för avläggande av teknologie doktorsexamen torsdagen, den 23 Jan 2025, kl. 10:00, i sal C312, Mittuniversitetet Sundsvall. Seminariet kommer att hållas på engelska.

Sustainable Engineering, Click Chemistry and Catalysis: Modification, Fabrication and Application of Cellulosic Materials

Printed by Mid Sweden University, Sundsvall

ISSN: 1652-893X

ISBN: 978-91-89786-87-5

Faculty of Science, Technology and Media (NMT)
Mid Sweden University, SE-85 170, Sundsvall, Sweden.
Phone: +46 (0)10 142 80 00

Mid Sweden University Doctoral Thesis 416

Look deep into nature, and then
you will understand everything better.

Albert Einstein

To my parents

Table of Contents

Abstract

Due to challenges such as sustainability and increasing carbon footprint, there is a growing demand to replace fossil-based materials with green sustainable alternatives like cellulosic materials. However, unmodified cellulosic materials often encounter issues like high wettability and low mechanical strength that limit their applicability. To overcome these drawbacks, functionalization and modification are crucial and inevitable. Reported methods often involve toxic/harsh conditions or reagents, and multi-step processes. The focus of this thesis is on the fabrication, functionalization, and modification of cellulosic materials through facile and eco-friendly approaches to enhance their properties and broaden their potential applications.

We started with immobilizing copper nanoparticles on controlled pore glass substrate and used it as a recyclable heterogenous catalyst for the copper-catalyzed alkyne-azide cycloaddition (CuAAC). Focusing on sustainability, we also employed cellulosic materials as catalyst supports. First, cellulose was functionalized using a mild organocatalytic approach. Then, copper or palladium nanoparticles were immobilized onto the functionalized cellulose and used as effective recyclable heterogeneous catalysts in different reactions.

Direct esterification of CNC materials with thioglycolic acid was performed enabling us to introduce thiol groups onto CNC materials. The reaction occurred under mild conditions using natural nontoxic organic acid as an organocatalyst. The method was applied on different CNC materials, producing the corresponding thiol-functionalized CNC materials. The thiol-functionalized CNC was used as a heterogeneous recyclable reducing agent to reduce Cu(II) to Cu(I), which is the active form of copper in CuAAC. The prepared thiol-functionalized CNC materials further functionalized with attaching UV active molecules via thiol-ene click chemistry.

Lactic acid (LA) functionalized CNFs were prepared by using an ecofriendly one-step reaction method in high yields. This was achieved by converting pulp fibers into nanofibrillated cellulose lactate under mild conditions, using LA as both reaction media and catalyst. The process was concurrent and involved an autocatalytic esterification reaction without using metal-based or harsh acid catalysts. Moreover, the LA media were recycled and reused in multiple reaction cycles.

In the fourth study, strong hydrophobic cellulosic materials were prepared via a facile, scalable and eco-friendly method. The method involves a betulin treatment and hot-pressing processes. First, a water-based betulin formulation was developed and used for the treatment of cellulosic materials. The betulin-treated samples were then hot-pressed. Hot-pressing altered the morphologies and led to dense structures. Moreover, it caused a polymorphic transformation of the betulin particles. Water contact angle and tensile tests revealed that the applied betulin/hot-pressing treatment method noticeably enhanced the samples' hydrophobicities as well as their tensile strengths. Furthermore, a synergistic effect was noticed between the hot-pressing, betulin treatment, and sulfonation during the pulping process.

Densified and strong large veneers were fabricated via a facile and scalable method. The method involves a combination of chemical modifications of aspen veneers followed by hot-pressing. The study showed that hot-pressing enhanced the tensile strengths. The chemical modifications further improved the efficiency of the hot-pressing, resulting in higher tensile strengths. The chemical modifications changed the wood's composition promoting wood softening and increasing the bonding. Since the method uses convenient and mild treatments combined with continuous hot-pressing, it enables the processing of large samples. It can also lower time/energy consumption, production costs and the environmental impact.

Sammanfattning

På grund av utmaningarna som ohållbarhet och ökat koldioxidavtryck, finns det en växande efterfrågan på att ersätta fossilbaserade material med gröna hållbara alternativ som cellulosamaterial. Omodifierade cellulosamaterial stöter dock ofta på problem som hög vätbarhet och låg mekanisk hållfasthet som begränsar deras tillämpbarhet. För att övervinna nackdelar är funktionalisering och modifiering avgörande och oundvikliga. Rapporterade metoder involverar ofta toxiska/hårda förhållanden eller reagens, och flerstegsprocesser. Fokus för denna avhandling är tillverkning, funktionalisering och modifiering av cellulosamaterial genom enkla och miljövänliga metoder för att förbättra deras egenskaper och bredda deras potentiella tillämpningar.

Vi började med att immobilisera kopparnanopartiklar på ett glassubstrat med kontrollerade porer och använde det som en återvinningsbar heterogen katalysator för den kopparkatalyserade alkynazid-cykloadditionen (CuAAC). Den yttersta klickreaktionen enligt Sharpless. Med fokus på hållbarhet använde vi också cellulosamaterial som katalysatorstöd. Först funktionaliserades cellulosa med ett milt organokatalytiskt tillvägagångssätt. Sedan immobiliserades nanopartiklar av koppar eller palladium på den funktionaliserade cellulosan och användes som effektiva återvinningsbara heterogena katalysatorer i olika reaktioner.

Direkt förestring av CNC-material med tioglykolsyra gjordes vilket gjorde det möjligt för oss att introducera tiolgrupper på CNC-material. Reaktionen utfördes under milda förhållanden med användning av naturlig ogiftig organisk syra som organokatalysator. Metoden användes på olika CNC-material och producerade motsvarande tiolfunktionaliserade CNC-material. Den tiolfunktionaliserade CNC:n användes som ett heterogent återvinningsbart reduktionsmedel för att reducera Cu(II) till Cu(I), vilket är den aktiva formen av koppar i CuAAC. De förberedda tiolfunktionaliserade CNC-materialen funktionaliserades ytterligare med att fästa UV-aktiva molekyler via tiolenklickkemi.

Mjölksyrafunktionaliserade CNF:er framställdes med en miljövänlig enstegsreaktionsmetod i höga utbyten. Detta uppnåddes genom att omvandla massafibrer till nanofibrillerat cellulosalaktat under milda förhållanden, med användning av mjölksyra (LA) som både reaktionsmedium och katalysator. Processen var samtidig och involverade autokatalytisk förestringsreaktion utan användning av metallbaserade eller hårda mineralsyrakatalysatorer. Dessutom återanvändes LA-medierna och återanvändes i flera reaktionscykler.

I den fjärde studien framställdes hydrofoba och starka cellulosamaterial via en enkel, skalbar och miljövänlig metod. Metoden innebär betulinbehandling och varmpressningsprocesser. Först utvecklades en vattenbaserad betulinformulering och användes för behandling av cellulosamaterial. De betulinbehandlade proverna varmpressades slutligen. Varmpressning förändrade morfologierna och ledde till täta strukturer. Dessutom orsakade det en polymorf omvandling av betulinpartiklar. Vattenkontaktvinkel och dragtester avslöjade att den applicerade betulin/varmpressningsbehandlingsmetoden märkbart förbättrade provets hydrofobicitet såväl som deras draghållfasthet. Dessutom noterades en synergistisk effekt mellan varmpressning, betulinbehandling och sulfonering under massaprocessen.

Förtätade och starka lättviktsmaterial tillverkades via en enkel och skalbar metod ifrån asp. Metoden innebär en kombination av kemisk förbehandling av aspfanér följt av varmpressning. Resultaten visade att varmpressning var effektiv och förbättrade draghållfastheten hos det tillverkade materialet. Kemisk-modifiering förbättrade ytterligare effektiviteten vid varmpressning, vilket resulterade i högre draghållfasthet. Den kemiska modifieringen förändrade träsammansättningen och främjade träets mjukning, vilket är fördelaktigt vid varmpressning. Eftersom metoden använder miljövänliga och milda modifieringar, kombinerat med kontinuerlig varmpressning, möjliggör den bearbetning av stora prover och kan sänka tids-/energiförbrukning, produktionskostnader och miljöpåverkan.

List of papers

I) Rafi, A. A.; Ibrahem, I.; Córdova, A. Copper Nanoparticles on Controlled Pore Glass (CPG) as Highly Efficient Heterogeneous Catalysts for "Click Reactions." *Sci Rep* **2020**, *10* (1), 20547

II) Alimohammadzadeh, R.; **Rafi, A. A.**; Goclik, L.; Tai, C.-W.; Cordova, A. Direct Organocatalytic Thioglycolic Acid Esterification of Cellulose Nanocrystals: A Simple Entry to Click Chemistry on the Surface of Nanocellulose. *Carbohydrate Polymer Technologies and Applications* **2022**, 3, 100205.

III) **Rafi, A. A.**; Alimohammadzadeh, R.; Avella, A.; Mõistlik, T.; Jűrisoo, M.; Kaaver, A.; Tai, C.-W.; Lo Re, G.; Cordova, A. A Facile Route for Concurrent Fabrication and Surface Selective Functionalization of Cellulose Nanofibers by Lactic Acid Mediated Catalysis. *Sci Rep* **2023**, 13 (1), 14730.

IV) **Rafi, A. A.**; Deiana, L.; Alimohammadzadeh, R.; Engstrand, P.; Granfeldt, T.; Nyström, S. K.; Cordova, A. Birch-bark Inspired Synergistic Fabrication of High-Performance Cellulosic Materials. *ACS Sustainable Resour. Manage.* **2024,** DOI: 10.1021/acssusresmgt.4c00266.

V) **Rafi, A. A.**; Nyström, S. K.; Garcia-Lindgren, C.; Engstrand, P.; Cordova, A. Continuous fabrication of strong, scalable, high yield and sustainable materials from aspen. *Manuscript*.

Author's contributions

Paper I

Participated in planning and performing the lab experiments, edited the manuscript and scientific discussions.

Paper II

Participated in planning and performing the experiments, scientific discussions, and preparing the manuscript (together with the second author).

Paper III

Participated in planning and performing lab experiments, analysis, scientific discussions, and preparing the manuscript.

Paper IV

Participated in planning and performing the lab experiments, analysis, scientific discussions, and preparing the manuscript.

Paper V

Participated in planning and performing the lab experiments, analysis, scientific discussions, and preparing the manuscript.

The related scientific contributions 2019-2024 (not included in the thesis)

I) Alimohammadzadeh, R.; Osong, S. H.; **Rafi, A. A.**; Dahlström, C.; Cordova, A. Sustainable Surface Engineering of Lignocellulose and Cellulose by Synergistic Combination of Metal-Free Catalysis and Polyelectrolyte Complexes. *Global Challenges* **2019**, *3* (7).

II) Li, M.; Yang, Y.; **Rafi, A. A.**; Oschmann, M.; Grape, E. S.; Inge, A. K.; Córdova, A.; Bäckvall, J. Silver-Triggered Activity of a Heterogeneous Palladium Catalyst in Oxidative Carbonylation Reactions. *Angewandte Chemie International Edition* **2020**, *59* (26), 10391–10395.

III) Deiana, L.; **Rafi, A. A.**; Naidu, V. R.; Tai, C.-W.; Bäckvall, J.-E.; Córdova, A. Artificial Plant Cell Walls as Multi-Catalyst Systems for Enzymatic Cooperative Asymmetric Catalysis in Non-Aqueous Media. *Chemical Communications* **2021**, *57* (70), 8814–8817.

IV) Zheng, Z.; Deiana, L.; Posevins, D.; **Rafi, A. A**.; Zhang, K.; Johansson, M. J.; Tai, C.-W.; Córdova, A.; Bäckvall, J.-E. Efficient Heterogeneous Copper-Catalyzed Alder-Ene Reaction of Allenynamides to Pyrrolines. *ACS Catal* **2022**, *12* (3), 1791–1796.

V) Deiana, L.; **Rafi, A. A.**; Bäckvall, J.-E.; Córdova, A. Subtilisin Integrated Artificial Plant Cell Walls as Heterogeneous Catalysts for Asymmetric Synthesis of (*S*)-Amides. *RSC Adv* **2023**, *13* (29), 19975–19980.

VI) Ramesh Naidu, V.; **Rafi, A. A**.; Tai, C.; Bäckvall, J.; Córdova, A. Regio- and Stereoselective Carbon-Boron Bond Formation via Heterogeneous Palladium-Catalyzed Hydroboration of Enallenes. *Chemistry – A European Journal* **2023**, *29* (24).

VII) Deiana, L.; Badali, E.; **Rafi, A. A.**; Tai, C.-W.; Bäckvall, J.-E.; Córdova, A. Cellulose-Supported Heterogeneous Gold-Catalyzed

Cycloisomerization Reactions of Alkynoic Acids and Allenynamides. *ACS Catal* **2023**, *13* (15), 10418–10424.

VIII) Deiana, L.; **Rafi, A. A.**; Tai, C.; Bäckvall, J.; Córdova, A. Artificial Arthropod Exoskeletons/Fungi Cell Walls Integrating Metal and Biocatalysts for Heterogeneous Synergistic Catalysis of Asymmetric Cascade Transformations. *ChemCatChem* **2023**, *15* (15).

IX) Avella, A.; **Rafi, A. A.**; Deiana, L.; Mincheva, R.; Córdova, A.; Lo Re, G. Organo-Mediated Ring-Opening Polymerization of Ethylene Brassylate from Cellulose Nanofibrils in Reactive Extrusion. *ACS Sustain Chem Eng* **2024**, *12* (29), 10727–10738.

X) Deiana, L.; Avella, A.; **Rafi, A. A.**; Mincheva, R.; De Winter, J.; Lo Re, G.; Córdova, A. In-situ enzymatic polymerization of ethylene brassylate mediated by artificial plant cell walls in reactive extrusion. *ACS Appl Polym Mater* **2024**, 6 (17), 10414-10422.

XI) Deiana, L.; **Rafi, A. A.**; Wu, H.; Mondal, S.; Bäckvall, J.; Córdova, A. Heterogeneous copper-catalyzed 1,4-conjugate additions of Grignard reagents to cyclic and linear enones. Manuscript submitted.

List of abbreviations

Acronyms	Definition
AGU	Anhydrous glucose unit
AMP	Aminopropyl group
BET	Betulin
CNC	Cellulose nano crystal
CNF	Cellulose nano fiber
CPG	Controlled pore glass
CTMP	Chemi-thermomechanical pulp
CuAAC	Copper-catalyzed alkyne-azide cycloaddition
DMPA	2,2-Dimethyl-2-Phenylacetophenone
DP	Degree of polymerization
DS	Degree of substitution
EB	Ethylene brasylate
HP	Hot-press
ILs	Ionic liquids
LA	Lactic acid
LCC	Lignin carbohydrate complex
MC	Moisture content
MCC	Microcrystalline cellulose
MFA	Microfiber angle
ML	Middle lamella
PCW	Primary cell wall
PDI	Poly dispersity index
RH	Relative humidity
SCW	Secondary cell wall
TEMPO	2,2,6,6-tetramethylpiperidine-1-oxyl
Tg	Glass transition temperature

TMP	Thermomechanical pulp
WCA	Water contact angle

1 Introduction

1.1 General

Wood is one the most abundant and available materials provided by the mother nature, and it has been used for many different purposes. A recent report revealed evidence of the earliest structural usage of wood around 500,000 years ago (found at Kalambo Falls, Zambia).[1] This shows the important role of wood in the development of civilizations over history. However, population growth and the development of civilization have increased demands for new materials with enhanced properties. With the advent of man-made materials with promising features such as fossil-based materials and alloys, the use of wood has been somewhat overtaken. Fossil-based materials such as plastics—with an approximate annual production of 440 million tons projected to reach 1.1 billion tons by 2050—offer great features; however, their ongoing use causes both resource scarcity, and serious environmental and health problems.[2,3] Therefore, unsustainable fossil-based materials became one of the utmost global challenges with increasing universal demand to be replaced with sustainable and ecologic alternatives.

Returning to wood or wood-based materials can improve the situation and comply with UN sustainable development goals. Despite the benefits of pristine wood and cellulosic materials, limitations in their mechanical properties and wettability hinder their use in advanced and high-performance applications. Therefore, improving such limitations can pave the way for employing this naturally abundant and lightweight material as a sustainable high-performance material in new and diverse applications.

1.2 Lignocellulosic biomass and plant cell walls

Lignocellulosic biomass is the most abundant sustainable carbon source on the planet, with estimated annual global production of over 200 billion tons. Lignocellulose is a composite material prepared by plant cells and mostly made of three different polymers (*i.e.*, cellulose, hemicelluloses and lignin) as well as small amounts of other components like pectin, inorganic compounds, and extractives.[4] Based on the source, the percentage of each component can be different. For instance, some materials such as cotton and ramie are rich in cellulose content (95 and 76 wt.%, respectively), while others like corn stalks and wheat straw can have lower amounts (35 and 30 wt.%, respectively).[5]

Figure 1.1 shows the cell wall structure in normal xylem (wood), which consists of different layers. The first layer is the primary cell wall (PCW), mainly composed of cellulose, hemicellulose, and pectin, which enables the enlargement of plants while maintaining their structural integrity. Cellulose microfibrils are randomly oriented in PCW. The secondary cell wall (SCW) is deposited after cell growth stops and contains mostly cellulose, hemicellulose, and lignin. This layer mostly provides the mechanical strength that enables plants to stand upright. Cellulose microfibrils are well oriented in SCW, and their orientation is commonly called the microfibril angle (MFA). The MFAs in S1 and S3 are within the range of 50–90° to the cell axis. S2 is the thickest part of cell walls and plays a critical role in their mechanical properties of cells wall. The MFA in S2 is less than that of S1 and S3 (usually ~10–30°).[6] The space between two adjacent cells is occupied with middle lamella (ML) which is poor in cellulose and rich in hemicellulose and lignin.[7,8]

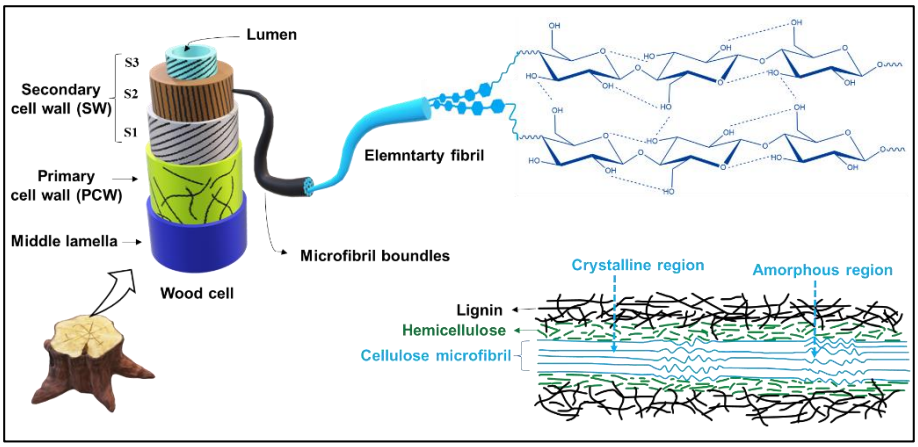

Figure 1.1. The structure of plant cell walls.

Depending on the tree species, wood can be categorized as softwood or hardwood. Generally, softwoods have simpler structures with a large volume of tracheids, which transport water and nutrients (mainly by thin-walled tracheids) and provide mechanical strength (mainly by thick-walled tracheids). On the other hand, hardwoods are more complex and mainly made up of fiber cells, ray cells, and large vessels.[9]

1.2.1 Hemicelluloses

Hemicelluloses are carbohydrate polymers that make up roughly 25 wt.% of the biomass. Unlike cellulose, hemicelluloses have a lower molecular weight (Mw) (degree of polymerization~100–200) and contain only the amorphous region. Hemicellulose is mainly composed of xylose, arabinose (pentoses), and glucose, mannose, and galactose (hexoses) that can be decorated with different groups such as acetyl and methyl groups. For example, xylan is one of the main hemicelluloses and consists mostly of xylose (Figure 1.2). Hemicelluloses bind to the surface of cellulose fibrils acting as an amorphous matrix holding cellulose fibrils. Functionalization with

hydrophobic groups like acetyl and methyl groups can increase the affinity of hemicellulose to lignin, thus improving cohesion between the three major lignocellulosic polymers. Hemicelluloses are more vulnerable to degradation than cellulose due to its non-crystalline structure.[7,10,11]

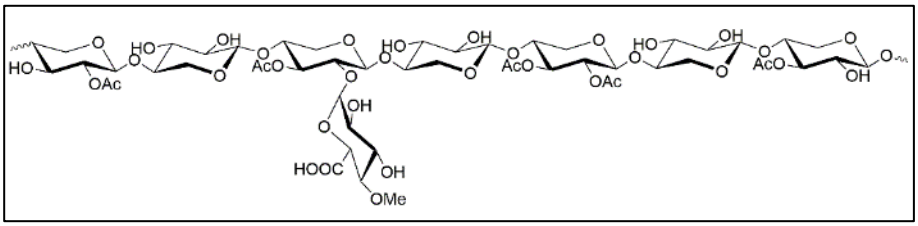

Figure 1.2. Representative structural formula for glucuronoxylan.

1.2.2 Lignin

The term lignin was first introduced by the Swiss botanist Augustin Pyramus de Candolle at the University of Geneva in 1813.[12] Lignin (~15–35 wt.%) is an aromatic polymer that becomes part of the cell wall after plant growth stops. Providing structural reinforcement, stiffness, water proofing, and resilience to decay are the main functions of lignin. The middle lamella is rich in lignin (>50%), having about 20-25% of the lignin in the whole tracheid. The main precursors or monomers of lignin biosynthesis are coniferyl alcohol, sinapyl alcohol and para-coumaryl alcohol that randomly polymerized via radical polymerization to produce a three-dimensional polymeric network. After polymerization, lignin units are identified by their aromatic ring structure and called guaiacyl (G), syringyl (S) and p-hydroxyphenyl (H) units, respectively (Figure 1.3). Lignin can bond to hemicellulose through a variety of non-covalent and covalent bonds (*e.g.*, ether and ester bonds). Lignin is the major obstacle for biomass deconstruction process and cellulose extraction.[7,13,14]

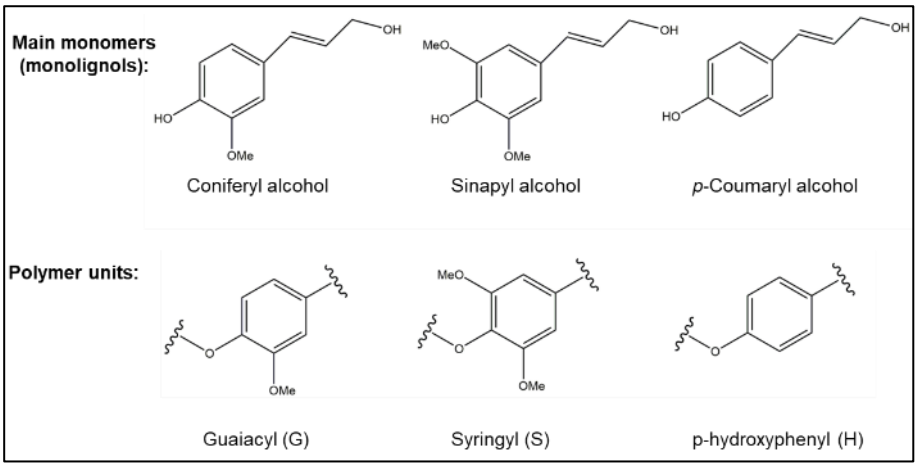

Figure 1.3. Main abundant monolignols and building blocks of lignin polymer.

1.2.3 Cellulose

Cellulose, the main component of lignocellulosic materials, is the most abundant biopolymer on Earth. It is estimated that nature produces approximately 10^{11} tons of cellulose annually through photosynthesis. In addition to plant cell walls, cellulose can be also produced by other creatures such as some bacteria, algae, fungal cell walls, and tunicate.[5] The term cellulose was coined in 1838 by the French chemist Anselme Payen, who discovered that all plants contain a white substance with the same composition as starch (made of glucose molecules and consisting of about 44% carbon, 6% hydrogen, and 49% oxygen).[15] As shown in Figure 1.4, cellulose is known as a linear homopolysaccharide and comprises chains of β-D-glucopyranose joined by β(1→4) glycosidic bonds with anhydro glucose units (AGUs) as repeating units.[7,8] AGU has three hydroxyl groups which not only undergo the typical reactions of hydroxyl groups (suitable for chemical modifications), but they also enable cellulose chains to form inter- and intra-molecular hydrogen bonds. The hydrogen bond formation in the cellulose structure strongly influences the cellulose's properties (*e.g.*, limited solubility in usual solvents, and the crystallinity of cellulose).[7,16]

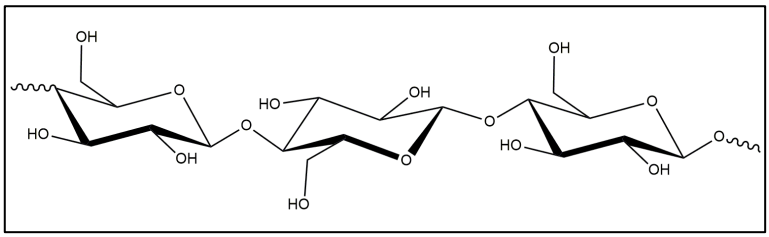

Figure 1.4. The molecular structure of a cellulose chain.

To liberate the cellulose fibers from the cell walls, pulping processes are carried out, which are categorized into different classifications. Mechanical methods (*e.g.* stone groundwood pulp) involve the use of mechanical energy to break the bonds between fibers, resulting in high-yield pulps. Combining mechanical refining with heat pretreatment (thermo-mechanical pulping, TMP) or chemical/heat pretreatment (chemi-thermomechanical pulping, CTMP) can improve the pulping process and quality of the final product, although it may slightly reduce the pulp yield. On the other hand, chemical pulping receives great help from chemical treatments to remove hemicellulose and lignin, which results in a high-cellulose-content pulp that can be used as high-strength and high-quality paper (pulp yield 40–55%). Kraft or sulfate pulping, which uses white liquor (Na_2S and NaOH) for digestion, is the most common approach worldwide. Sulfite pulping is another type of chemical pulping.[5,17,18]

1.2.4 Nanocelluloses

Studies related to microcrystalline cellulose (MCC) and nanocellulose began appearing in the 1950s, when Battista produced microcrystalline cellulose via the hydrolysis and sonication of cellulose fibers.[19] Nanocelluloses with high surface areas are interesting candidates for new materials such as reinforcement agents in nanocomposites.[20,21] Nanocelluloses can be classified into the following four categories: cellulose nanocrystals (CNCs), cellulose nanofibrils (CNFs NFCs),

regenerated nanocellulose (RNC), and bacterial cellulose (BC).[22] In this thesis, we will focus only on CNCs and CNFs. As shown in Figure 1.5, cellulose fibrils contain both crystalline and amorphous regions. The chains are orderly stacked in the crystalline regions, which contributes to cellulose's high stiffness and strength. In contrast, the amorphous regions contribute to flexibility.[20,23]

1.2.4.1 CNCs

In 1947, Nickerson and Habrle obtained CNCs via the acid hydrolysis of cotton, and a few years later, Rånby reported the generation of cellulose nanocrystals suspensions.[12,24,25] CNCs are highly crystalline rod-like particles (commonly 200–500 nm in length and 3–35 nm in diameter), that are obtained after the hydrolysis of the amorphous parts of fibrils.[23] The most common method for isolating CNCs is via acid hydrolysis (*e.g.*, using sulfuric acid), which hydrolyses the amorphous parts of the elementary cellulose fibrils, thus leaving the crystalline regions (Figure 1.5). The benefit of using sulfuric acid is that it can introduce anionic sulfate ester groups onto the cellulose's surface, and the repulsive forces between identical electrostatic charges enable the dispersion of nanocelluloses.[20,22]

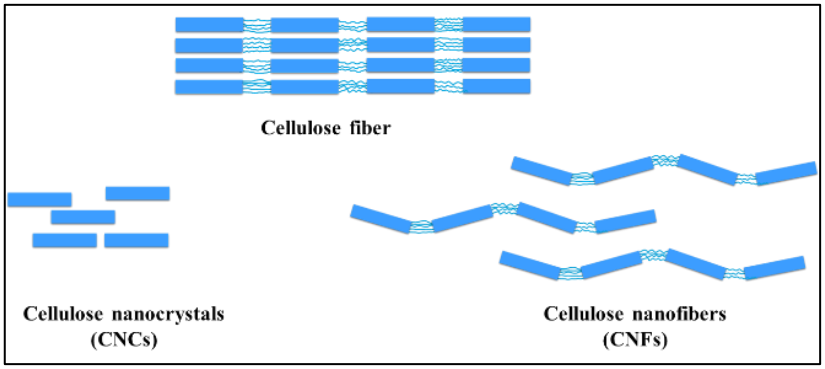

Figure 1.5. Components of cellulose fibers.

1.2.4.2 CNFs

Herrick *et al.* and Turbak *et al.* described the isolation of microfibrillated cellulose for the first time in 1983.[26,27] CNFs are long entangled fibrils (3–500 nm in diameter, with lengths up to several μm) which, unlike CNCs, consist of both crystalline and amorphous regions.[22] Mechanical agitation (mechanical disintegration) is a common method for CNF fabrication. The method is simple and straightforward; moreover, since no chemicals are used, the products are suitable for sensitive applications in fields such as food and medicine. However, high energy consumption is the main drawback of this method. Combining a mechanical process with different pretreatments can ease the process and reduce energy consumption.[22,28] For example, 2,2,6,6-tetramethylpiperidine-1-oxyl radical (TEMPO)-mediated oxidation could reduce the energy consumption of mechanical defibrillation. TEMPO is used as the catalyst in the presence of sodium hypochlorite (NaClO) as a primary oxidant to oxidize the hydroxyl group of cellulose to carboxylates.[29,30] Introducing negative charges onto the fibrils helps dispersity of the nanofibers. Despite its advantages, issues such as the high-cost of TEMPO catalysts and using active radical initiators and a chlorine-based oxidant are the main drawbacks of this approach.[22,29] Enzymatic treatment can also be used for preparing CNFs. Although the enzymatic approach has a low environmental impact, it is usually time-consuming, pricy and less stable (which may lead to the addition of biocides).[31]

1.3 Catalysis

In 1835, Berzelius coined the term "catalysis" to describe reactions that are accelerated by substances that remain unconsumed after the reaction. Catalysis has become fundamental in chemistry by enabling

processes in various fields, from industrial synthesis to environmental science.[32] Generally, there are three major types of catalysis: organocatalysis, biocatalysis, and metal catalysis. Biocatalysts are biological components (enzymes as the most common example) that are used to accelerate reactions with high efficiency and selectivity. Enzymes are considered a sustainable choice since they are biodegradable and derived from renewable resources. However, their applications are limited due to some challenges; for example, enzymes are generally expensive, sensitive to harsh conditions, and their effective use is mostly limited to aqueous media.[33]

In organocatalysis, an organic molecule is used to accelerate chemical reactions. In contrast to organometallics and enzymes, organocatalysis does not require the use of metals or large complex molecules to accomplish catalytic activation. Organocatalysts are generally not as efficient as other catalysts, requiring the use higher catalyst loadings. However, organocatalysis holds much promise for achieving sustainable chemistry since most of organocatalysts are inexpensive, readily available, less air/moisture sensitive, metal-free, and less toxic. The first example of organocatalysis was demonstrated by Liebig (in 1859) using pure acetaldehyde as the organocatalyst for the transformation of cyanogen to oxamide. Amino acids and secondary amines are examples of organocatalysts that are widely used in reactions.[34–36] The organocatalytic activities of green natural organic acids (*e.g.*, tartaric acid, citric acid, and lactic acid) were first reported by Casas *et al.*, who used these natural organic acids for the ring-opening of caprolactones.[37] In 2005, Hafren & Cordova used these natural organic acids for direct polymerization of cellulose fibers.[38]

Transition metal catalysts are indeed one of the most powerful and efficient tools in organic synthesis to synthesize valuable compounds.

They have been employed extensively in different industrial applications, from the petrochemical to pharmaceutical industries. The incompletely filled d-orbitals in transition metals give them their unique features for their use as catalysts. The possibility to obtain multiple oxidation states by accepting or giving electrons enables them to form temporary bonds with substrates. This facilitates reactions by stabilizing reaction intermediates and lowering activation energies.[39]

The concept and guidelines of sustainable chemistry demand that chemical products and processes be designed in a way that eliminates or reduces the use and generation of hazardous substances. Therefore, the attempt to develop eco-friendly and sustainable chemical processes is a primary aim of chemical and material societies. In this context, employing catalysis is one of the principles for sustainable processes. Moreover, heterogeneous catalysts (immobilized catalyst onto heterogeneous supports) offer further advantages from both economic and environmental points of views. Catalysts can be expensive and hazardous. Using heterogenous catalysts facilitate catalyst recovery and recyclability, thereby reducing costs and waste. Additionally, immobilization significantly mitigates catalyst leaching, a critical factor in preventing contamination (*e.g.*, heavy metals), especially in sensitive applications such as pharmaceutical products.[40–44]

Among catalyst supports, cellulosic materials become one of the advantageous candidates and have been employed to immobilize different catalysts such as metal nanoparticles. For example, Moores *et al.*, employed Pd nanoparticles immobilized onto CNC for enantioselective ketone hydrogenation reaction.[45] N-Methylimidazole functionalized carboxymethyl cellulose supported PdNPs catalyst was used in Suzuki reaction. The prepared catalyst was effective than that prepared via depositing palladium nanoparticles directly onto

cellulose in absence of N-methylimidazole.[46] CNFs functionalized with aminopropyl moieties, were also used for immobilization of Pd nanoparticles for Suzuki-Miyaura reaction where the prepared catalyst was recyclable and yield the corresponding products in high yields.[47,48]

1.3.1 Click reactions

The concept of "click chemistry" was first introduced by Sharpless in 2001. It is known as a powerful tool in chemistry and material science to produce new materials. Overall, click reactions are efficient and stereospecific reactions that are simple to perform and need mild conditions. According to Devaraj and Finn, the word 'Click' mimics the molecular building blocks annotating the 'seat belt buckle' module that can be easily conjoined but is inseparable.[49] The most generally used click reaction is the copper-catalyzed azide-alkyne cycloaddition (CuAAC). The non-catalyzed reaction is slow, needs elevated temperatures to proceed, and results in a mixture of 1,4 and 1,5- regio-isomer products. In 2002, Sharpless (a two-time Chemistry Nobel prize winner) and Meldal independently reported that the reaction is catalyzed by Cu^{I}, resulting in a completely selective formation of the 1,4-isomer (Figure 1.9).[50–52]

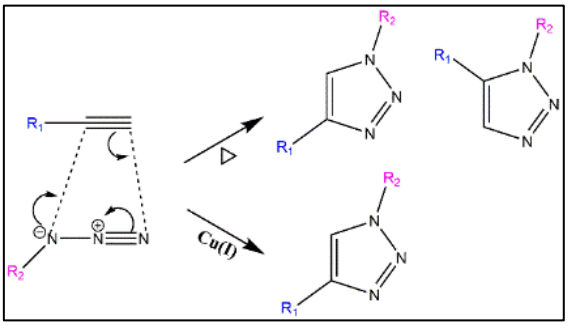

Figure 1.9. Alkyne-azide cycloaddition and formation of 1,4 and 1,5 triazoles.

Another type of click chemistry is the radical-mediated thiol-ene click reaction, which occurs between an alkene and a thiol to form a

thioether. The reaction has been known about for over 100 years, and it takes place through a free-radical addition which can be activated thermally or photochemically (Figure 1.8).[53]

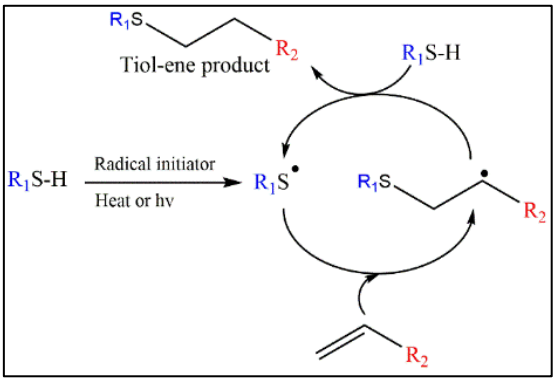

Figure 1.8. The mechanism of radical-mediated thiol-ene click reaction.

1.3.1.1 Modification and functionalization of cellulose

Thanks to the hydroxyl groups in its structure, cellulose can undergo various chemical modifications to introduce desired functional groups. Surface modification of nanocelluloses alters their surface properties by introducing charges or functional groups. Modifications can be performed during the production of nanocelluloses or after production (post-modification). These modifications can fulfill several purposes, such as facilitating nanocellulose fabrication, enhancing hydrophobicity and compatibility with other materials, and enabling covalent grafting with other compounds. Chemical modifications can also facilitate nano fibrillation by decreasing the energy consumption of the process. For example, Wågberg *et al.* were the first to employ the carboxymethylation of fibers to produce CNFs.[54] The main drawbacks of carboxymethylation are the use of toxic chemicals such as monochloroacetic acid and methanol in the procedure.[55]

The functionalization of cellulosic materials can be achieved through the chemical grafting of different molecules directly onto the hydroxyl

groups or onto existing functional groups on the cellulosic materials. Silylation and esterification are two common methods used for functionalization and modification. The silylation of cellulose is a versatile approach for cellulose modification. Silane groups can graft onto nanocelluloses via silyl ether bonds, enabling further functionalization and surface design (Figure 1.6). For example, the functionalization of cellulosic materials with 3-aminopropyltriethoxysilane (APTES) can introduce aminopropyl (AMP) groups grafted onto the cellulosic materials. Robles *et al.* used AMP-functionalized nanocellulose as a reinforcement agent in a polymeric network to improve the mechanical properties in the prepared nanocomposite. This improvement can be explained by the enhanced distribution of AMP-functionalized nanocellulose in the polymer.[56] AMP functionalized nanocellulose can also bind to metals, which opens up opportunities for the adsorption and removal of metals, and preparing heterogeneous catalysts for chemical reactions. Hokkanen *et al.* used APS-functionalized micro-fibrillated cellulose for the adsorption of different metals such as Ni(II), Cd(II), and Cu(II) from water.[57] Another possible type of functionalization involves grafting alkyl-containing silanes onto cellulosic materials. Our group recently used a combination of silylation and an organocatalytic approach to produce hydrophobic CNC films.[58,59]

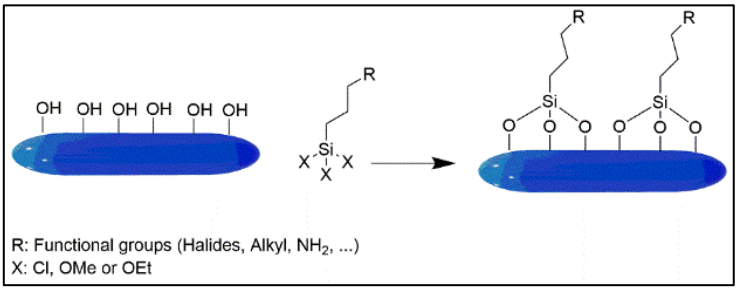

Figure 1.6. Silylation of cellulosic materials.

Esterification is another versatile chemical approach for introducing functional groups onto nanocelluloses. Cellulose esters can be categorized into inorganic esters (*e.g.*, cellulose nitrate) and organic cellulose esters (*e.g.*, cellulose acetate). Esterification can be carried out via Fischer esterification (Figure 1.7). In the presence of an acid catalyst such as HCl, carboxylic acids (as acylating agents) bind to the nanocelluloses through the formation of ester bonds.

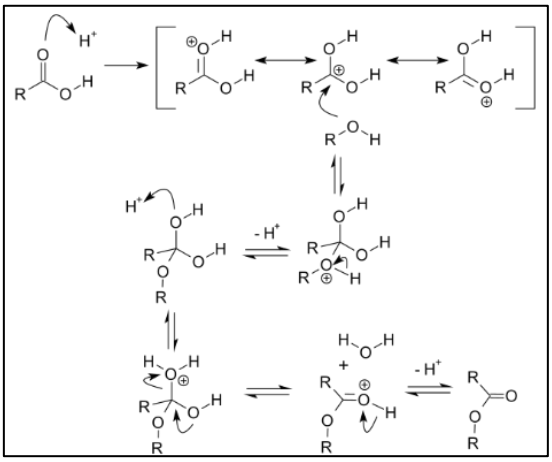

Figure 1.7. Chemical mechanism of Fischer esterification.

It is advantageous to perform esterification under mild conditions to avoid the severe disintegration and decomposition of nanocelluloses.[60] Milder conditions and green processes are more desirable, so a variety of methods have been employed to achieve the aims of sustainable chemistry. In the context of the esterification of cellulosic materials, Hafren and Cordova have previously reported on a straightforward, ecological and direct organocatalytic approach for the esterification of cellulose fibers using natural and nontoxic organic acids (*e.g.*, L-tartaric acid, citric acid) as catalysts.[38,61–63] Hafren and Cordova also reported on the functionalization of cellulose by introducing different organic molecules onto the solid cellulose. The method first involved the organocatalytic esterification and functionalization of cellulose with 5-

hexynoic acid and tartaric acid a catalyst. Next, a fluorescent moiety was attached via the CuAAC click reaction.[62] In another work, they first performed the organocatalytic esterification of cellulose with different alkenes. Then, different thiol groups attached onto the cellulose via the thiol-ene click reaction.[63]

The use of natural organic acids as organocatalysts has been successfully applied to the direct esterification of bacterial nanocellulose with acetic acid and propionic acid by Ramirez *et al*.[64] They also carried out esterification of CNC with acetic anhydride in the presence of citric acid as an organo-catalyst. They discovered that the reaction time, temperature, and catalyst amount affected the degree of substitution (DS).[65] Organic acids can be used as both solvent and reagent. For example, Espino-perez *et al.* used different carboxylic acids such as benzoic acid for the esterification of an aqueous suspension of CNCs. Termed "Sol React," this method used carboxylic acids as solvents during the reaction. A critical key of this study was performing the reaction at temperatures above both the melting point of the carboxylic acids and the boiling point of water. The functionalized CNCs had higher WCAs (~75°) and better dispersion in solvents.[66]

In addition to the post-modification of nanocelluloses, the esterification method can also be employed concurrently for nanocellulose fabrication and functionalization. By using various organic acids (with a catalytic amount of HCl), different esterified nanocelluloses can be produced.[67–70] For example, acetylated and butylated CNCs were synthesized via Fischer esterification using the related carboxylic acids and HCl as a catalyst.[71] Espinella *et al*. produced functionalized CNCs using a similar methodology and different organic acids (*e.g.*, citric, malonic, or malic acids). The highest

yield was obtained when 0.05 M HCl was used. Moreover, the functionalized CNCs showed less thermal stability than non-functionalized CNCs.[67] Li *et al.* reported the fabrication and esterification of nanocellulose using oxalic acid. Oxalate-functionalized nanocellulose with a DS of 0.35 was obtained using this method.[69] Formic acid was also used for the fabrication of functionalized nanocelluloses.[70,72] Our group reported direct fabrication of CNFs from wood pulp using formic acid. The fabricated CNF was esterified by formic acid, and the used acid could be reused. Further functionalization of CNFs was also achieved through organocatalytic silylation followed by the thiol-ene click reaction.[72]

Esterification reactions can be used to introduce different functional groups, such as thiol groups, that can be used for different applications. For example, Felpin *et al.* esterified cellulose with thioglycolic acid using *p*-toluene sulfonic acid, and the thiol-functionalized paper was then used for copper detection.[73] As mentioned before, thiol-functionalized materials can also undergo further functionalization via the thiol-ene click reaction. For example, the thiol-functionalized CNC can be used as crosslinking and reinforcing agents in a natural rubber matrix.[21] Maleki *et al.*, introduced thiol groups onto hemicellulose via ring-opening of γ-thiobutyrolactone, then performed thiole-ene click reactions to obtain different hydrogels.[74] The thiol-ene click reaction between vinyl-functionalized nanocelluloses and perfluoroalkyl thiols under UV irradiation results in hydrophobic cellulosic materials.[75,76] Through ester bond formation, Navarro *et al*., introduced functional groups as polymerization initiators onto nanocelluloses. The resulting cellulose-based macroinitiator started the polymerization of stearyl acrylate, producing hydrophobic polymer-grafted nanocellulose.[77,78] A similar methodology was used to create zwitterionic polymer-grafted CNCs, which were applied for the adsorption of metal ions and dyes.[79]

1.3.2 Wood Extractives

Wood extractives are the chemical compounds that are extractable from wood using different neutral solvents. Extractives generally make up less than 5% of dry wood mass, except for some tropical and subtropical woods, that this amount can be high and up to nearly 20 wt.%. The amount of extractives can be different between similar trees or even in the different parts of a single tree. Despite their minor amount, wood extractives play various important roles, including protecting living trees against pathogen attacks and contributing to the metabolism of trees. Wood extractives are often categorized based on their chemical structure and hydrophilicity. Sugars and phenolic compounds such as tannins are hydrophilic extractives, whereas aliphatic compounds (*e.g.*, fatty acids) and terpenes (*e.g.*, terpenoids, and resin acids) are considered lipophilic extractives and generally called wood resin.[80,81] Even though the content of lipophilic extractives in wood is generally lower than that of hydrophilic extractives, lipophilic extractives are more important from a pulp and paper manufacturing point of view since they can cause problems such as pitch deposits and lower the quality of the final products. On the other hand, due to wood extractives' interesting properties, they can be used in different applications such as in wood protection or platform chemicals. For example, pine extractives have been used for hundreds of years for paintings, coatings, and the caulking seams of wooden vessels.[80,82] Sablík *et al.* [83] also reported that treatment of non-durable European beech wood with *Robinia pseudoacacia* extracts increases the wood's decay resistance (treated and untreated wood samples showed a mass loss of 13 and 44 wt.%, respectively).

Betulin (or betulinol, $C_{30}H_{50}O_2$) is a naturally occurring triterpene of the lupane type (Figure 1.10). It was first isolated from birch bark by

Johann T. Lovitz in 1778. Its name comes from the Latin word "Betula," meaning birch (coined by Masson, 1831). In fact, the white color of birch bark is attributed to the presence of betulin, and its main function is to protect birch trees from fungal and bacterial attacks. Besides its ecological role, betulin is nontoxic and has health-benefit properties, making it an interesting compound in different fields such as pharmaceutics and cosmetics. The outer bark of birch is considered the main source of betulin where it constitutes 20-35% of the dry mass of the outer bark.[81,84,85] An average pulp mill using birch wood produces roughly 10,000 tons of birch bark annually, from which it would be possible to produce 1,800 tons of betulin. Rather than simply getting incinerated together with the bark to produce energy, betulin can be extracted and employed to fabricate value-added products.[86,87]

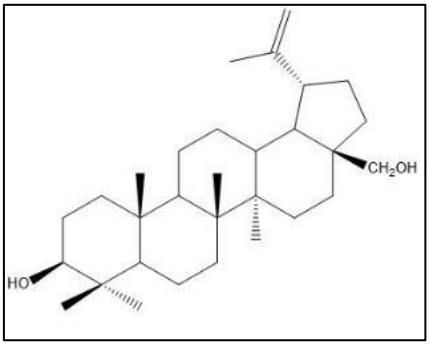

Figure 1.10. The chemical structure of betulin.

Betulin and its derivatives can be used to fabricate hydrophobic cellulosic materials. Huang *et al.* reported that the impregnation of cotton textile with betulin or betulin terephthaloyl chloride copolymer creates hydrophobic surfaces (WCA 151°).[88] This approach involves using chemicals and organic solvents like THF, toluene, and pyridine. Niu *et al.* demonstrated that a coating made of betulin, fossil-based polydimethylsiloxane, and a curing agent in 2-isopropanol can

increase cellulose substrate hydrophobicity (WCA 149°).[89] The fabrication of hydrophobic cellulosic materials utilizing betulin and betulinic acid using ionic liquids (ILs) as solvents has been reported.[90] The prepared nonwovens and yarn samples contained 10 wt.% of betulin and had a WCA of ~100°. However, ILs are not widely used for commercial purposes currently. They are considered toxic and hazardous, and their residuals can be entrapped inside the cellulosic products causing health/environmental issues.[91,92]

1.4 Hot pressing

Manipulating the composition and structure of wood cells can lead to improvements in the mechanical properties of wood. The relationship between density and mechanical properties suggests that wood densification could be an effective method for enhancing the mechanical properties of cellulosic materials. Generally, a significant part of wood's volume consists of open and empty pores, and by eliminating them, the density of wood increases. Hot-pressing is a densification method that compresses and densifies wood by subjecting it to elevated temperatures and pressure (Figure 1.11). Compression can be applied in different directions (longitudinal, radial, and tangential); however, the most common is radial direction. Through hot-pressing, lumen and void spaces within the wood structure shrink, resulting in denser structure. When open volumes in the structure decrease, the contacting surfaces increase, interactions are improved, and the mechanical properties are enhanced.[8,93,94] Hot pressing has been investigated for over a century, and the first patent for the mechanical compression of wood was issued in 1900 in the USA.[95] Nonetheless, many researchers and engineers have been investigating the field from different points of views.

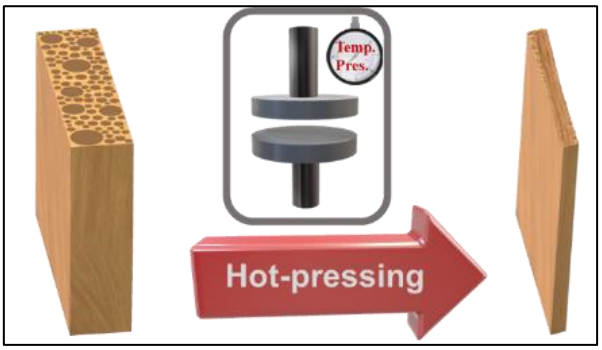

Figure 1.11. Hot-pressing of wood resulting in densified samples with compact structures.

An important factor in the hot-pressing process is wood softening. Wood softening happens when wood reaches a temperature over the glass-transition temperature (Tg) of its polymers. Tg is an approximate temperature at which the material begins to soften. When wood temperature exceeds the Tg, its characteristics change from a glassy to a rubber elastic state (plasticized).[93,96] Compression under plasticized conditions allows the material to be compressed without being crushed. Compression in these conditions causes the lignin to flow, which leads to a relief of internal compression stresses that stabilizes set recovery.[97] Generally, decreasing Tg is beneficial and facilitates the hot-pressing process. Tg is moisture-dependent, and with increasing moisture content (MC), the softening temperature (Tg) decreases (Figure 1.12).[98] Wood softening can also occur through chemical treatments; for example, sulfonation of lignin reduces the degree of crosslinking, which consequently reduces the Tg and softening temperature.[99,100]

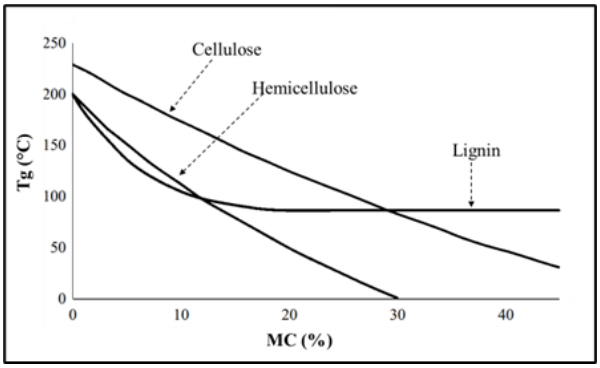

Figure 1.12. Tg vs MC for wood's main components.[98]

Delignified cellulose pulps (*e.g.*, kraft pulp) have higher tensile strengths than lignocellulosic pulps.[101] However, hot pressing has been found to be highly beneficial and effective for lignocellulosic materials resulting in significant enhancement in mechanical properties. Early studies by Mason showed that lignin-rich fibers could be fused together through hot pressing, resulting in a densified structure and strengthened bonds between fibers.[102] Song *et al*.[103] reported that partially removing lignin and hemicelluloses from bulk wood samples (increase in porosity and decrease in rigidity) followed by hot pressing results in a significant enhancement in tensile strengths. In densified lignocellulosic materials, lignin plays an important role in achieving the significantly improved strength by acting as a phenolic binder between the fibrils. Research have shown that densification of fully delignified wood without adding an additional matrix leads to a less pronounced enhancement of the mechanical strength.[8,104] Joelsson *et al.* also reported that the strengths of hot-pressed papers made from lignin-rich wood fibers (CTMP pulps) were higher than those made from low-lignin fibers such as sulfite and bleached kraft pulp.[105] Jiang *et al.* have reported that adding lignin to the cellulose network followed by long-time hot pressing (T=100 °C, P=5 MPa, for 3 days) produces strong paper samples with a tensile strength of 200 MPa (five

times higher than typical cellulose paper).[104] In another study, a record high tensile strength of 1 GPa was reported for partially delignified and densified bamboo samples.[106] In other words, hot pressing of lignin-containing materials (*e.g.*, paper[104,105,107] or wood[103]) at temperatures above the Tg of lignin allows for a plastic-like flow of lignin and improves the adhesion between fibers, where lignin acts as a natural binder. Moreover, wood softening by sulfonation is beneficial and facilitates the hot-pressing process. In this context, recent studies by the groups of Engstrand and Berglund have reported that sulfonation increases softening and conformability at lower temperatures, resulting in effective hot pressing and higher strengths.[99,100]

Research on hot pressing indicates that densification is a promising approach for improving wood properties and developing new materials, thus providing significant opportunities to expand wood applications. Despite these advantages, however, densified wood has not yet become a mass-produced product (only few successful industrial cases). One of the obstacles hindering the large-scale production of densified wood is the reliance on static and batch-type hot-pressing processes. Static hot-pressing machines need to be loaded and unloaded after each batch, and their press plates need to be heated before pressing and sometimes cooled down afterwards. Subsequently, the process is energy- and time-consuming, making it inappropriate from the production standpoints. Continuous hot pressing provides a promising solution for decreasing time and energy consumption, thus enhancing the cost-effectiveness and environmental impact of the densification process and making mass production more feasible.[108–111]

2 Results & Discussions

This chapter presents the results extracted from the research conducted in this thesis as well as the related discussions. To make reading convenient, this chapter is divided into five subsections, with each subsection describing one study (or paper). Each section starts with a brief description of the work and its objectives; followed by the related results and discussions.

2.1 Heterogeneous catalysts

2.1.1 Heterogeneous nanocopper catalyst

I began my research by investigating the Cu(I)-catalyzed alkyne-azide cycloaddition (CuAAC) using immobilized copper on controlled pore glass as a heterogeneous catalyst. The CuAAC is widely used in many fields, and it is desired due to its efficiency, selectivity, and the fact that it requires mild conditions. CuX (copper(I) halide) or $CuSO_4$/sodium ascorbate are commonly used as Cu^I catalyst sources. Although CuX is a good choice as a direct source of Cu^I, its limited solubility is the main disadvantage. $CuSO_4$/sodium ascorbate that generates Cu^I in situ is usually preferred; however, the use of reducing agents cause some limitations. For example, they are not recyclable, and ascorbates cause side effects in biological reactions.[112]

A well-established way to facilitate catalyst recycling is to immobilize nanocatalysts onto solid supports. Among the different supports that can be prepared with tunable morphology and specific surface functionalization, controlled pore glass (CPG) remains a relatively underdeveloped support within the nanocatalysis field. CPG, which belongs to the family of silica-based materials, provides several advantages since it is cost-effective, commercially available with different types of surface functionalities, and it has efficient mass-transfer, a high surface area, tunable morphology, and stability. Moreover, palladium[113] and copper[114] nanocatalysts, immobilized on CPG, showed notable levels of performance in catalytic activity.

We reported herein that the prepared Cu-AMP-CPG heterogeneous catalyst (immobilized $Cu^{I/II}$ nanoparticles onto aminopropyl functionalized CPG) acts under environmentally friendly conditions, and it serves as an efficient and recyclable catalyst in the CuAAC

reaction. In the next step, different cellulose-based heterogeneous nanocatalysts were also prepared that could be used in various organic reactions.

We started with preparing the Cu-AMP-CPG as a heterogenous catalyst.[114] Briefly, AMP-CPG was mixed with an aqueous solution of $Cu(OTf)_2$ to furnish with Cu^{II} (Cu^{II}-AMP-CPG). In the next step, Cu^{II}-AMP-CPG was reduced by $NaBH_4$ to generate the mixed valence $Cu^{I/II}$ heterogeneous nanocatalyst (Cu-AMP-CPG). The XPS analysis revealed that the catalyst had a Cu^{II}/Cu^{I} atomic ratio of 3.2:1. The total amount of copper in the prepared catalyst was determined by elemental analysis (3.3 wt.%).

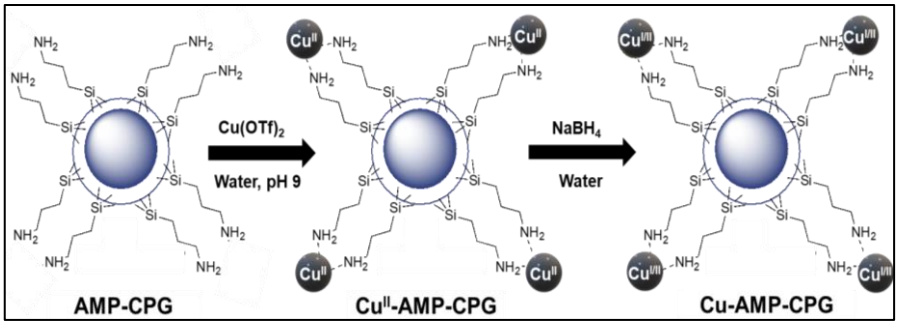

Figure 2.1.1. A schematic overview of the synthesis of Cu-AMP-CPG nanocatalyst.

The SEM images show the porous morphology of the prepared catalyst (Figure 2.1.2a,b), and the TEM images (Figure 2.1.2c,d) show nanoparticles in the size range of 1–20 nm.

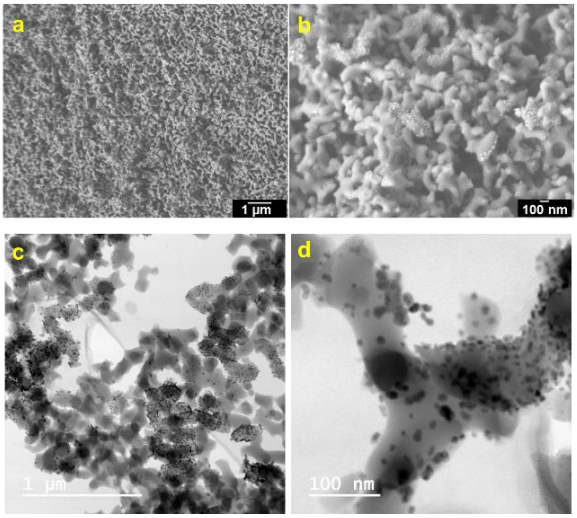

Figure 2.1.2. SEM (a,b) and TEM (c,d) of the prepared Cu-AMP-CPG nanocatalyst.

The prepared heterogeneous catalyst was used in the CuAAC reaction between benzyl azide **2a** and propargyl alcohol **3a** in *t*-BuOH/H_2O 1:1 as a solvent (Table 2.1.1). The initial experiment was successful and produced triazole **4a** in a high yield (entry 1), while the reaction didn't proceed in the control reaction (No Cat., entry 8). Encouraged by this, we continued to probe the reaction conditions. For example, it was also possible to run the reaction with a lower catalyst loading (1, 2 mol%), giving nearly full conversion within 1 h (entry 2, 3). Changing the ratio between **2a** and **3a** to 1:1 (instead of 1:1.5) and using low catalyst loadings gave almost full conversion to **4a** (entries 9–12). The neat reaction was also effective (entry 12). However, we chose *t*-BuOH/H_2O as a solvent over the neat condition due to practical reasons (*e.g.*, difficulties in miscibility of solid reagents).

Table 2.1.1. The model CuAAC reaction between benzyl azide (2a) and propargyl alcohol (3a) using the prepared catalyst to produce product (4a).

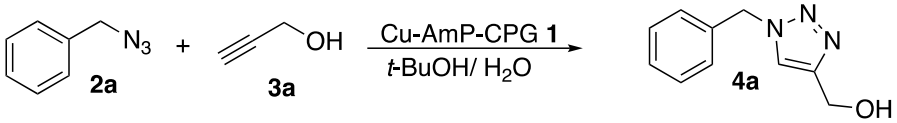

2a 3a 4a

Entry[a]	Cu-AMP-CPG (%)	Temp. (°C)	Time (h)	Conv. (%)[b]
1	5	70	0.3	>98
2	2	70	0.5	>98
3	1	70	0.7	>98
4	1	r.t.	2	15
5	1	r.t.	18	>98
6	1	50	2	73
7	1	50	2.4	>98
8	-	70	3	-
9[c]	1	70	0.8	>98
10[c]	0.5	70	3	>98
11[c]	0.25	70	4.7	98
12[d]	0.25	70	3	98

[a] 2a (0.1 mmol) and 3a (0.15 mmol) in 0.5 mL *t*-BuOH/H_2O (1:1). [b] Conversion determined by HNMR analysis using xylene as an internal standard. [c] 2a (0.1 mmol) and 3a (0.1 mmol) in *t*-BuOH/H_2O; 1:1 (0.5 mL). [d] 2a (0.1 mmol) and 3a (0.1 mmol), neat.

A range of different substrates were used to study the reaction scope (Table 2.1.2). Although prolonged reaction times were required in some cases (*e.g.*, entries 3 and 14), the reactions were successful, and the corresponding triazoles (**4a**–**4k**) were obtained in high yields.

The catalyst recycling was performed according to Table 2.1.3, and it was observed that product **4a** was obtained over eight consecutive reaction runs at high conversions.

Table 2.1.2. Scope of the CuAAC reaction using the prepared nanocatalyst.

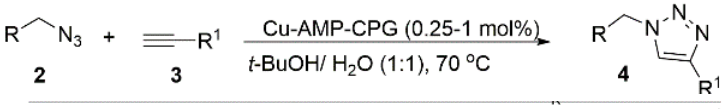

2 **3** **4**

Entry[a]	R	R^1	Cat.(mol%)	Product	Time (h)	Yield [%][b]
1	Ph	CH_2OH	0.25	**4a**	4.7	95
2	Ph	*n*-Butyl	0.25	**4b**	6	93
3	Ph	Ph	1	**4c**	48	85
4	Ph	$CH_2CH(CO_2Me)_2$	0.5	**4d**	3	92
5	Ph	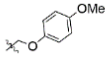	0.25	**4e**	7	95
6	Ph	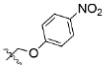	0.5	**4f**	3	87
7	Ph	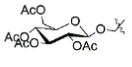	0.25	**4g**	5	92
8	Ph		1	**4h**	9	93
9	n-$C_{15}H_{31}$	CH_2OH	0.25	**4i**	6	90, (81)[c]
10	n-$C_{15}H_{31}$	n-C_4H_9	0.5	**4j**	7	81
11	n-$C_{15}H_{31}$	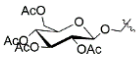	0.25	**4k**	4	94
12	Ph	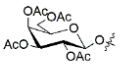	0.5	**4l**	4	94
13	Ph	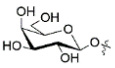	0.5	**4m**	3	93
14	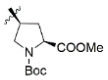	CH_2OH	0.5	**4n**	24	94

[a] Reactions performed using Cu-AMP-CPG catalyst, 2 (0.4 mmol) and 3 (0.4 mmol) in *t*-BuOH/H_2O; 1:1 (2 mL) at 70 °C. [b] Isolated yields. [c] Neat, catalyst (1 mol%), 2 h.

Table 2.1.3. Catalyst recycling after the CuAAC reaction between (2a) and (3a).[a]

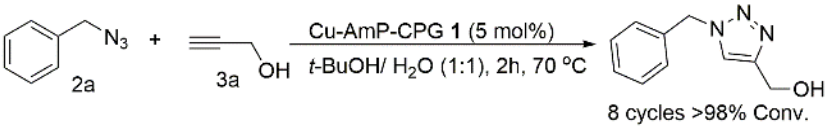

Reaction cycles	Conversion (%)[b]
1	99
2	99
3	99
4	99
5	99
6	99
7	99
8	99

[a] Reactions performed using 2a (0.25 mmol, 1 equiv.), 3a (0.38 mmol, 1.5 equiv.), and Cu-AMP-CPG (5 mol%) in 1.3 mL solvent for 2 h at 70 °C. [b] Determined by ^{1}HNMR.

Through investigating the kinetics of the first three reaction cycles, we noticed that that the rate of reaction started to decrease after two cycles (Figure 2.1.3). We can say that although we were successful in recycling the catalyst and achieving high reaction conversions over 8 reactions, we had been using more catalyst than needed to achieve full conversion within the allotted time shown in Table 2.1.3 (*i.e.*, 2 h).[115]

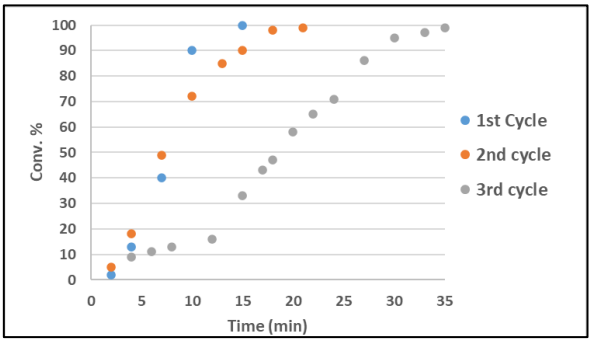

Figure 2.1.3. The reaction conversions during the 1st, 2nd, and 3rd reaction cycles.

We were also able to recycle and utilize the catalyst by using different substrates for the reaction, and the recycled catalyst was able to produce the corresponding product in high yields (Table 2.1.4).

Table 2.1.4. Recycling after reaction with different alkynes.

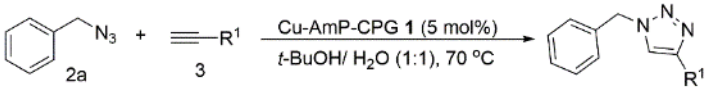

Cycle	R^1	Product	Time (min)	Conv.(%)
1	CH_2OH	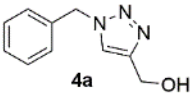 4a	15	>99
2	*n*-C_4H_9	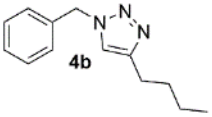 4b	40	>99
3	O-*p*-MeO-C_6H_4	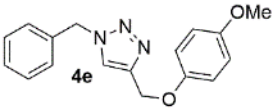 4e	40	>99

To investigate catalyst leaching, the reaction was performed and after full conversion, the catalyst was filtered from the reaction mixture and the reaction mixture was then sent for elemental analysis The analyses revealed no catalyst leaching. In addition, a hot-filtration experiment was performed where catalyst was removed from the reaction mixture when product formation reaches ~15%. Next, the reaction mixture (after catalyst removal) was continued to stir for 2 days. No further formation of product 4a was observed.

2.1.2 Cellulose-based heterogeneous catalysts

Intrigued by this work and with a focus on sustainability, we also utilized cellulose-based materials as catalyst supports for the preparation of heterogeneous catalysts (Figure 2.1.4).

The preparation procedures are described in detail in Appendix 2. Briefly, in the first step, aminopropyl functional groups (AMP) were introduced onto microcrystalline cellulose (MCC) via silylation with 3-aminopropyltrimethoxysilane. The applied method was eco-friendly

and performed in mild conditions using L-tartaric acid as a green nontoxic organocatalyst in dry toluene. In the next step, and by using Li_2PdCl_4 or $Cu(OTf)_2$, palladium (II) or copper (II) cations were furnished on the prepared MCC-AMP, thus producing MCC-AMP-Pd^{II} and MCC-AMP-Cu^{II}, respectively. Subsequent reduction by $NaBH_4$ resulted in mixed-valence MCC-AMP-Cu (Cu^{I}/Cu^{II} ratio 1.3:1) and MCC-AMP-Pd (Pd^{0}/Pd^{II} ratio 3.5:1) heterogeneous catalysts.

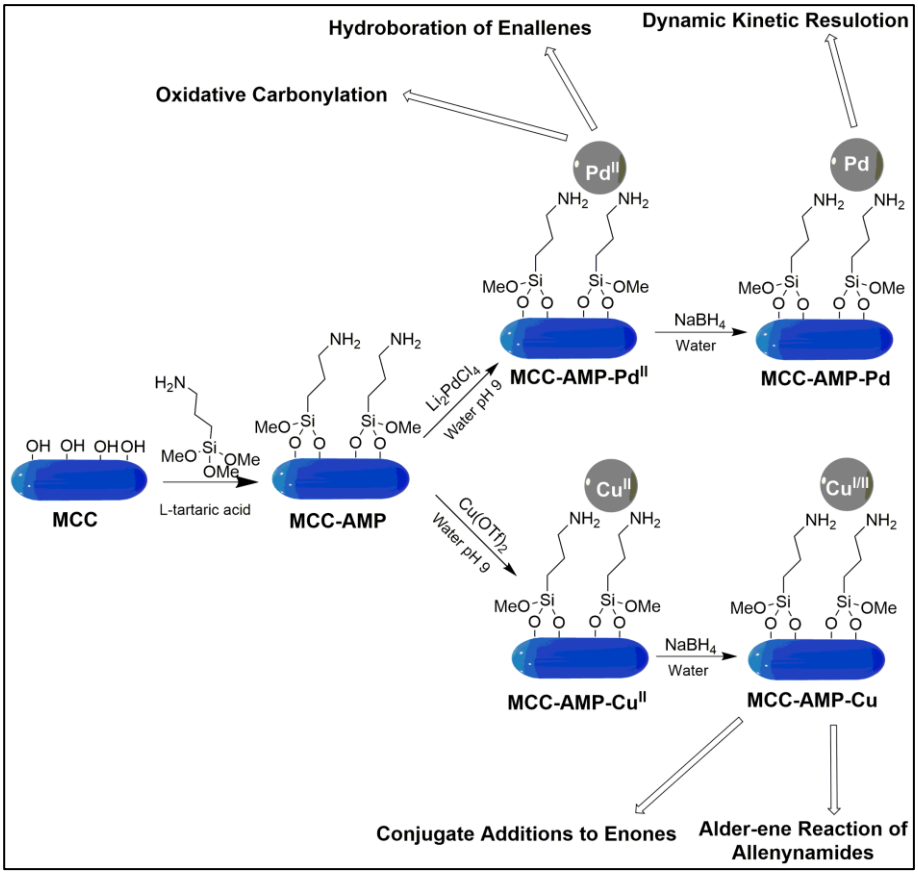

Figure 2.1.4. A schematic overview of the preparation of different MCC-based heterogeneous catalysts and their applications in different organic reactions.

The TEM images of the prepared catalysts revealed well-dispersed particles with sizes smaller than 8 nm (Figure 2.1.5). The prepared

heterogenous catalysts were employed as efficient and recyclable catalysts for selective organic synthesis (*e.g.*, dynamic kinetic resolutions, conjugate additions, carbocyclizations, hydroborations) yielding the corresponding products in high yields.[116–120] This concept was also extended to gold nanoparticles where the prepared catalyst used as recyclable catalyst for cycloisomerization of alkynoic acids.[121]

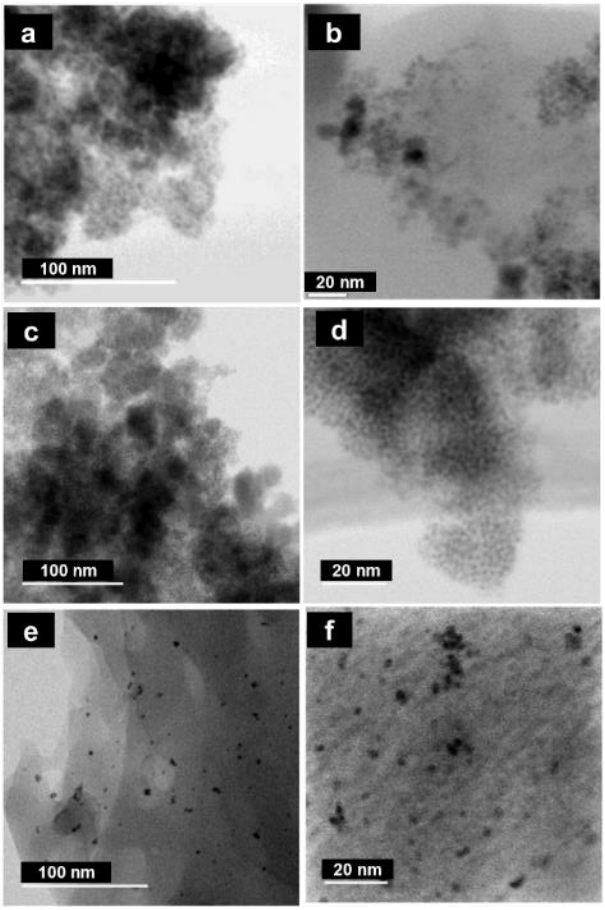

Figure 2.1.5. TEM images of a,b) MCC-AMP-Cu and c,d) MCC-AMP-Pd^{II}, and e,f) MCC-AMP-Pd.

2.2 Thiol functionalization of CNCs via direct organocatalytic esterification (Paper II)

Grafting thiol groups onto CNCs provides opportunities for different applications and further functionalization.[53,63] For example, cellulose-SH can be used in sensors and detectors,[73] metal removal,[122] as a cross-linking agent in nanocomposites,[21]and as a reducing agent in chemical reactions.[73,123] Introduction of -SH groups can be achieved by a variety of chemical reactions such as silylation with mercapto silanes[72] or by esterification with thiol carboxylic acids.[21] Generally, esterification is preferred when the cost of mercapto silanes matters. Moreover, cross-linking and self-condensation occur with alkoxysilane reagents in aqueous media. Therefore, we opted for esterification with thioglycolic acid for grafting the thiol groups onto CNCs. Some studies have reported the direct esterification of cellulosic materials with thioglycolic acid using strong inorganic acids under harsh conditions.[73,123]

Herein, we investigated the direct esterification of CNCs with thioglycolic acid under mild conditions using natural, nontoxic organic acids as organocatalysts. We applied the method to both solid CNCs materials (foam and film) and CNCs in suspension, producing the corresponding thiol-functionalized CNC materials (CNC foam-SH, CNC film-SH, and CNC suspension-SH). The prepared CNC suspension-SH was redispersible after esterification and could be used for further processes. Briefly, the aims of this study can be listed as follows: (I) Organocatalytic functionalization of CNC suspensions, foams and films using natural green organic acid as a catalyst, (II) Further functionalization of the prepared CNC-SH by thiol-ene click chemistry, and (III) Using the CNC-SH foam as a recyclable reducing agent in Cu-catalyzed cycloaddition reactions.

The starting water-suspension CNC (3 wt.%) with a size of 2-20 nm in diameter and 20-500 nm in length was provided by Melodea Ltd. The CNC films were prepared by vacuum-assisted filtration. A homogenized and well-dispersed CNC suspension (0.05 wt.%) was passed through a filtration system equipped with a glass filter support and a membrane filter. The formed CNC wet cake was dried via a Rapid-Köthen sheet former (93 °C, 96 kPa, 10 min). Figure 2.2.1 shows the main steps used in this work for the esterification of different CNC materials (solid forms and suspensions) with thioglycolic acid.

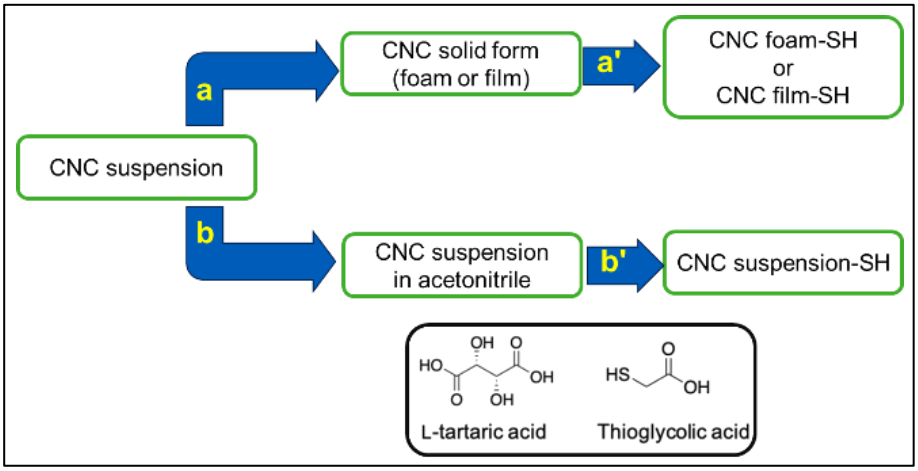

Figure 2.2.1. Organocatalytic esterification of CNC materials with thioglycolic acid. (a) lyophilization or vacuum filtration of the CNC suspension to prepare CNC foam or a CNC film, respectively. (a') Esterification of the CNC film or foam samples (1 equiv. dry CNC, 2 equiv.thioglycolic acid, 5 mol% L-tartaric acid in toluene), refluxed under nitrogen for 24 h. (b) CNC 3 wt.% suspension (3.76 mmol) was dispersed in 200 mL acetonitrile. (b') Esterification of the CNC suspension (7.5 mmol thioglycolic acid, refluxed under nitrogen for 24 h). Final products were washed by Soxhlet extraction with acetone.

We began with the organocatalytic esterification of CNC foam with thioglycolic acid in toluene using L-tartaric acid (5 mol%) as a green catalyst (Table 2.2.1). DS was improved from 0.08 to 0.22 when the thioglycolic acid to CNC ratio was increased from 0.5:1 to 2:1 (Entries 1 & 2). It can be concluded from the low DS values that surface

functionalization has occurred. It was also observed that the reaction was autocatalytic and produced CNC foam-SH with a DS of 0.08 (Entry 3); however, the DS was lower compared to that of Entry 2, where L-tartaric acid was used as the catalyst (DS = 0.22, Entry 2). The DS increased to 0.35 by performing the reaction in the neat thioglycolic acid (Entry 4). Other solid cellulose substrates such as CNC film and filter paper could also be esterified via this organocatalytic direct esterification method (entries 11-13).

CNC in dried forms irreversibly aggregate and can't be redispersed. It is beneficial for some applications to esterify CNC directly in suspension to give the corresponding CNC suspension-SH, which can be then processed and used in the preparation of films. Therefore, we also investigated the organocatalytic esterification of CNC suspensions under various conditions. In toluene as a solvent, the CNC suspension aggregated during the reaction because of the immiscibility of water and toluene. The absence of ester bonds in the FT-IR spectrum and the DS value showed that esterification didn't work in 3-methyl-3-pentanol as a solvent (Entry 10). The catalytic esterification worked in acetonitrile (Entries 5-10), and performing the reaction without adding catalyst in acetonitrile gave a DS of 0.13 (Entry 6). The corresponding CNC suspensions-SH were dispersible in water, which allowed us to make CNC film-SH afterwards.

Table 2.2.1. Esterification of CNC materials with thioglycolic acid (TGA).[a]

Entry	CNC materials	Conc (M)[b]	Catalyst	Solvent	CNC:TGA (equiv.)	DS[c]
1	Foam	0.075	L-tartaric acid	Toluene	1:0.5	0.08
2	Foam	0.075	L-tartaric acid	Toluene	1:2	0.22
3	Foam	0.075	-	Toluene	1:2	0.08
4[d]	Foam	-	-	Neat	1:10	0.35
5	Suspension	0.018	L-tartaric acid	Acetonitrile	1:2	0.08
6	Suspension	0.018	-	Acetonitrile	1:2	0.13
7	Suspension	0.018	Citric acid	Acetonitrile	1:2	0.08
8	Suspension	0.018	Acetic acid	Acetonitrile	1:2	0.06
9[d]	Suspension	0.18	-	Neat	1:2	0.03
10	Suspension	0.018	L-tartaric acid	3-methyl-3-pentanol	1:2	0.0
11	Film	0.018	L-tartaric acid	Toluene	1:2	0.09
12	Filter paper	0.018	-	Acetonitrile	1:2	0.06
13	Filter paper	0.047	-	Toluene	1:3	0.45

[a] General procedure: CNC (1 equiv.), thioglycolic acid (2 equiv.), catalyst (5 mol % of CNC), reflux for 24 h under N_2. [b] Concentration is based on the AGUs of dry mass of CNC in total volume. [c] DS estimated by alkali hydrolysis and back titration. [d] Temp. 105 °C.

2.2.1 Characterization of the prepared CNC-SH

Figure 2.2.2 shows the FT-IR spectra of the esterified CNC samples. The peaks in all spectra at around 3330, 2898 and 1636 cm^{-1} correspond to the O-H, C-H stretching vibrations and the O-H bending vibrations of the absorbed water, respectively. The peaks at 1160 and 1104 cm^{-1} are attributed to the stretching vibrations of C–C and C–O, respectively. The absorption peaks at 1030 cm^{-1} comes from the vibration of C-O-C in the pyranose ring. In comparison with the pristine CNC spectrum (a), a new peak appears around 1726 cm^{-1} in the spectra of the esterified samples (CNC foam-SH, CNC film-SH, and CNC suspension-SH), which is assigned as the characteristic peak of the ester bond. This

confirms esterification and the attachment of the thioglycolic acid onto the CNC materials.[124,125]

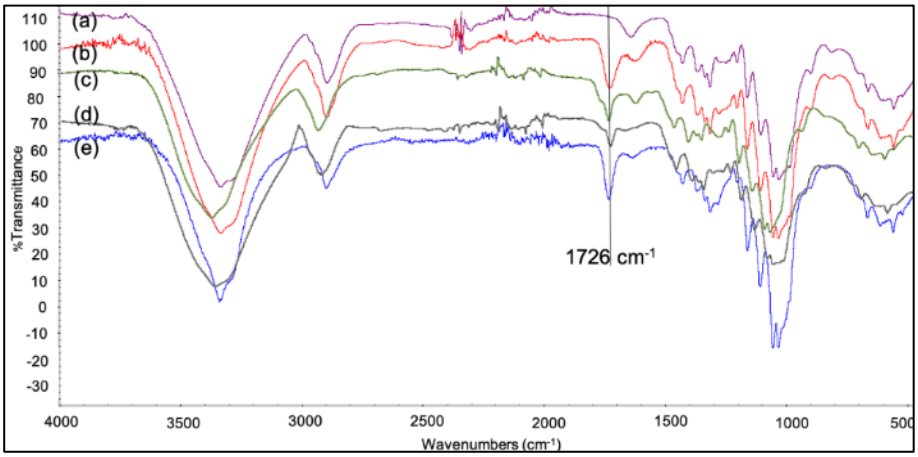

Figure 2.2.2. The FT-IR spectra of (a) pristine CNC; (b) CNC foam-SH (L-tartaric acid used as a catalyst, reaction in toluene (Entry 2 in table 2.2.1); (c) CNC suspension-SH, reaction in acetonitrile (Entry 6); (d) CNC foam-SH, reaction in toluene (Entry 3); (e) CNC foam-SH (neat, Entry 4).

Figure 2.2.3 shows the solid state ^{13}CNMR spectra of pristine CNC and CNC foam-SH. The spectrum of pristine CNC shows the characteristic peaks of cellulose at 105, 89, and 65 ppm for C1, C4, and C6, respectively. C4′ and C6′ are assigned to the amorphous parts that appear at 84 and 63 ppm, while C4 and C6 correspond to the ordered cellulose structure. The cluster at 72-75 ppm is attributed to C2-C3-C5 in cellulose.[65] Compared to the pristine CNC spectrum, the CNC foam-SH spectrum shows two new signals at 26 ppm (CH_2 of thioglycolic acid) and 175 ppm (carbonyl group), thus confirming the esterification reaction and the attachment of thioglycolic acid onto the CNC.

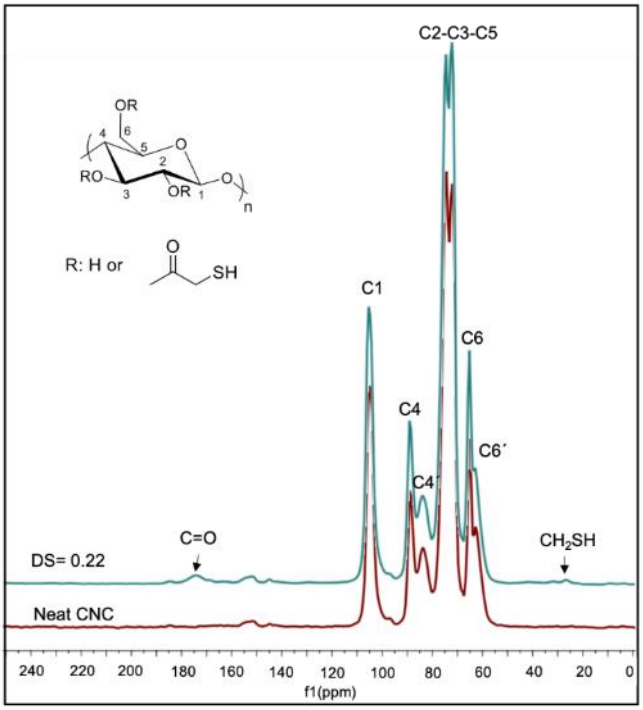

Figure 2.2.3. Solid state ^{13}CNMR spectra of pristine CNC and CNC foam-SH.

The TEM images show that the CNC-SH suspension consists of nano-sized cellulose particles with a similar size as to the pristine CNC (Figure 2.2.4).

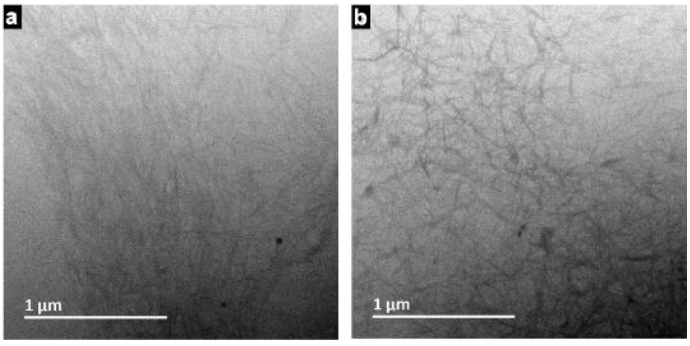

Figure 2.2.4. The TEM images of (a) pristine CNC and (b) CNC suspension-SH.

The thermal stabilities of the CNC-SH and pristine CNC were investigated by TGA (Figure 2.2.5). The pristine CNC spectrum shows a two-step degradation at 293 and 389 °C corresponding to the degradation of the outer parts and interior regions of the CNC particles, respectively.[126] The CNC foam-SH showed a similar degradation behavior with slightly increased stability.

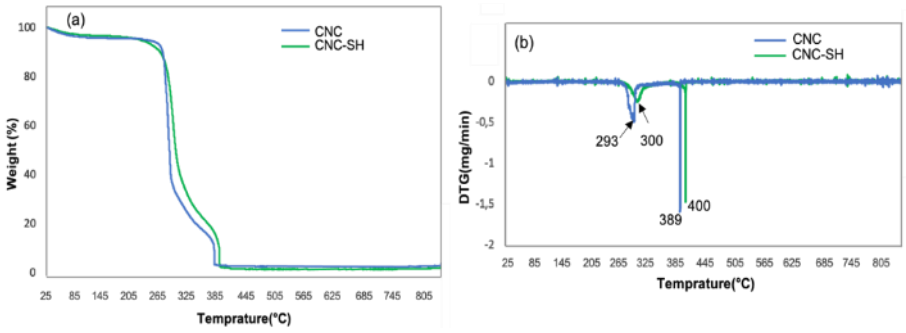

Figure 2.2.5. (a) TGA and (b) derivative thermogravimetry (DTG) of the pristine CNC and CNC foam-SH.

2.2.2 CNC foam-SH as a heterogeneous reducing agent in the CuAAC

CNC foam-SH was used as a co-catalyst (heterogeneous reducing agent) for the CuAAC. Cu^{I} is generally generated in situ via the reduction of Cu^{II} with an extra amount of reducing agent such as sodium ascorbate. Ascorbate is not recyclable and shows side effects in biological reactions.[112] On the other hand, heterogeneous reducing agents are useful since they are readily separated from the reaction mixture and can be reused.

In this context, we used the prepared CNC foam-SH as a heterogeneous reducing agent. A model reaction between benzyl azide and propargyl alcohol in the presence of $CuSO_4.5H_2O$ and CNC foam-SH was performed in a water/t-BuOH 1:1 as a solvent (Figure 2.2.6).

The reaction was completed within 8 h and the corresponding 1,4-triazole was isolated (90% isolated yield). This result confirms that the CNC foam-SH successfully worked as a heterogeneous reducing agent for the reduction of Cu^{II} to Cu^{I}.

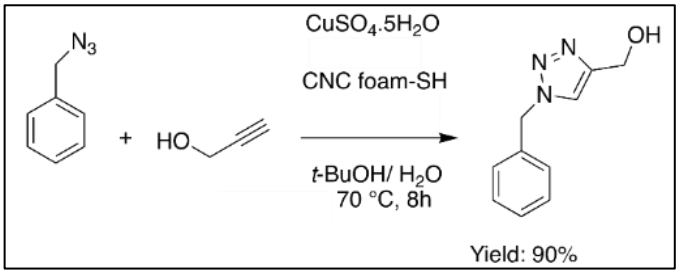

Figure 2.2.6. The CuAAC using CNC foam-SH (DS=0.22) as a heterogeneous reducing agent. Reaction conditions: benzyl azide (0.1 mmol), propargyl alcohol (0.15 mmol), $CuSO_4 \cdot 5H_2O$ (2 mol% of azide), and CNC foam-SH (13 mg, 16 mol% SH).

The CNC foam-SH was separated by centrifugation and reused for 9 reaction cycles. An increase in reaction time was observed after cycle 3; however, the corresponding product was produced in high conversions in all cycles (96-99%).

Table 2.2.2. Recycling of CNC foam-SH as a heterogeneous reducing agent in CuAAC reaction.[a]

Reaction run	Time (h)	Conversion (%)[b]
1	8	97
2	8	96
3	9	98
4	14	98
5	16	99
6	18	97
7	19	96
8	20	98
9	21	99
10	22	97

[a] Reactions performed as described in Figure 2.2.6. [b] Conversion was determined by ^{1}H NMR analysis of the crude reaction mixture.

2.2.3 Grafting fluorescent or UV active compounds onto CNC-SH materials

Grafting UV-active and fluorescent molecules opens new applications in different areas such as in sensors, biology, cell uptake and viability, and surface monitoring.[127,128] In this context, after thiol functionalization of CNC samples, we used thiol-ene click reaction to attach UV-active and fluorescent molecules onto the prepared CNC-SH samples. The thiol-ene click reaction was performed in the presence of a photo-initiator (DMPA) under UV irradiation to graft Allyl-TAMRA (a fluorescent molecule) or quinidine (as a natural UV active molecule) onto CNC suspensions-SH and CNC film-SH (Figure 2.2.8).

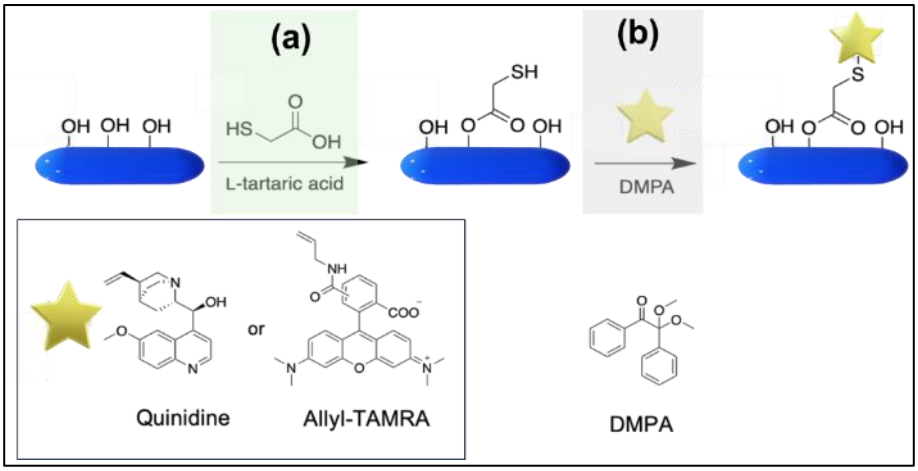

Figure 2.2.8. (a) Thiol functionalization of CNC materials. (b) Grafting UV active and fluorescent compounds (quinidine and TAMRA) onto CNC-SH [Quinidine (10 mol %) or Allyl-TAMRA (1 mol %), DMPA (5 mol %) in DMF under UV radiation for 24 h]. The prepared materials were washed with acetone Soxhlet extraction then dried.

In the case of the CNC suspension-SH, UV labeling was performed via the thiol-ene click reaction to graft quinidine (producing CNC suspension-S-quinidine). Afterwards, a corresponding film (CNC-S-quinidine film) was made via the filtration of the prepared CNC suspension-S-quinidine.

It was also possible to graft quinidine onto the CNC film-SH to obtain the corresponding CNC film-S-quinidine. As shown in Figure 2.2.9d, both methods produced UV active films, while the CNC film-SH was not shining under UV irradiation. Using the thiol-ene click reaction approach, allyl-TAMRA was also attached onto the prepared CNC films-SH.

CLSM was performed using specific emission ranges for TAMRA (λ=561 nm) and quinidine (λ=405 nm) on the CNC film-S-TAMRA and CNC film-S-quinidine, respectively (Figure 2.2.9c). A uniform distribution of TAMRA and quinidine was observed in the corresponding films.

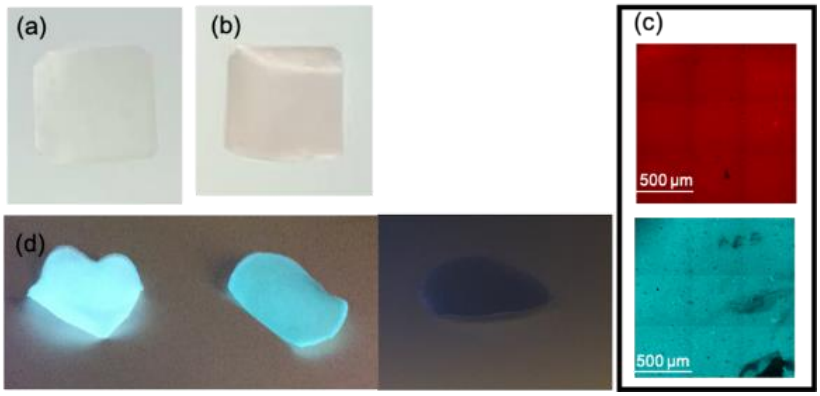

Figure 2.2.9. UV or fluorescent active molecules grafted onto CNC-SH materials. (a) photograph of pristine CNC film, size: 2.5 cm x 2.5 cm; (b) photograph of CNC film-S-TAMRA, size: 2.5 cm x 2.5 cm; (c) CLSM images of CNC film-S-TAMRA (top), and CNC film-S-quinidine (bottom); (d) photograph of CNC-S-quinidine film prepared from CNC suspension-S-quinidine (left), CNC film-S-quinidine prepared from click reaction on CNC-SH film (middle), and CNC-SH film (left) under a UV lamp.

2.3 Fabrication and functionalization of CNFs using lactic acid mediated catalysis approach (Paper III)

Different methods such as mechanical agitation, TEMPO oxidation, and enzymatic methods can be used for the preparation of CNFs; however, high energy consumption and using expensive and toxic chemicals are the main drawbacks of these methods. Organic acids like oxalic acid,[69] citric acid,[67] formic acid,[70] benzoic acid,[66] lactic acid,[68] and acetic acid[68] have been used as neat reaction media for fabrication of organic acid-grafted CNCs (using a strong mineral acid as a catalyst). Recently, a direct and concurrent fabrication of CNFs using formic acid was reported in our group. The prepared CNF was esterified by formic acid, and the used formic acid could be recycled and reused.[47,72]

Herein, we investigate the fabrication of esterified CNFs through lactic acid mediated catalysis. Lactic acid (LA) was obtained from sour milk for the first time in 1780 by a Swedish Scientist (Carl Scheele). LA is environmentally friendly since it has less environmental impact during its disposal and can be produced via the microbial fermentation of renewable resources.[129] Additionally, LA-esterification of nanocelluloses could make nanocelluloses more applicable and compatible with polymers. One possible way to produce LA-nanocellulose is by concurrent LA-esterification and fabrication using a strong mineral acid like HCl as a catalyst. In this context, it was recently reported that LA-functionalized CNCs can be fabricated from cotton using a mixture of LA and HCl at 150°C under high pressure.[68] Furthermore, post-modification of CNFs with lactic acid ester groups was reported using metal-based compounds as catalysts.[130,131] Strong acids such as HCl are corrosive and pollutant, moreover these challenges become even more challenging and costly during scale-up.

We study herein an approach for direct one-step esterification and fabrication of CNFs from wood-derived pulp in high yields. LA is used as both reaction media and catalyst (a mild, organocatalytic and metal-free method). The LA media can be reused for the preparation of LA-CNFs without affecting the yield or DS of the produced LA-CNFs.

The procedure that we used in this work to fabricate lactic acid-functionalized CNFs (LA-CNFs) is briefly demonstrated in Figure 2.3.1. Bleached sulfite pulp (dissolved softwood pulp [70% spruce and 30% pine]) was mixed with lactic acid (as neat reaction media), and the mixture was vigorously stirred at 105 °C for 24 h. The reaction mixture was centrifuged, and the supernatant was collected for another reaction run (recycling). The solids were washed several times with water, then homogenized in water.

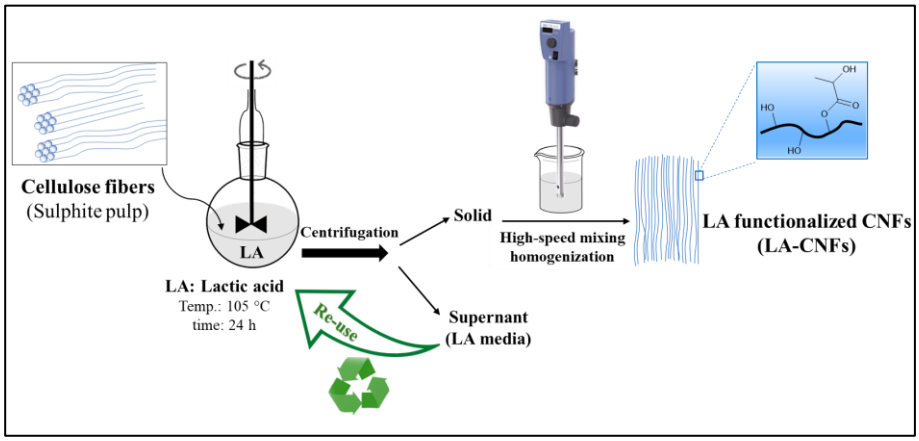

Figure 2.3.1. Fabrication of LA-CNFs. Sulfite pulp (5 g) and LA 90% (200 mL) was mixed with a mechanical stirrer (1400 rpm). The mixture was centrifuged (12000 rpm) and the supernatant was collected and reused as the reaction medium for another reaction cycle. The solid part was washed with water and then homogenized in 200 mL water using IKA® T25 ULTRA TURAX, 14000 rpm for 90 min (LA-CNFs).

Entry 1 and 2 in Table 2.3.1 show that when only lactic acid (either D,L-lactic acid (LA) or L-Lactic acid (LLA)) was used, the yields of LA-CNFs were 92% and 91%, respectively. It was observed that the addition of a catalytic amount of HCl to the LA medium reduced the production yields. Entries 3 and 4 show that by using 0.05 M and 0.1 M HCl, the yields dropped to 73% and 65%, respectively. The DS of fabricated LA-CNFs were between 0.20-0.22. Therefore, the data in

Table 2.3.1 revealed that the approach is autocatalytic and doesn't need to use harsh acid reagents and conditions.

Table 2.3.1. Fabrication of LA-CNFs in different conditions.

Entry	Reaction Medium[a]	HCl Conc.[b]	Yields (%)	DS[c]
1	LA	-	92	0.21
2	LLA	-	91	0.21
3	LA+HCl	0.05 M	73	0.20
4	LA+HCl	0.1 M	65	0.22

[a] Temp.: 105°C, reaction time: 24 h. [b] Total Concentration of HCl in the reaction medium. [c] CNF isolated yields. [d] DS determined by alkali hydrolysis and back titration method.

The LA media was collected after the reaction and reused for the subsequent reactions (recycling). Table 2.3.2 shows the isolated yields of the fabricated LA-CNFs in different cycles and in different reaction media. When only LA was used as the reaction medium, the yields for different cycles were high and almost the same (91-92%); however, by adding a catalytic amount of HCl to the LA medium (0.05 M), the yields decreased (73-85%). It was also observed that in the latter case, the yields are increased as the number of reaction cycles increased owing to the decrease in acidity of the medium (HCl evaporation). The reaction was also performed in larger scale, and similar results were observed.

Table 2.3.2. Recycling and reusing of the LA media for the fabrication of LA-CNFs.[a]

Cycles	Yields (%)	Yields (%)[b]
1st	92	73
2nd	91	77
3rd	91	82
4th	92	85
5th	91	83
6th	92	84
7th	92	85
8th	92	N.d.

[a] Reaction condition as described at Figure 2.3.1. [b] HCl (total concentration of 0.05 M) was also added to the reaction media.

2.3.1 FT-IR spectra

FT-IR spectra of the starting material and fabricated LA-CNFs are shown in Figure 2.3.2. Comparing the spectrum of the starting material with the LA-CNFs' spectra revealed that a new peak appeared around 1737 cm^{-1} in the LA-CNFs spectra, which corresponds to the ester bond.[132] The presence of this peak confirms the attachment of the LA onto the CNFs via ester linkage.

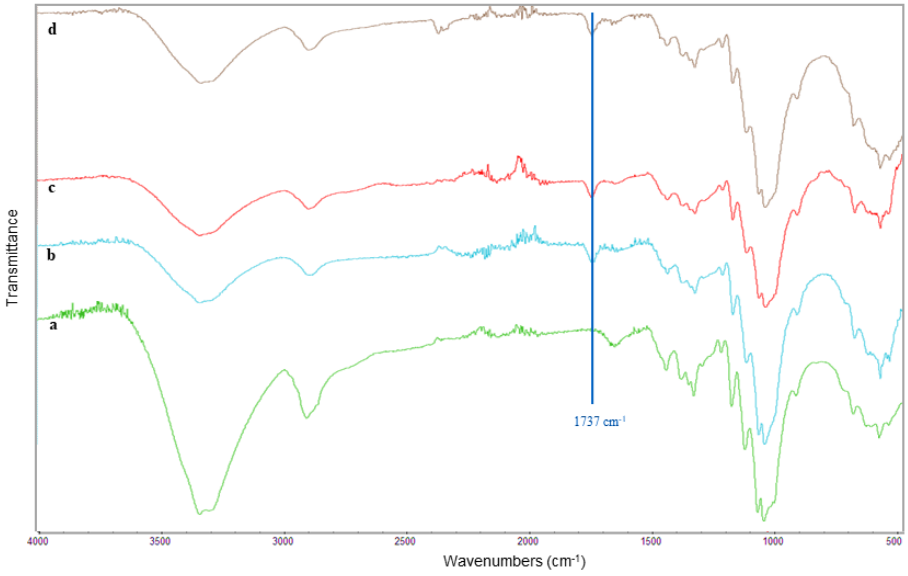

Figure 2.3.2. FT-IR spectra of (a) sulfite pulp starting material; (b) LA-CNFs (in the presence of HCl 0.1 M); (c) LA-CNFs (in the presence of HCl 0.05 M); (d) LA-CNFs (without HCl).

2.3.2 Solid state ^{13}CNMR

The Solid state CNMR spectrum of the starting material shows the characteristic peaks of cellulose at 105, 89, and 66 ppm for C1, C4, and C6, respectively. C4′ and C6′ are assigned to the amorphous parts that come at 84 and 63 ppm, while C4 and C6 correspond to the ordered

cellulose structure. The cluster at 72-75 ppm is attributed to C2-C3-C5 in cellulose.[65] Compared to starting material, LA-CNFs has two new signals, one at 20 ppm (–CH_3 of LA) and the other at 176 ppm (carbonyl group) confirming the attachment of LA onto the CNFs. No peaks corresponding to the oligomeric or polymeric lactide was observed. Moreover, by dividing the area under the C4 crystalline peak by the total area of the C4 resonances from both crystalline and amorphous regions (C4+C4′), the crystallinity indexes were calculated to be 0.52 and 0.53 for the sulfite pulp (starting material) and the LA-CNFs, respectively.[133]

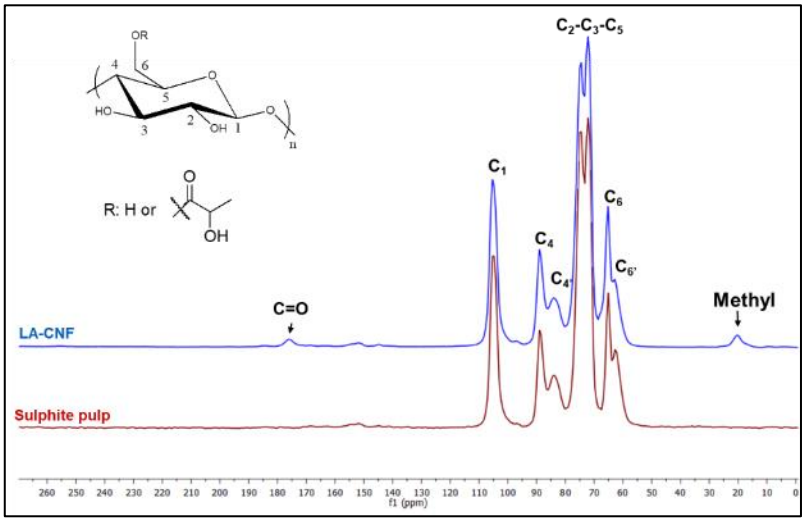

Figure 2.3.3. Solid state ^{13}CNMR spectra for the sulfite pulp and the prepared LA-CNFs.

The mean crystal sizes were calculated from the XRD spectra via *Scherrer* equation, and they were calculated to be 3.6 and 3.1 nm for the sulfite pulp and the fabricated LA-CNFs, respectively. These sizes are in the same range as those reported for Norway spruce *Picea abies (L.) Karst*. (3.2 nm), and Scots pine *Pinus sylvestris L.* (3.1 nm), respectively.[134]

2.3.3 SEM and AFM images

SEM images of the starting sulfite pulp and the fabricated LA-CNFs are shown in Figure 2.3.4, revealing the big fibers in the sulfite pulp (a,b) as well as the fabricated LA-CNFs (c,d).

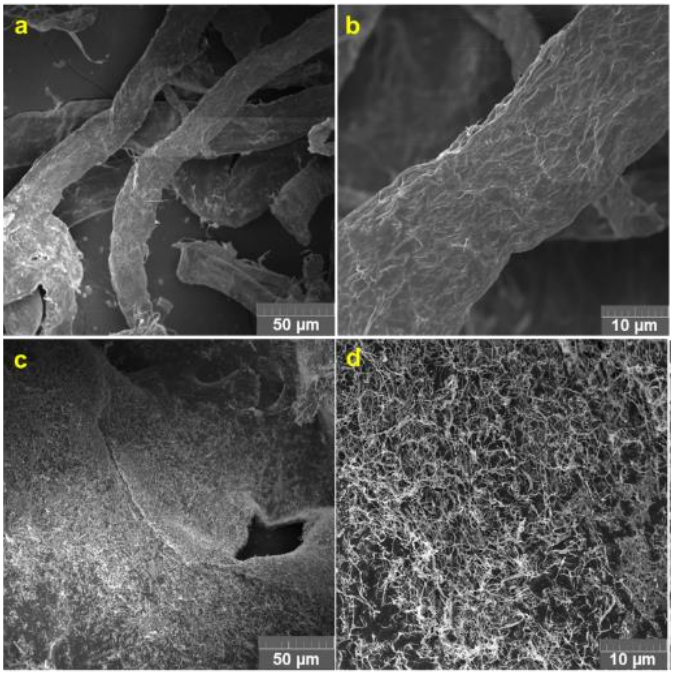

Figure 2.3.4. SEM images of the sulfite pulp (a,b), and the fabricated LA-CNFs (c,d) at different magnifications.

The AFM image of the fabricated LA-CNFs is shown in Figure 2.3.5, revealing long thin fibers. From the AFM images, the aspect ratio of the fabricated LA-CNFs was calculated to be 162±24 by measuring of around 100 different individualized CNFs (with an average length of 1236±214 nm and a diameter of 8±2 nm).

The size exclusion chromatography (SEC) technique was used to determine the molecular weight distribution and degree of polymerization (DP) of the fabricated LA-CNFs. The average Mw, Mn, poly dispersity index (PDI) and DP were 112,639 g/mol, 21,142 g/mol,

5.3 and 131, respectively. The average molecular weight was very similar to that of the formic acid-generated CNFs in the previous study (Mw=112,360 g/mol a PDI=6.8).[72]

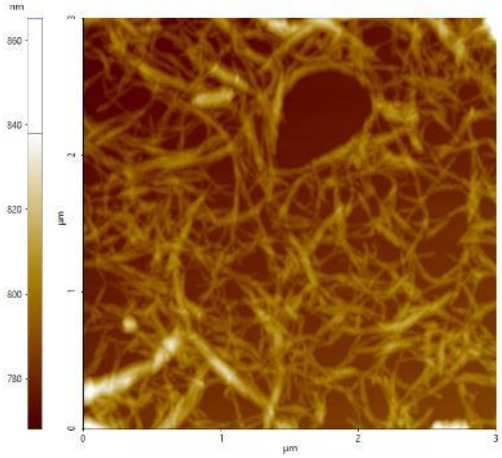

Figure 2.3.5. AFM image of the fabricated LA-CNFs.

2.3.4 Thermal studies

Thermal analyses of the cellulose sulfite pulp, fabricated LA-CNFs (prepared in LA+HCl 0.1 M), the fabricated LA-CNFs (No HCl) as well as the latter material before the homogenization step were performed, and the related TGA and DTG curves are shown in Figure 2.3.6. For each sample, two main weight losses were observed in the TGA curves. The initial one happened around 90 °C that was corresponded to the water evaporation from the samples. The next one was a significant weight loss due to the decomposition and degradation of the sample. No significant differences among the curves of the samples were observed; however, the thermal stability of the LA-CNFs is slightly lower than that of the sulfite pulp. Moreover, the thermal analyses of the LA-CNFs before and after the homogenization step are slightly different. In fact, the degradation temperature of the samples after homogenization is lower (324 °C) than that of the sample before the

homogenization step (336 °C). The lower degradation temperature of the fabricated LA-CNFs samples compared to the starting material is due to the smaller fiber dimensions of the fabricated materials compared to that of the sulfite pulp.[135]

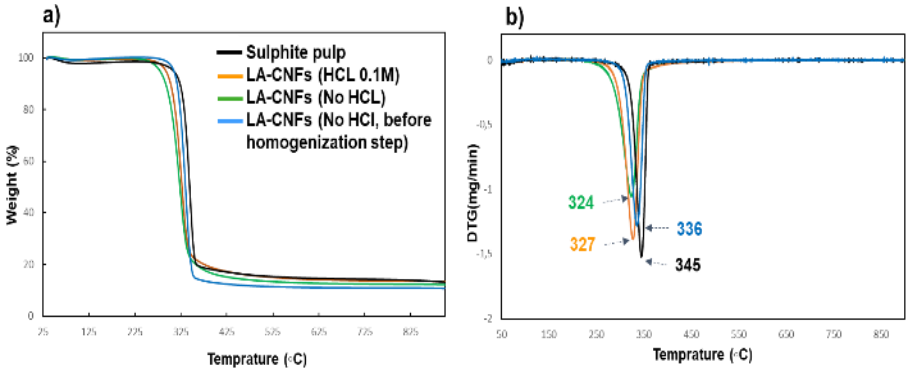

Figure 2.3.6. a) TGA curves of the sulfite pulp, the fabricated LA-CNFs (prepared in LA+HCl 0.1 M), and the fabricated LA-CNFs (without HCl as a co-catalyst) before and after the homogenization step; b) DTG curves of the related samples.

2.3.5 Further investigations

We also prepared CNFs (without LA functional groups) through removal of the attached LA groups from the prepared LA-CNFs via the alkaline hydrolysis of the ester bonds (Figure 2.3.7). The removal of ester bond peak in the FT-IR spectrum (1735 cm^{-1}) confirms the removal of the LA from the LA-CNFs (Figure 2.3.9, Spectrum b).

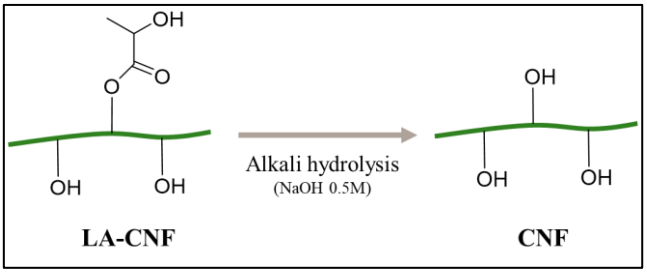

Figure 2.3.7. Preparation of the CNF via the alkali hydrolysis of LA-CNFs. LA-CNFs (500 mg) was mixed with 30 mL of NaOH (0.5 M) in 40 mL EtOH (*aq*) at 60 °C for 24 h.

The corresponding films made of LA-CNFs and CNFs were prepared to investigate their mechanical properties and measure the WCAs. The mechanical measurements (Table 2.3.3) show that both films were in the same range, with the LA-CNF film having a slightly higher tensile strength compared to that of the CNF film.

Table 2.3.3. Mechanical test of the LA-CNF and CNF films.

Sample	Tensile strength [MPa]	E-modulus [GPa]	Strain at break [%]
LA-CNF film	42 ± 1	5.7 ± 0.3	1.3 ± 0.3
CNF film	39 ± 2	5.1 ± 0.4	1.3 ± 0.2

The effect of adding the fabricated LA-CNF to poly lactic acid (PLA) was investigated. This was done by mixing the fabricated LA-CNFs with PLA using a twin-screw micro-compounder (Xplore, 15 mL) at 190 °C under nitrogen. The addition of CNF components to the neat PLA was effective and increased the tensile strength. By adding 1 wt.% of LA-CNFs or CNFs, the tensile strengths of the neat PLA (66 MPa) were increased by 5% and 9%, respectively (Appendix 3).

The WCA measurements showed that the LA-CNF film had a slightly higher contact angle compared to that of the CNF film, and they were measured to be around 58±1° for the LA-CNFs film and 42±3° for the CNFs film.

In collaboration with Chalmers University, the fabricated LA-CNFs and CNFs were used to make nanocomposites of ethylene brassylate (EB), which is a monomer originating from castor oil.[136] Using reactive extrusion, the related polyethylenebrassylate (PEB)/CNFs and PEB/LA-CNFs samples were prepared (Figure 2.3.8). The study showed that adding LA-CNFs or CNFs were effective and enhanced the properties of neat PEB. For example, by adding 1 wt.% of LA-CNFs

or CNFs, the tensile strengths of the neat PEB (8.9 MPa) were increased by 54 and 44%, respectively.[136]

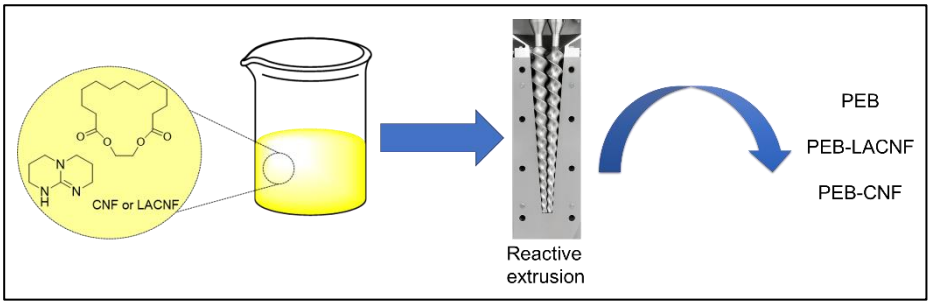

Figure 2.3.8. ROP polymerization of EB (54.9 mmol) using reactive extrusion in the presence of: TBD (1.3 mmol, as an initiator), with or without the CNFs or LA-CNFs (1 wt.%.). The reaction was performed in an Xplore micro compounder (total volume of 15 cm^3) at 130 °C and 100 rpm for 60 min under a constant N_2 flow.

The prepared (PEB)/CNFs and PEB/LA-CNFs were well dispersed, and no sedimentation of nanofibers was observed. This suggests their surface modification with PEB (*i.e.,* polymer grafting from the nanofibril surface hydroxyl groups). The possibility of grafting PEB from the CNF moieties was investigated as a strategy to promote CNF dispersion and interaction with PEB. An effective way to confirm the grafting of PEB onto the CNFs is to investigate the presence of ester bonds in the CNFs separated from PEB-CNFs nanocomposite. To do this, extensive Soxhlet extraction of the PEB-CNFs nanocomposite was performed first to remove all noncovalently bonded PEB from the insoluble CNF fraction. Comparing the FT-IR spectrum of the starting CNFs with spectrum of CNFs separated from the PEB-CNFs nanocomposite shows the presence of an ester peak at 1735 cm^{-1} in the latter sample, thus confirming the grafting of PEB onto the CNFs (Figure 2.3.9).

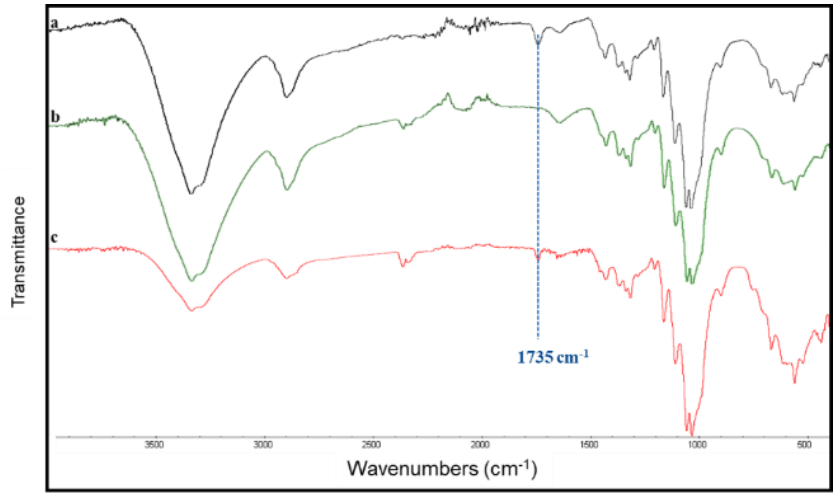

Figure 2.3.9. FT-IR spectra of a) LA-CNFs, b) CNFs (alkali hydrolyzed LA-CNFs), and c) CNF separated from PEB-CNFs nanocomposite (after Soxhlet extraction with $CHCl_3$).

Furthermore, the solid state ^{13}CNMR of PEB-CNFs after soxhlation was also performed (Figure 2.3.10). In addition to the characteristic peaks of cellulose, peaks for carbonyl and methylene were also observed confirming the covalent bonding of PEB onto the CNFs.

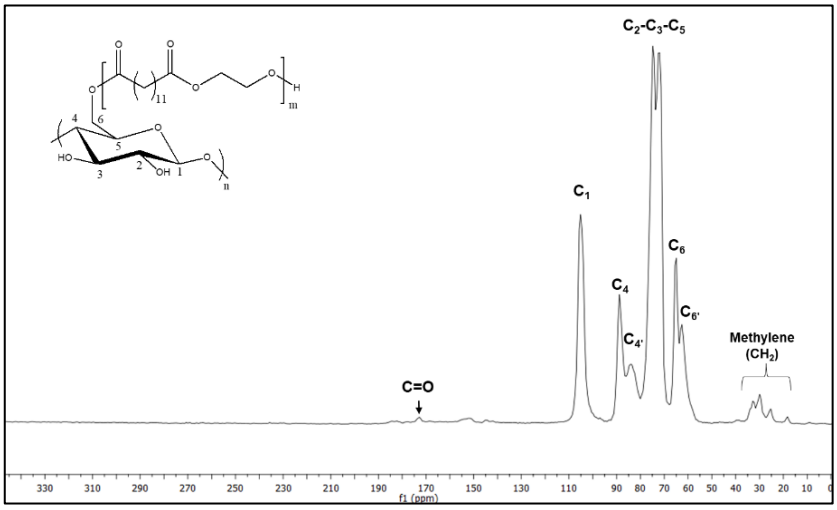

Figure 2.3.10. Solid state ^{13}CNMR spectrum of CNF separated from PEB-CNFs (after Soxhlet extraction with $CHCl_3$).

2.4 Fabrication of strong hydrophobic cellulosic materials by combination of an aqueous betulin treatment with hot-pressing (Paper IV)

High wettability and low wet-strength are inherent drawbacks of unmodified cellulosic materials that limit their applications. There have been numerous reports about improving these drawbacks. In the context of water repellency, various methods have been applied; for example, using fluorinated compounds, functional silanes, and grafting polymers.[58,64,137,138] However, most methods face multiple obstacles like using costly and fossil-based chemicals and/or organic solvents, multiple chemical reactions, and time-consuming processing steps, as well as difficulties in scaling up.

Using natural and ecological materials has received much interest and shown many benefits. Betulin, an abundant naturally occurring triterpene extracted from birch bark, can be employed to increase the hydrophobicity of cellulosic materials. Huang *et al*.[88] and Moriam *et al*.[90] reported hydrophobization of cellulosic materials by impregnating them with betulin; however, the use of unsustainable and hazardous chemicals (*e.g.*, ILs, organic solvents) can be challenging from both ecological and industrial perspectives.

In the context of mechanical strength, several commercially available wet-strength chemicals and hydrophobic agents used for the treatment of cellulosic materials (*e.g.,* epichlorohydrin, fluorocarbons, formaldehyde-based resins). These materials are mostly fossil-based and have been shown to be unsafe.[137–140] Hot pressing is considered a convenient and effective method for the fabrication of densified samples with improved mechanical properties.[103–105,107] Moreover, the

process has been found to be very effective in the case of lingocellulosic materials, and especially after wood softening.[99,100]

The main objective of this work was to develop an eco-friendly and scalable approach for the fabrication of strong hydrophobic cellulosic materials. Herein, we developed a water-based betulin formulation and applied it for the eco-friendly hydrophobization of cellulosic materials. Cellulosic samples were treated by spraying them with the prepared aqueous betulin formulation, and then hot pressing. It was observed that hot pressing changed the morphology of the samples, resulting in a dense and compact structure, with the betulin particles undergoing polymorphic transformations from prismatic crystals into orthorhombic whiskers. The process improved the hydrophobicity of the samples. Significant enhancements in the tensile strengths (especially wet strength) of the samples were observed, where a synergistic effect occurred between the hot pressing, betulin particles, and sulfonation.

At the beginning of study, we started with treatment of different cellulosic materials by impregnation of the samples in ethanolic betulin solution. For this aim, the cellulosic materials were impregnated with a betulin/EtOH solution (8.5 mM) and then air dried. Although the WCAs were improved, they didn't reach 90° after a long impregnation time (Appendix 4). Since it is advantageous to use a water medium, in the next step we developed an aqueous colloidal suspension formulation of betulin to use in this study (Appendix 5). The impregnation of cellulosic materials with the prepared aqueous betulin suspension followed by heat treatment in an oven, increased hydrophobicity of different cellulosic materials up to 130° (Appendix 6).

2.4.1 Betulin treatment and hot-pressing

Due to the advantages of aqueous media, we applied the prepared aqueous betulin suspension to treat the cellulosic materials. Figure 2.4.1 schematically demonstrates the entire process and indicates the nomenclature of the different prepared samples in this work.

First, we obtained different CTMP samples, and the corresponding laboratory handmade paper sheets were prepared. The following CTMPs with different amounts of bound sulfur (S) were used: *CTMP1* (total bound S of 2.4 g (S)/kg), and *CTMP2* (total bound S of 1.0 g (S)/kg). *CTMP1* and *CTMP2* with 28% dryness were from the primary high consistency refiner. *CTMP3* with 85% dryness was form final step and was the same as CTMP2 (total bound S of 1.0 g (S)/kg). For more details and information, see Appendix 7.[141]

The initial samples (*i.e.*, neither betulin treated nor hot-pressed) named *starting samples*; for example, the initial handmade paper sheet made of CTMP1 is called CTMP1-starting. The prepared starting samples

were treated by spraying them with the prepared aqueous betulin suspension then dried in an oven 55 °C. The resulting samples were named *BET-NoHP samples* (*e.g.*, the betulin treatment of CTMP1-starting gives CTMP1-BET-NoHP). The samples treated with betulin (*i.e.*, BET-NoHP samples) underwent hot pressing (at 3 bar and 250 °C for 1 min) giving *BET-HP samples* (*e.g.*, hot pressing of CTMP1-BET-NoHP produces CTMP1-BET-HP). Moreover, some starting samples were also directly hot-pressed without betulin treatment producing *NoBET-HP samples*.

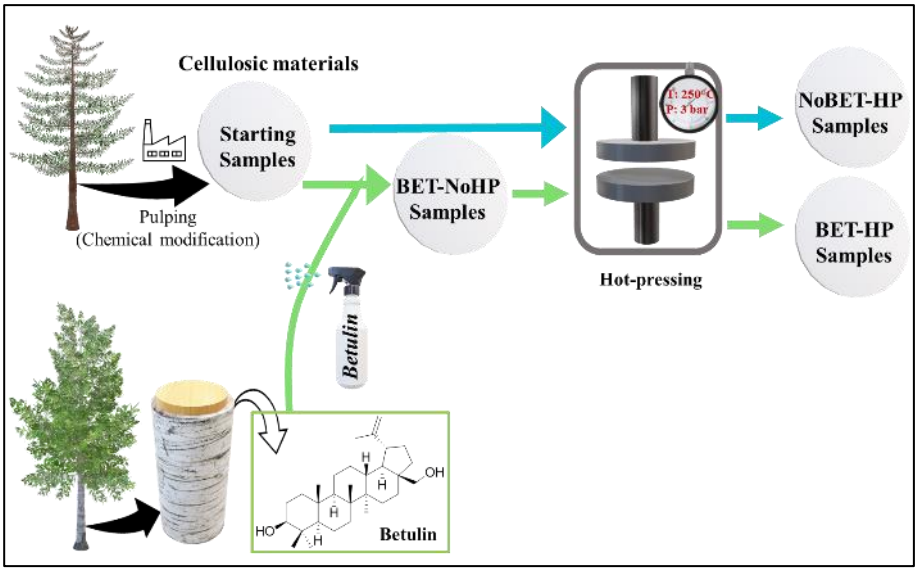

Figure 2.4.1. A schematic demonstration of the procedure and the nomenclatures of the prepared samples (BET=Betulin, HP=Hot-pressing).

All corresponding samples for all CTMPs as well as filter paper were prepared and shown in Figure 2.4.2a. Compared to the starting samples, the BET-NoHP samples had a brighter color because of the presence of betulin in the paper sheets (~6 wt.% of the sample). The NMR spectra of the starting pure betulin powder and the sample scraped off from the surface of the BET-HP samples were identical

(Figure 2.4.2b,c). Betulin, which had been melted at 280 °C, had also identical spectra. This confirms that betulin chemical composition was stable upon hot pressing; however, the morphology of the betulin crystals was altered upon hot pressing, as explained in the SEM and XRD sections.

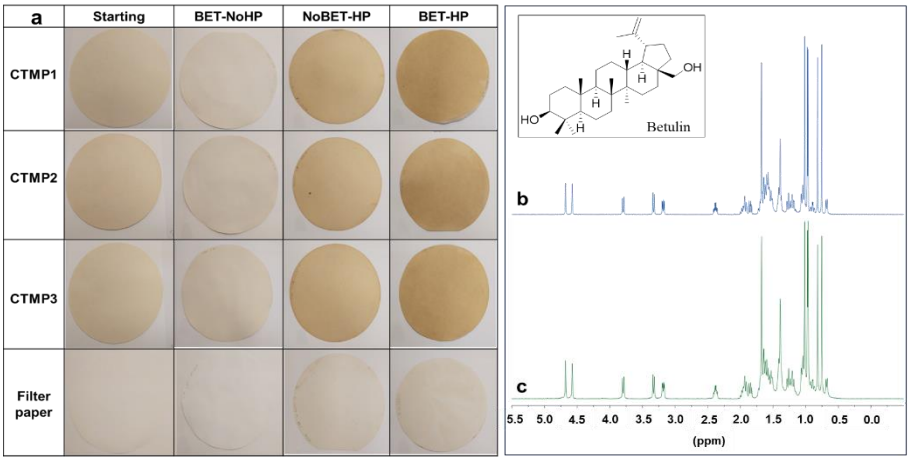

Figure 2.4.2. a) Photographs of filter paper and all CTMP samples without betulin and without hot pressing (starting samples), with betulin without hot pressing (BET-NoHP), without betulin but hot pressed (NoBET-HP), and with betulin and with hot pressing (BET-HP), b) ^{1}HNMR spectra of betulin, c) ^{1}HNMR spectra of betulin taken from the BET-HP sample.

2.4.2 FT-IR spectra

Figure 2.4.3 displays the FT-IR spectra corresponding to the CTMP1 samples (CTMP1-starting, CTMP1-NoBET-HP, CTMP1-BET-NoHP, and CTMP1-BET-HP). Here, only the spectra of the CTMP1 samples are shown as an example since the FT-IR spectra of all the other CTMP samples exhibited similar characteristics. The peaks in all the spectra around 3331 and 2895 cm^{-1} are related to the O-H and C-H stretching vibrations, respectively. The bands around 1631 cm^{-1} correspond to the O-H bending vibrations of hydroxyl groups from absorbed water. The peaks around 1730 and 1509 cm^{-1} are related to C=O stretching (hemicellulose) and aromatic ring skeleton vibration (lignin),

respectively. The bands around 1158, 1105, and 1028 cm^{-1} are attributed to the stretching vibrations of C–C, C–O, and C-O-C bonds, respectively.[100,125] The spectra of samples containing betulin (c, d) show new peaks around 2895 cm^{-1} originating from betulin (aliphatic C-H stretching).

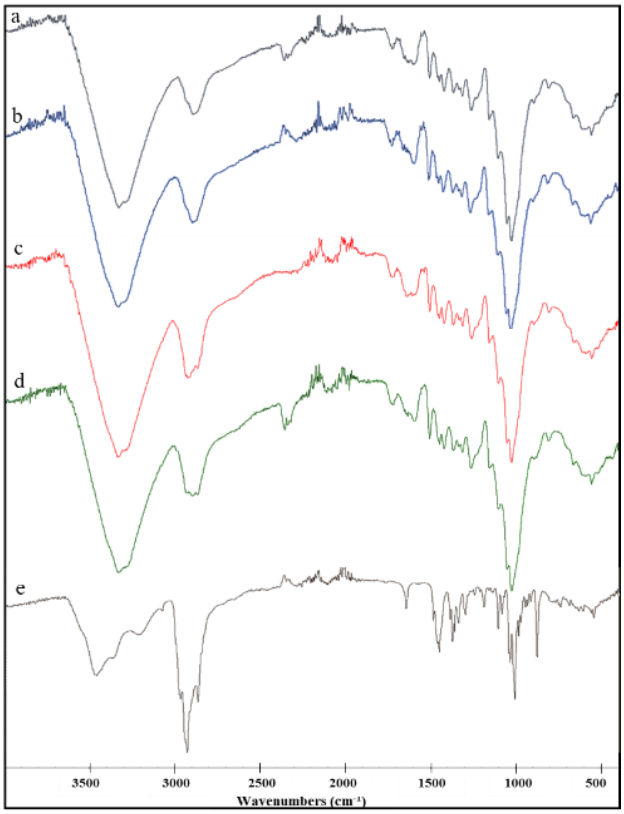

Figure 2.4.3. FT-IR spectrum of CTMP1-starting (a), CTMP1-NoBET-HP (b), CTMP1-BET-NoHP (c), CTMP1-BET-HP (d), and betulin (e).

2.4.3 SEM images

SEM analyses were conducted to reveal the morphology of the samples. The SEM images of the starting initial betulin powder and the aqueous betulin suspension (freeze-dried) revealed a similar morphology with a prismatic crystal structure (Figure 2.4.4).

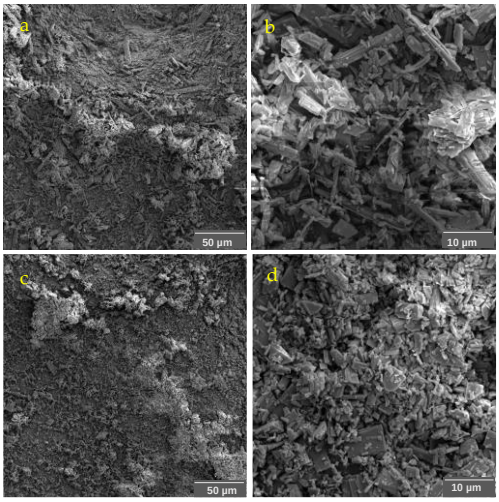

Figure 2.4.4. SEM of the starting betulin powder (a,b) and the freeze-dried betulin aqueous suspension (c,d).

The SEM image of CTMP1-starting shows a network of intertwined cellulose fibers (Figure 2.4.5a). Comparison of CTMP1-starting (a-c) with CTMP1-NoBET-HP (d-f) indicates that hot pressing alters the surface morphology, resulting in a more compact and dense structure. After spraying with the aqueous betulin suspension, the fibers are covered with betulin particles resulting in CTMP1-BET-NoHP sample (g-i). The betulin particles has the prismatic shape of the reported betulin hydrate (betulin III).[142,143] The SEM images of CTMP1-BET-HP (j,k,l) reveal the polymorphic transformation of betulin from prismatic crystals (betulin III) to long whiskers (betulin I).[142] Betulin I whiskers are also observed in the SEM images of the CTMP2-BET-HP, CTMP3-BET-HP, and filter paper-BET-HP samples (m, n, and o, respectively). The SEM of corresponding samples of CTMP2, CTMP3, and filter paper also revealed that treating with betulin and hot pressing cause the same structural morphology changes, and as shown for CTMP1 to finally form long betulin whiskers intertwined with the cellulosic fibers (m-o). All the SEM images related to CTMP2, CTMP3 and filter paper are shown in Appendix 9.

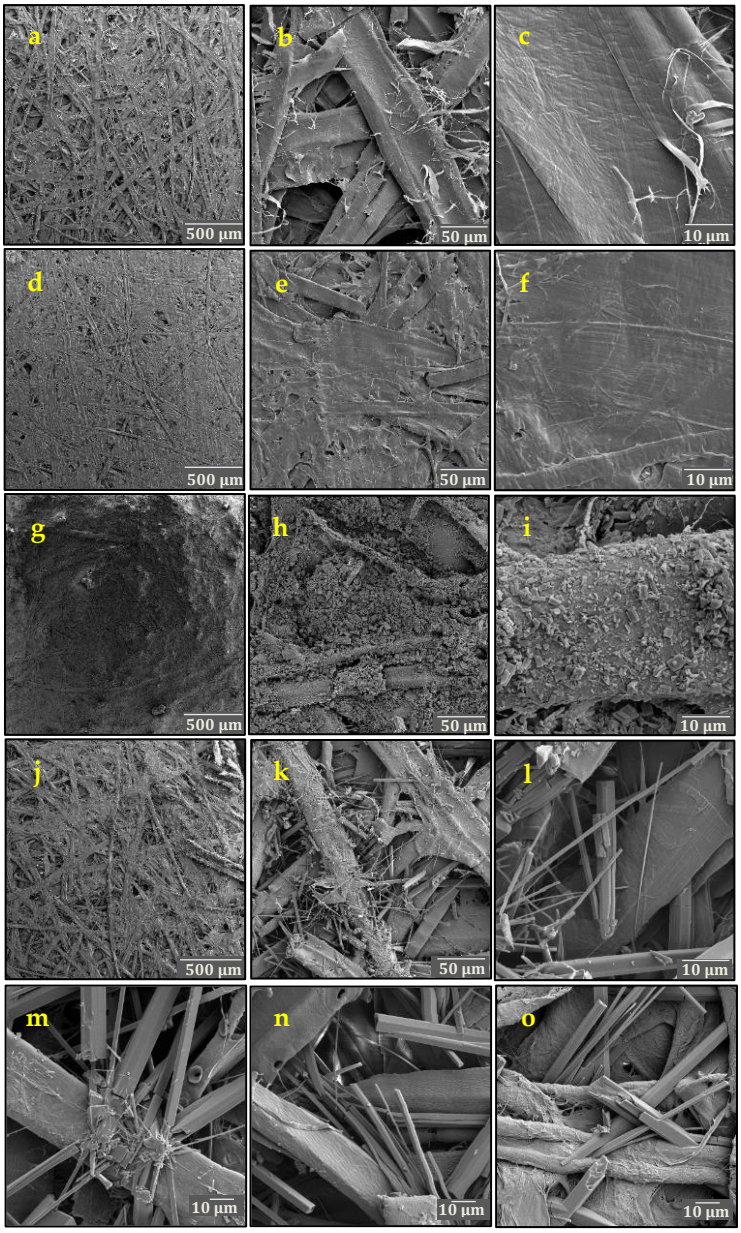

Figure 2.4.5. SEM images of CTMP1-starting (a, b, c), CTMP1-NoBET-HP (d, e, f), CTMP1-BET-NoHP (g, h, i), CTMP1-BET-HP (j, k, l), CTMP2-BET-HP (m), CTMP3-BET-HP (n), and filter paper-BET-HP (o).

The cross-sectional SEM image of CTMP1-starting (Figure 2.4.6a,b) exhibits a loosely packed structure with some inter fiber pores and

open fiber lumens. CTMP1-BET-NoHP shows that the betulin particles are mainly located close to the surface of the sheet (c,d). CTMP1-BET-NoHP also exhibits a looser structure with larger pores compared to CTMP1-starting, having a thicker cross section. After hot pressing, the fiber pores mostly disappeared, the thickness decreases and a densely packed structure is formed (g,h).

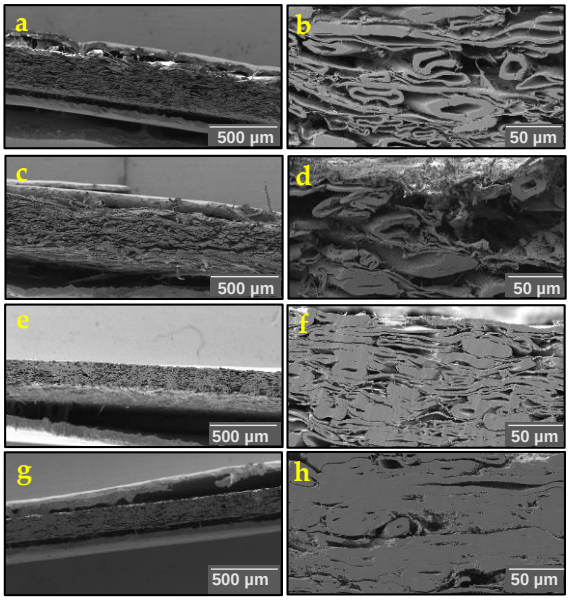

Figure 2.4.6. The cross-sectional SEM images of CTMP1-starting (a, b), CTMP1-BET-NoHP (c, d), CTMP1-NoBET-HP (e, f), and CTMP1-BET-HP (g, h).

2.4.4 XRD spectra

As mentioned earlier, the SEM images of the starting betulin powder and freeze-dried betulin aqueous suspension revealed a similar morphology with a prismatic crystal structure (Figure 2.4.4). The XRD spectra of the starting betulin powder and betulin aqueous suspension (freeze-dried and oven dried) also exhibited similar patterns showing the same polymorph with a prismatic crystal structure.

Betulin can undergo polymorphic transformation and form different types of crystal structures.[142,143] It can form prismatic crystals of betulin

hydrate (betulin III) and long whiskers (betulin I). These types of crystal structures were indeed observed in the SEM images of the betulin treated samples (Figure 2.4.5).

Figure 2.4.7 displays the XRD patterns of the starting betulin powder, CTMP1-starting, CTMP1-BET-NoHP, and CTMP1-BET-HP samples. The starting betulin powder spectrum shows distinct peaks corresponding to the prismatic crystals of betulin hydrate (betulin III).[142] Comparing the spectra of CTMP1-BET-NoHP with CTMP1-starting reveals the presence of more peaks in CTMP1-BET-NoHP (at 6.26°, 7.77°, 9.39°, 12.27°, 12.71°, 14.09°, 14.61°, 15.00°, 15.36°, 16.82°, 18.94°, 19.59°, 20.36°, 24.39°) which correspond to the presence of the prismatic betulin III structure. The CTMP1-BET-HP spectrum reveals that a polymorphic transformation has occurred, forming betulin orthorhombic whiskers (betulin I) [142] with new peaks appearing at 10.83°, 11.88°, 12.31°, 12.97°, 13.48°, 15.24°, 15.56°, 15.44°, 16.84°, 18.07°, 18.96°, 19.91°, 24.87°. Therefore, the staring betulin prismatic crystals were converted to the betulin whiskers at 250 °C. These changes are also in accordance with what the SEM images of these samples revealed (Figure 2.4.5).

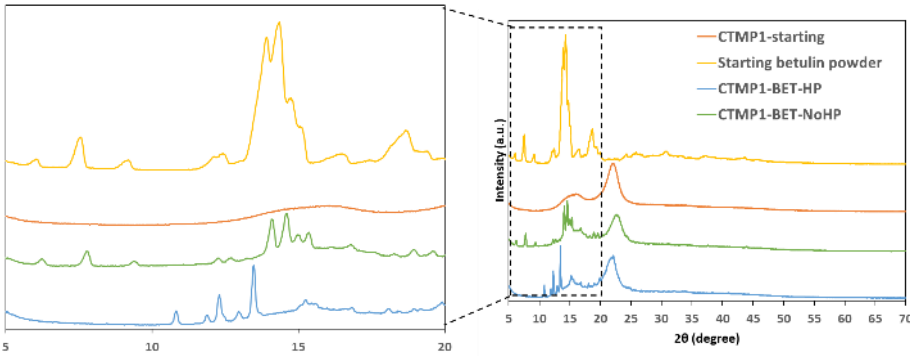

Figure 2.4.7. XRD spectra of the starting betulin powder, CTMP1-starting, CTMP1-BET-NoHP and CTMP1-BET-HP.

2.4.5 WCAs

The WCAs of different samples after 5 min are reported in Table 2.4.1. It was noticed that the betulin treatment/hot-pressing approach was synergistically effective and increase the WCAs of the BET-HP samples reaching 132° (Entries 1-4). The WCAs for the starting samples were 0° (Entries 5-8), and the applied water drops for the measurements started to adsorb immediately into the surface of the samples. The WCAs of the hot-pressed samples without betulin treatment were 0° (Entries 9-12). It was also observed that only the spraying of the betulin suspension onto the filter paper sample without hot pressing (Entry 13) or with hot pressing at a low temperature (97 °C, Entry 14) were not effective, and the WCAs were 0°. Therefore, there is a synergistic effect for achieving a hydrophobic surface via betulin treatment combined with hot pressing, where the polymorphic transformation of betulin from prismatic crystals to long whiskers has occurred.

Table 2.4.1. The WCA measurements for different prepared samples.

Entry	Cellulosic material	WCAs (θ)[a]
1[b]	Filter paper-BET-HP	121°±2
2[b]	CTMP3-BET-HP	132°±1
3[b]	CTMP2-BET-HP	121 °±2
4[b]	CTMP1-BET-HP	130 °±1
5	Filter paper-starting	0°
6	CTMP3- starting	0°
7	CTMP2- starting	0°
8	CTMP1- starting	0°
9[b]	Filter paper- NoBET-HP	0°
10[b]	CTMP3- NoBET-HP	0°
11[b]	CTMP2- NoBET-HP	0°
12[b]	CTMP1- NoBET-HP	0°
13	Filter paper-BET-NoHP	0°
14[c]	Filter paper-BET-HP	0°

[a] The WCAs were measured after 5 min. [b] BET-HP, and NoBET-HP samples are hot-pressed at 250 °C, 3 bars for 1 min. [c] Hot pressed for 20 min at 1 bar and 97 °C.

2.4.6 Tensile indices

Dry tensile indices

The dry tensile indices of the samples are shown in Figure 2.4.8a. The dry tensile index of CTMP1-starting (blue bar) is higher than that of CTMP2-starting. This is due to the higher degree of sulfonation (higher amount of S) in CTMP1.[99,144] The dry tensile indices of CTMP-starting samples decreased after treatment with betulin (BET-NoHP samples, orange bars). This is in accordance with previous observation that the addition of betulin can decrease the strength of cellulosic materials by 10-20%.[145] This was attributed to the presence of additives that can interfere with the structure and network of cellulosic materials creating discontinuities in the structure of cellulosic materials, which results in lower strengths.[90,146] Hot pressing noticeably increases the dry tensile indices of the starting samples (blue vs grey bars).[105] Moreover, the highest improvement in the dry tensile indices was noticed when hot pressing was performed on the cellulosic samples treated with betulin (orange vs yellow bars). In the case of filter paper, adding betulin increased the dry tensile index of the pure cellulose paper up to 30% (blue bar vs orange bar), and the hot pressing of Filter paper-BET-NoHP showed only a slight improvement (orange bar vs yellow bar). Overall, by comparing the tensile indices of the starting samples (blue bars) with the corresponding BET-HP samples (yellow bars), obvious improvements in dry tensile indices were observed for all samples throughout the betulin treatment/hot-pressing process.

Wet tensile indices

The wet tensile indices of the samples are displayed in Figure 2.4.8b. All the starting samples (blue bars) had very low wet strengths, with filter paper showing the lowest wet tensile strength. Spraying the aqueous betulin suspension onto the different starting samples further

reduced their wet tensile indices (blue vs orange bars). It is worth noting that the hot pressing of the samples significantly increased the wet tensile indices. For instance, hot pressing of CTMP1-starting enhanced the wet strength to ~21 kNm/Kg (blue bar vs gray bar). This can be explained by that upon hot pressing at temperatures above lignin Tg, lignin softens allowing for a plastic like flow. The network is densified, and the softened lignin facilitates robust inter-fiber bonding, effectively adhering fibers together. In other words, lignin serves as a natural wet-strength additive.[103,105,107] Furthermore, the wet tensile index of the CTMP1-NoBET-HP sample was slightly higher than that of CTMP2-NoBET-HP (~10%), that can be attributed to the greater amount of sulfur present in CTMP1-NoBET-HP (*i.e.*, higher sulfonation during pulping). Higher sulfonation reduces lignin Tg, and that can make the hot-pressing process more efficient resulting in enhancement of the sample strength.[104,105]

All the starting samples treated with the aqueous betulin suspension experienced a decline in wet strengths (blue vs orange bars). However, a significant synergistic enhancement in the wet tensile indices of the CTMP samples was observed when hot pressing was combined with the betulin treatment and chemical modification (sulfonation during pulping). In other words, hot pressing of the betulin treated samples was more effective than the hot pressing of the starting samples. By the synergistic betulin/hot-pressing treatment, for example, the wet tensile index of CTMP3-starting increased from 2.0 to 26.9 kNm/Kg in CTMP3-BET-HP (yellow bar), while just hot pressing of CTMP3-starting alone resulted in an increase to 15.8 kNm/kg in CTMP3-HP (gray bar). A similar trend was also noticed for the other samples. Therefore, it was the hot-pressing of samples synergistically acting with the polymorphic transformation of the betulin crystals during hot

pressing, that contributed to the additional increase in the wet tensile indices.

According to the observations from the SEM and XRD analyses, the following mechanism can be suggested for the betulin/hot-pressing treatment process. During hot pressing, the fibers undergo densification, and simultaneously, betulin undergoes a polymorphic transformation into long whiskers. These whiskers interconnect through the cellulose fiber network, serving as reinforcement/armature within the newly formed structure. In the case of lignocellulosic fibers (CTMP), a further synergistic effect happens upon hot pressing when chemical modification (sulfonation) reduces the Tg of lignin, facilitating strong inter-fiber bonding and gluing of the fibers together, coupled with the polymorphic transformation of betulin into long whiskers. In other words, chemical modification has also a synergistic effect, when the higher degree of sulfonation, combined with the betulin treatment as well as the hot pressing (*i.e.*, CTMP1-BET-HP) results in the highest wet strength.

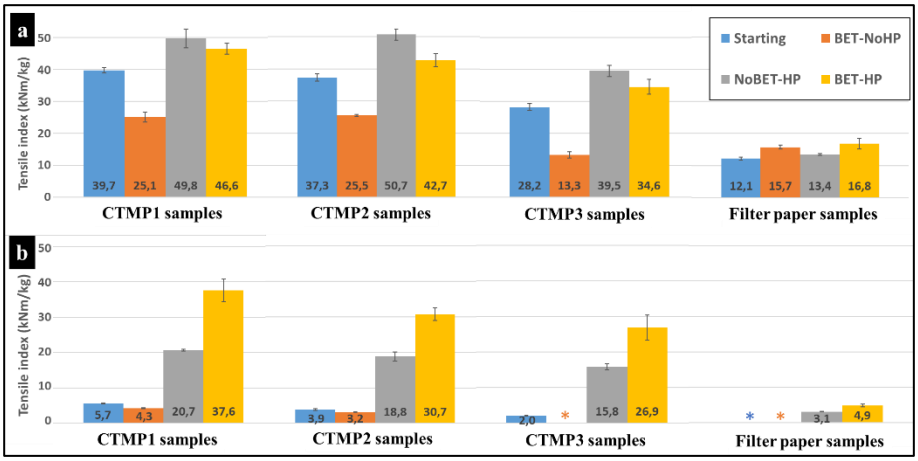

Figure 2.4.8. (a) Dry tensile indices and, (b) wet tensile indices of the different fabricated samples (∗: tensile strength<0.01 kN/m).

2.5 Fabrication of strong materials from aspen veneer in a sustainable, continuous, scalable, and high yield approach (Paper V)

Strong, lightweight materials are highly desirable for advanced applications in various fields. Due to the advantages of wood—such as affordability, biocompatibility, and sustainability—strengthened wood materials have garnered significant interest. A convenient approach to improves the mechanical properties of wood is hot pressing. A concern in this area is wood pretreatment before hot pressing. Pretreatments can facilitate and increase the efficiency of hot pressing, resulting in addressing hot pressing challenges and increasing mechanical strength. For example, partially removal of lignin and hemicelluloses before hot pressing can increase the mechanical strength of hot-pressed wood samples.[103,106] Wood softening or decreasing the Tg (*e.g.*, by lignin sulfonation) can also increase hot-pressing efficiency.[99] Pretreatments can hinder the process for mass production, especially when harsh and intense conditions are employed (*e.g.*, treatment with boiling solutions under high pressures, using special instruments such as autoclaves).[100,103] These obstacles become even more challenging when trying to hot press large samples.

Another concern in the context of hot pressing is employing batch-type static hot pressing, which is energy and time-consuming with having limitations for sample sizes. Continuous hot pressing can provide a way to address these challenges and improve the cost-effectiveness and environmental impact of the densification process, making mass production more feasible.[108–111]

This work demonstrates continuous large-scale production of lightweight, strong, renewable, scalable and high-yield materials from aspen, a fast-growing and readily available wood. The approach involves synergistic combination of mild chemical modifications (using of readily available chemicals from the pulp and paper industry), with the industrially relevant continuous steel belt hot press technique. The approach was high yield and resulted in up to 530% increase in tensile strengths, reaching values exceeding specific strengths of materials such as PET, brass, stainless steel, magnesium alloy and aluminum alloy. These high strengths are attributed to factors such as wood softening, increased bonding, fiber alignment, and cross-linking of the lignin upon heating. Moreover, the applied chemical modification/continuous hot-pressing approach does not require complex or harsh procedure. This can reduce time/energy consumption and enables processing of larger samples with lower production costs and environmental impacts.

2.5.1 Initial study (static hot pressing)

To evaluate the effects of chemical modification and hot pressing, we started our studies using aspen veneer as the wood substrate and static hot pressing. Figure 2.5.1 depicts the steps for fabrication of different veneers using static hot pressing and their nomenclatures. First, the veneer samples with the size of 6 × 20 cm^2 were soaked under vacuum in either water, Na_2SO_3 (1M), or NaOH (0.5 M) solutions and then heat-treated in a reactor. Next, the samples were dried in an oven and, hot-pressed using static hot press machinery. The veneer that was only hot pressed without any chemical modification is named NoTr.-HPst. The veneers treated with Na_2SO_3 and NaOH were labeled Sulfite-HPst. and Alkali-HPst., respectively.

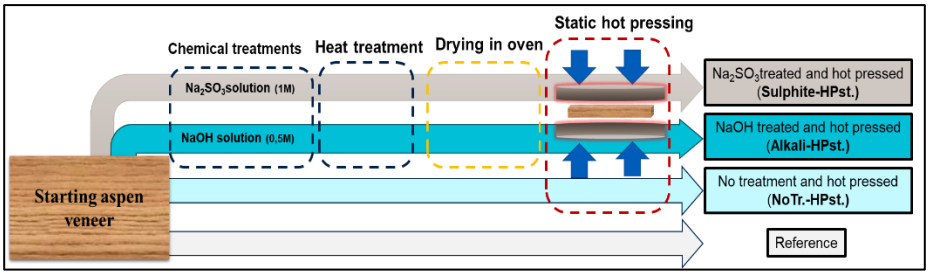

Figure 2.5.1. Illustration of the preparation steps for static hot pressing and products nomenclatures (initial study).

It was noticed that all hot-pressed veneers had higher tensile strengths than reference veneer (49 MPa, entry 4, Table 2.5.1). It was also observed that chemical modification was effective and improved strength of the hot-pressed veneers. Among these, Alkali-HPst showed the highest breaking strength of 331 MPa (entry 2). The Sulfite-HPst also demonstrated a high tensile strength of 325 MPa (entry 3). During the chemical modification steps, the wood composition changes. For instance, treatment with Na_2SO_3 results in the sulfonation of lignin and an increased anionic charges, while alkali treatment deacetylates,

introduces carboxylates and alters the structure of lignin and hemicelluloses. Both treatments ultimately lead to wood softening.

Table 2.5.1. The tensile strengths of static hot pressed aspen veneers.

Entry [a]	Veneers	Pressure [b] (bar)	Density [c] (kg/m^3)	Tensile strength (MPa)
1	NoTr.-HPst.	181	1183	254
2	Alkali-HPst.	111	1393	331
3	Sulfite-HPst	184	1346	325
4	Reference veneer	-	385	49

[a)] Temperature for hot pressing was 190±5 °C; Moisture content before hot pressing: 5%; puls time: 60s. For experimental details see (Appendix 10). [b)] Applied pressure in hot pressing. [c)] Density of the sample after hot pressing.

2.5.2 Fabrication of strong veneers by combination of chemical modification and continuous hot pressing

Building upon the results from the static hot-pressing (initial study), that showed the positive effect of hot pressing and its combination with chemical modifications, we aimed to perform hot pressing of the veneers via continuous steel belt pressing. This can offer faster process and feasibility for larger veneers. Figure 2.5.2 demonstrates the steps involved in the fabrication of the different aspen veneer materials using continuous steel belt hot pressing and their nomenclatures in this work. First, the starting aspen veneers were modified by immersing in the desired solution (water, Na_2SO_3 and NaOH) for 24 h. The veneers were then placed in an oven (50 °C) to decrease their moisture content to around 20 wt.% (based on the dry masses of the corresponding starting veneers) since the samples with high moisture content (>30 wt.%) were prone to burst upon applied hot pressing condition. Finally, the veneers underwent hot-pressing using continuous steel belt hot pressing. For example, the veneer which was

not chemically modified but hot pressed was named NoTr.-HP, and the alkali-treated and hot-pressed one was labeled Alkali-HP.

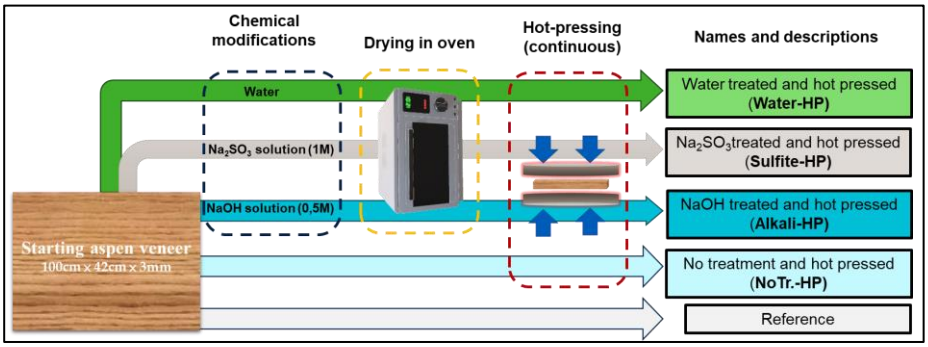

Figure 2.5.2. Schematic illustration of the different steps for preparation of the different veneer materials.

After the impregnation step, some veneers were dried in an oven (at 110 °C for 24 h), and the weight measurements revealed weight losses of 2.3 wt.% and 0.4 wt.% in case of veneers treated with alkali solution and plain water, respectively. The veneer treated in sulfite solution showed around 7.1 wt.%. weight gain.

As mentioned earlier, our aim was to densify and increase the tensile strengths of large veneer samples in more industrially benign approach using combination of facile simple chemical modification and continuous hot-pressing technique. Therefore, we employed a unique continuous steel belt hot-press machine from IPCO, Germany. As demonstrated in Figure 2.5.3, the machinery comprises of different parts and zones. The rotating drums and carrying belts transport the sample and can be preheated. Zones 1-3 can heat up and press the sample, while zone 4 is for cooling down the hot-pressed samples. The total line speed, as well as the temperature and applied pressure in each zone can be programmed and adjusted. Unless it is mentioned, the following set up was applied for the hot pressing of the samples: Line speed of 0.5 $m.min^{-1}$; drum Temp.: 80 °C; applied pressure (bar)

in different zones (Z1=20, Z2=245, Z3=230, Z4=none); applied Temp. (°C) in different zones (Z1=220, Z2=240, Z3=80, Z4=none).

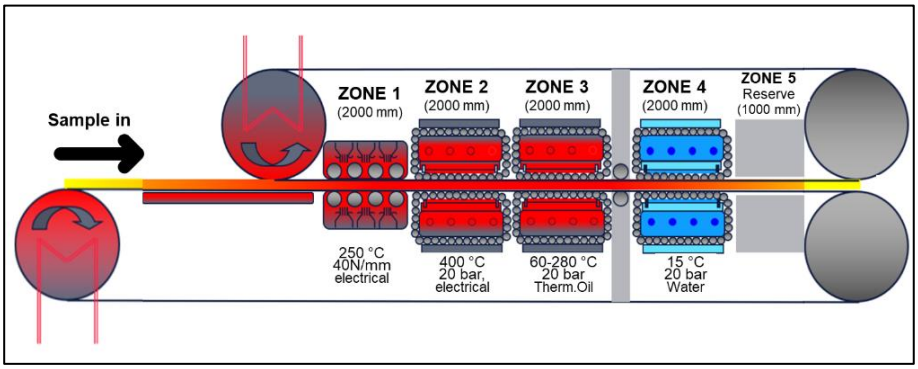

Figure 2.5.3. Modular continuous steel belt hot-press machinery at IPCO (more pictures at Appendix 11).

The hot-pressed veneers had a different appearance compared to the reference veneer, and they become thinner, smoother, and darker after hot pressing. Figure 2.5.4 displays the veneers, wherein the Alkali-HP has a notably darkened hue. The color change can be explained by the formation of new chromophore substances upon the process.[147,148]

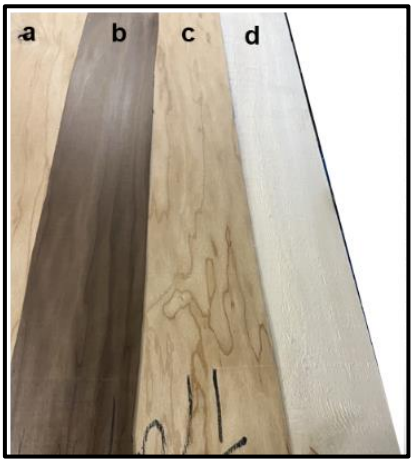

Figure 2.5.4. Photographs of the (a) NoTr-HP, (b) Alkali-HP, (c) Sulfite-HP, and (d) reference.

2.5.3 FT-IR spectra

The FT-IR spectra of the reference and hot-pressed veneers are displayed in Figure 2.5.5. The wide absorption peaks observed in all the spectra around 3338 cm^{-1} and the peaks around 2894 cm^{-1} correspond to the hydroxyl group and aliphatic C-H stretching vibrations, respectively. The peak around 1731 cm^{-1} is related to C=O stretching (ester bonds in hemicellulose). Peaks at 1502 and 1591 cm^{-1} correspond to aromatic ring vibrations in lignin (C=C) and carboxylate (CO_2^-) groups. The stretching vibrations of ether bonds (C-O-C) in lignin and hemicellulose appear at 1234 cm^{-1}. The peaks around 1159, 1103, and 1030 cm^{-1} correspond to the stretching vibrations of C–C, C–O, and C-O-C (pyranose), respectively.[125,147–149]

The FT-IR spectra of NoTr.-HP (Spectrum b) and Water-HP (Spectrum c) were similar to that of reference (Spectrum a). The spectrum of Sulfite-HP (Spectrum d) shows the S=O stretching vibration of sulfonic groups at 1205 cm^{-1}, indicating sulfonation of the veneer.[150] In the Alkali treated veneer (Spectrum e), the peak around 1731 cm^{-1} (ester bonds) has disappeared and the peak around 1234 cm^{-1} (C-O-C) is weakened. In addition, the peak at 1591 cm^{-1} has increased due to the formation of carboxylate (CO_2^-).

These changes reveal that upon chemical modifications wood's composition changes (*e.g.*, depolymerization of lignin, breakage of ester bonds, deacetylation and degradation of hemicellulose).[14,147,151,152] These changes disturb the wood's structure, weaken lignin carbohydrate complexes (LCCs) resulting in wood softening and increasing hot pressing efficiency. Furthermore, upon elevated temperatures, lignin undergoes softening through glass transition overlapped with depolymerization, and is followed by the solidification of the softened material by cross-linking reactions.[153] The

FT-IR spectra also showed that more charges were introduced for the chemically modified veneers promoting ion-bonding between the fibers.

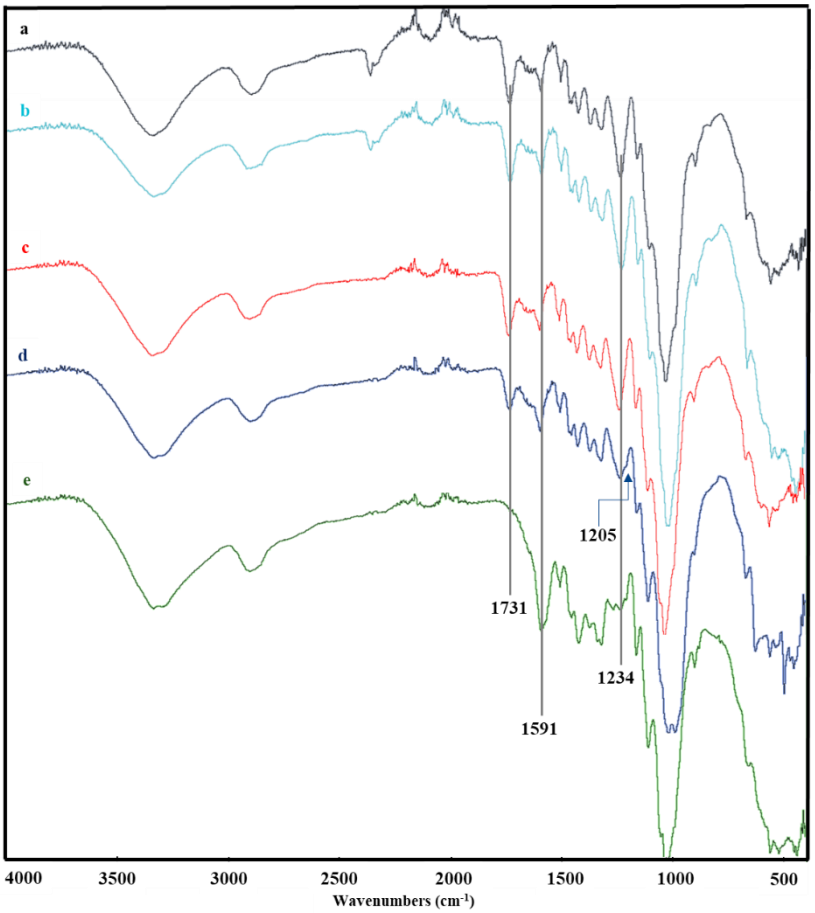

Figure 2.5.5. FT-IR spectra of the (a) reference, (b) NoTr.-HP, (c) Water-HP, (d) Sulfite-HP, and (e) Alkali-HP.

2.5.4 SEM images

Figure 2.5.6 exhibits the surface morphology of the reference and hot-pressed veneers at different magnifications. The SEM images reveal

that reference (a, b) has a coarse and uneven surface. Hot pressing aligns the fibers, compacts and flattens surfaces resulting in a denser structure with more uniform and smoother surfaces. Among the hot-pressed veneers, the Alkali-HP displays the smoothest and most uniform surface (g, h). Compared to the Alkali-HP, the Sulfite-HP (e, f) has a less uniform surface with some separation and gaps between fibers; however, its surface is more compact than that of the Water-HP (c, d).

The cross-sectional SEM images of the veneers are displayed in Figure 2.5.7. The image of reference (a, b) displays the wood's structure, which mainly consists of large open pores (vessels) and fibers with open lumens and ray cells. In the Water-HP (c, d), the structure started to alter, and pores are partially closed. Further structural collapse and pore closure are observed in the Sulfite-HP (e, f). Remarkably, in the Alkali-HP (g, h), the pores and lumens have mostly disappeared, and the wood structure has collapsed, resulting in a densely packed structure. This demonstrates that the modifications (especially the alkali treatment) play a significant role in enhancing the efficiency of hot pressing. Consequently, tighter structures and denser samples are obtained. Additionally, the increased contact area between cell walls leads to more interactions and bondings that ultimately can result in higher tensile strengths.

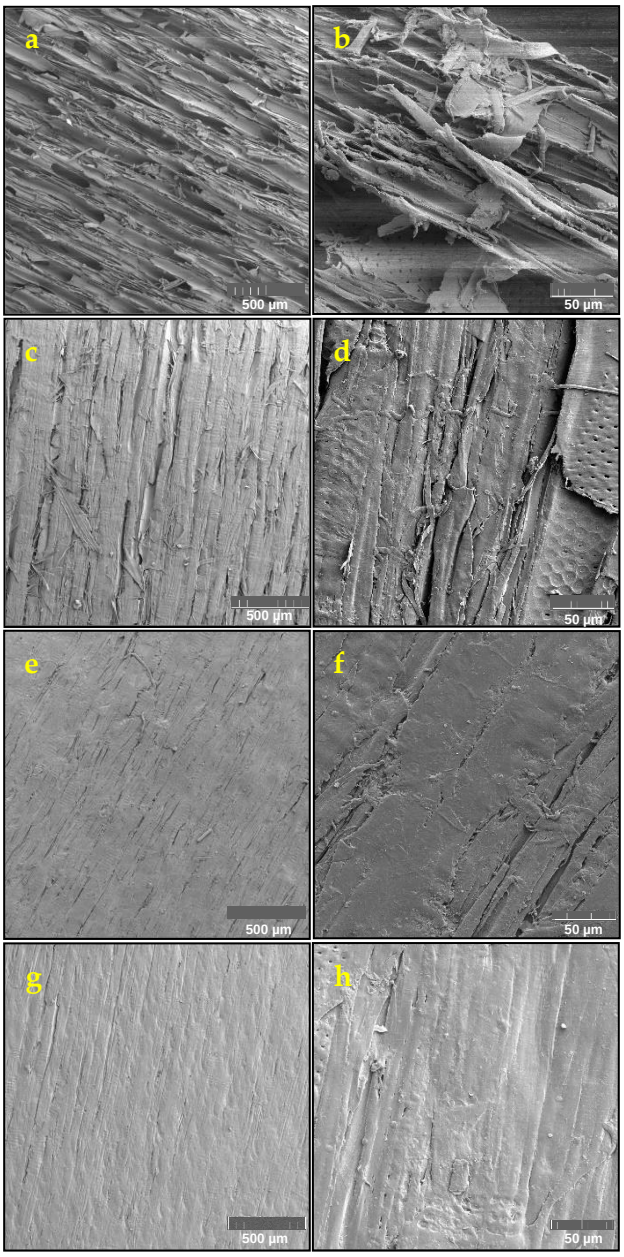

Figure 2.5.6. The SEM images of the reference and hot-pressed veneers in different magnifications: reference (a, b), Water-HP (c, d), Sulfite-HP (e, f), and Alkali-HP (g, h).

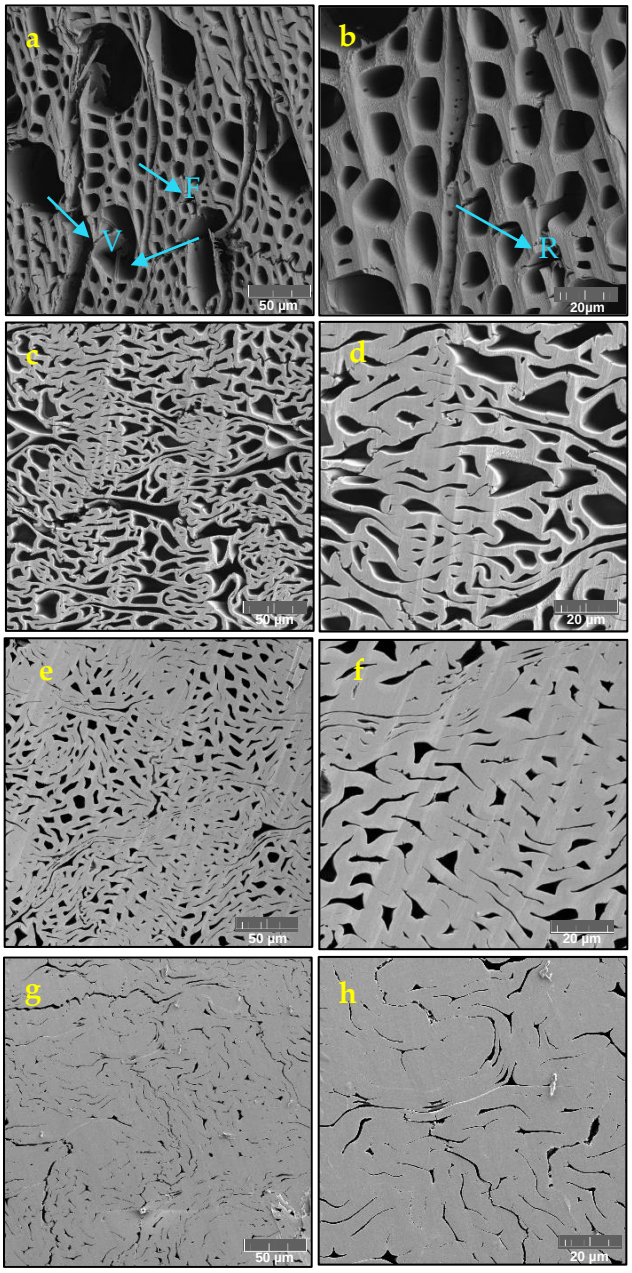

Figure 2.5.7. The cross-sectional SEM images of the reference and hot-pressed veneers at different magnifications: reference (a, b) (V: vessels; F: fibers; R: ray cells), Water-HP (c, d), Sulfite-HP (e, f), and Alkali-HP (g, h).

2.5.5 Tensile strengths

Table 2.5.2 shows the tensile strengths of the reference and hot-pressed veneers by continuous steel belt hot pressing. It was observed that all the hot-pressed veneers had higher tensile strengths than that of reference veneer (49 MPa, Entry 7). This indicated that regardless of chemical modifications only hot pressing itself strengthens the veneer. Comparing Entries 1 and 2 shows that breaking strengths increase with decreasing line speed (*i.e.,* prolonged hot-pressing time). By increasing the maximum applied pressure in the system to 245 bar and slightly decreasing the line speed, the densification process becomes more effective and increases the tensile strength (from 80 to 113 MPa, Entries 2 and 3). Increasing the moisture content of the veneer before hot-pressing from around 7 to 20 wt.% led to a slight increase in the tensile strength (comparing Entries 3 and 4). This can be due to the decrease in the Tg of wood polymers in higher moisture contents.[98] The tensile strength of the Sulfite-HP increased to 151 MPa (Entry 5). The sulfite treatment lowers lignin Tg (wood softening), thereby enhances the efficiency of hot pressing and sample's strength.[99,100] A lower Tg is generally beneficial in hot pressing since the softening of the polymers can occur at lower temperatures allowing them to flow and reshape more easily. This facilitates hot pressing of wood samples since it lowers required force and energy for hot pressing, and less breaks in the wood's cell walls occur during the process. Remarkably, the tensile strength of the Alkali-HP is elevated to 258 MPa (Entry 6), showing the highest tensile strength. FT-IR revealed that the alkali treatment alters wood's chemical structure (*e.g.*, disturbing the ester bonds, hemicellulose degradation, carboxylate formation), resulting in wood softening which is beneficial for hot pressing.[14,148,151] As a consequent, for both the sulfonated and alkali-hydrolyzed wood fibers and polymer matrix become more flexible and can easily move, rearrange,

and find the most stable arrangement during the hot-pressing process (less breakage, stress, and tension in the structure). Moreover, the sulfite and alkali modified lignocellulosic fibers have higher charges, and the alignment during hot-pressing promote the ion-bindings. Furthermore, the increased availability of hydroxyl groups (*e.g.*, due to breakage of ester bonds) facilitates the formation new and additional inter- and intramolecular hydrogen bonds upon hot pressing, thus strengthening the structure.[103,154] Hot pressing also collapses the porous structure of wood and increases the contact area between cell walls (Figure 2.5.7), resulting in enhanced interactions and higher tensile strengths.

Table 2.5.2. The tensile strengths of the hot-pressed and reference veneers.

Entry[a]	Veneers	MC (%)[b]	Line speed ($m.min^{-1}$)	Density[c] (kg/m^3)	Tensile strength (MPa)[d]
1[e]	NoTr.-HP	7	0.8	560	77 (14)
2[e]	NoTr.-HP	7	0.6	612	80 (12)
3	NoTr.-HP	7	0.5	858	113 (18)
4	Water-HP	20	0.5	938	117 (21)
5	Sulfite-HP	20	0.5	1001	151 (24)
6	Alkali-HP	20	0.5	1274	258 (34)
7	Reference	7	-	385	49 (4)

[a] Hot-pressing set-up: applied pressure (bar) in hot-pressing process in different zones (Z1=20, Z2=245, Z3=230, Z4=none); applied Temp. (°C) in hot-pressing process in different zones (Z1=220, Z2=240, Z3=80, Z4=none); belts preheating Temp.: none; Temp. of drums: 80 °C.

[b] Moisture content of the sample before hot pressing (based on the dry mass of the starting sample).

[c] Density of the sample after hot pressing.

[d] Tensile measurements were performed via MTS (Flex Test SE) instrument at 23 °C, 50% RH. An average of at least 10 tests is reported (standard deviations in parentheses).

[e] Hot-pressing set-up: applied pressure (bar) in hot pressing process in different zones (Z1=125, Z2=125, Z3=125, Z4=40); Temp. (°C) in hot-pressing process in different zones (Z1=200, Z2=230, Z3=180, Z4=20); drums and belts preheating Temp.: 120 °C.

3 Conclusion

According to the UN Sustainable Development Goals, it is crucial to adopt measures that enhance the use of sustainable and eco-friendly materials such as cellulosic materials. This thesis focused on addressing the drawbacks and limitations of unmodified cellulosic materials by applying sustainable chemistry principles, promoting sustainability, and minimizing the use of toxic reagents and harsh conditions. As a result, the potential applications of cellulosic materials could expand.

Heterogeneous catalysts are beneficial from both an environmental and industrial point of views, as they can be easily recycled and reused. In the first part, different efficient heterogeneous and recyclable catalysts were prepared. For example, after a successful silylation and functionalization of nano- and microcrystalline celluloses using a naturall nontoxic organocatalyst, copper and palladium nanoparticles immobilized onto cellulosic substrates, providing a sustainable alternative to traditional homogeneous catalyst supports.

Thiol functionalization of cellulosic materials opens new windows for further functionalization and applications. Thiol functionalized CNCs were produced via the direct esterification method using mild conditions and L-tartaric acid as a catalyst. The method worked on both solid and suspension forms of CNC materials producing versatile materials that could be used in different applications.

Lactic acid functionalized CNFs (LA-CNFs) can be fabricated in high yields using a one-step reaction process and without using metal or harsh acid catalysts. Lactic acid acted as both reaction media and catalyst, and it could be recycled and reused. The prepared CNFs,

along with their application in nanocomposites, highlight the significance of this approach for scalability and sustainability.

Wettability and strength of the cellulosic materials were improved via a simple and environmentally friendly method, where betulin treatment was combined with hot pressing. The study revealed a significant improvement in both mechanical and hydrophobic properties, particularly through a synergistic effect between hot pressing, aqueous betulin treatment (polymorphic transformations) and sulfonation during pulping.

The thesis also outlined that strong large veneers can be fabricated via combination of chemical modifications with continuous hot pressing. The chemical modifications softened the wood, facilitated the hot pressing, increased the charges, and promote bonding, resulting in a further improvement in tensile strengths of the hot pressed veneers. Additionally, employing continuous hot pressing together with facile chemical pretreatment (without using harsh or complex processes), improves the limitations of the similar methods such as limitations in sample size, and time/energy consumption.

Overall, the thesis demonstrates the sustainable and eco-friendly approaches for the functionalization and modification of cellulosic materials. It also lays a solid foundation for further advancements in the use of cellulosic materials in a wide range of applications, from catalysts to advanced high-performance materials.

4 Acknowledgements

I would like to begin by expressing my deep gratitude to my main supervisor, **Prof. Cordova,** for giving me the opportunity to perform my PhD study in the group. Your knowledge, support and guidance have been the greatest help throughout this journey. I am also very thankful to **Prof. Engstrand** and **Prof. Bäckvall**: your valuable suggestions and feedback have greatly contributed to the quality of this work. A special thanks to **Dr. Birgitta Engberg** for helps, affability and fostering a supportive environment.

I am grateful to **Prof. Ek, Prof. Norgen, Prof. Svedberg, Prof. Kers** and **Prof. Edlund** for reviewing the thesis and sharing their ideas.

I extend my appreciation to **Håkan Norberg** for the assistance in the lab that made the experimental phase of this work so much smoother.

I acknowledge **Prof**. **Kaarlo Niskanen, Prof. Dan Bylund, Prof. Håkan Edlund, Dr. Claes Mattsson, Staffan Nyström, Dr. Magnus Hummelgård, Dr. Christina Dahlström, Dr. Cherryleen Lindgren, Dr. Amanda Mattsson, Dr. Alireza Eivazi, Dr. Gunilla Pettersson, Dr. Thomas Granfeldt, Prof**. **Gaida Lo-Re, Dr. Angelica Avella, Dr. Madelen Olofsson, Annelie Ervasti, John Håkansson, Dr. Erika Wallin, Dr. Jennie Sandström,** and all people at **FCSN**, **O-huset**, and **Tork-huset**. **MIUN**, **FSCN**, **Neopulp (financed by the Knowledge Foundation)**, **European Union funding**, **SCA, Holmen**, **IPCO**, and **Billerud** for their supports and collaborations.

I wish to express my gratitude to my colleagues in the chemistry lab during these years—**Rana, Luca, Italo, Ismail, Lin,** and **Kaiheng**—thank you for your friendship, discussions, and collaborations.

I would like to gratitude **Prof. Mahkam** for introducing and encouraging me to the chemistry and material research.

Last but not least, my heartfelt thanks go to **my friends** (accept my excuse for not naming you!), **my parents**, **Hannaneh**, **Sobhan** and **Sabrina** for all the supports and favors. I love you and thanks for everything.

Thank you all again for making this journey rewarding and memorable.

5 References

1. Barham, L. *et al.* Evidence for the earliest structural use of wood at least 476,000 years ago. *Nature* **622**, 107–111 (2023).
2. Tsakona, M. *et al. Drowning in Plastics – Marine Litter and Plastic Waste Vital Graphics*. (United Nations Environment Programme, 2021).
3. Raabe, D., Tasan, C. C. & Olivetti, E. A. Strategies for improving the sustainability of structural metals. *Nature* **575**, 64–74 (2019).
4. Liu, Y.-J., Li, B., Feng, Y. & Cui, Q. Consolidated bio-saccharification: Leading lignocellulose bioconversion into the real world. *Biotechnol Adv* **40**, 107535 (2020).
5. Heinze, T., El Seoud, O. A. & Koschella, A. Production and Characteristics of Cellulose from Different Sources. in 1–38 (2018). doi:10.1007/978-3-319-73168-1_1.
6. Li, J., Chen, C., Zhu, J. Y., Ragauskas, A. J. & Hu, L. In Situ Wood Delignification toward Sustainable Applications. *Acc Mater Res* **2**, 606–620 (2021).
7. Brandt, A., Gräsvik, J., Hallett, J. P. & Welton, T. Deconstruction of lignocellulosic biomass with ionic liquids. *Green Chemistry* **15**, 550 (2013).
8. Chen, C. *et al.* Structure–property–function relationships of natural and engineered wood. *Nat Rev Mater* **5**, 642–666 (2020).
9. Henriksson, G., Brännvall, E. & Lennholm, H. 2. The Trees. in *Wood Chemistry and Wood Biotechnology* 13–44 (Walter de Gruyter, 2009). doi:10.1515/9783110213409.13.
10. Rao, J., Lv, Z., Chen, G. & Peng, F. Hemicellulose: Structure, chemical modification, and application. *Prog Polym Sci* **140**, 101675 (2023).

11. Teleman, A. 5. Hemicelluloses and Pectins. in *Wood Chemistry and Wood Biotechnology* 101–120 (Walter de Gruyter, 2009). doi:10.1515/9783110213409.101.

12. Mai, C., Schmitt, U. & Niemz, P. A brief overview on the development of wood research. *Holzforschung* **76**, 102–119 (2022).

13. Katahira, R., Elder, T. J. & Beckham, G. T. Chapter 1. A Brief Introduction to Lignin Structure. in 1–20 (2018). doi:10.1039/9781788010351-00001.

14. Jeffries, T. W. Biodegradation of lignin-carbohydrate complexes. *Biodegradation* **1**, 163–176 (1990).

15. Payen, A. Mémoire sur la composition du tissu propre des plantes et du ligneux (Memoir on the composition of the tissue of plants and of woody [material]). *C. R. Hebd. Seances Acad. Sci.* **7**, 1052–1056 (1838).

16. Heinze, T., El Seoud, O. A. & Koschella, A. Structure and Properties of Cellulose and Its Derivatives. in 39–172 (2018). doi:10.1007/978-3-319-73168-1_2.

17. Mboowa, D. A review of the traditional pulping methods and the recent improvements in the pulping processes. *Biomass Convers Biorefin* **14**, 1–12 (2024).

18. Li, P. *et al.* Development of Raw Materials and Technology for Pulping—A Brief Review. *Polymers (Basel)* **15**, 4465 (2023).

19. Battista, O. A. Hydrolysis and Crystallization of Cellulose. *Ind Eng Chem* **42**, 502–507 (1950).

20. Phanthong, P. *et al.* Nanocellulose: Extraction and application. *Carbon Resources Conversion* **1**, 32–43 (2018).

21. Parambath Kanoth, B., Claudino, M., Johansson, M., Berglund, L. A. & Zhou, Q. Biocomposites from Natural Rubber: Synergistic Effects of Functionalized Cellulose Nanocrystals as Both Reinforcing and Cross-Linking Agents via Free-Radical

Thiol–ene Chemistry. *ACS Appl Mater Interfaces* **7**, 16303–16310 (2015).

22. Qi, Y. *et al.* Nanocellulose: a review on preparation routes and applications in functional materials. *Cellulose* **30**, 4115–4147 (2023).

23. Nasir, M., Hashim, R., Sulaiman, O. & Asim, M. Nanocellulose. in *Cellulose-Reinforced Nanofibre Composites* 261–276 (Elsevier, 2017). doi:10.1016/B978-0-08-100957-4.00011-5.

24. Nickerson, R. F. & Habrle, J. A. Cellulose Intercrystalline Structure. *Ind Eng Chem* **39**, 1507–1512 (1947).

25. Rånby, B. G., Banderet, A. & Sillén, L. G. Aqueous Colloidal Solutions of Cellulose Micelles. *Acta Chem Scand* **3**, 649–650 (1949).

26. Herrick, F. W., Casebier, R. L., Hamilton, J. K. & Sandberg, K. R. Microfibrillated cellulose: morphology and accessibility. *J Appl Polym Sci Symp* **37**, 797–813 (1983).

27. Tubrak, A. F., Snyder, F. W. & Sandberg, K. R. MICROFIBRILLATED CELLULOSE, A NEW CELLULOSE PRODUCT: PROPERTIES, USES, AND COMMERCIAL POTENTIAL. *J Appl Polym Sci Symp* **37**, 815–827 (1983).

28. Abdul Khalil, H. P. S. *et al.* Production and modification of nanofibrillated cellulose using various mechanical processes: A review. *Carbohydr Polym* **99**, 649–665 (2014).

29. Isogai, A., Saito, T. & Fukuzumi, H. TEMPO-oxidized cellulose nanofibers. *Nanoscale* **3**, 71–85 (2011).

30. Saito, T., Nishiyama, Y., Putaux, J.-L., Vignon, M. & Isogai, A. Homogeneous Suspensions of Individualized Microfibrils from TEMPO-Catalyzed Oxidation of Native Cellulose. *Biomacromolecules* **7**, 1687–1691 (2006).

31. Yarbrough, John. M. *et al.* Multifunctional Cellulolytic Enzymes Outperform Processive Fungal Cellulases for

Coproduction of Nanocellulose and Biofuels. *ACS Nano* **11**, 3101–3109 (2017).

32. Roberts, M. W. Birth of the catalytic concept. *Catal Letters* **67**, 1–4 (2000).

33. Bell, E. L. *et al.* Biocatalysis. *Nature Reviews Methods Primers* **1**, 46 (2021).

34. List, B. Introduction: Organocatalysis. *Chem Rev* **107**, 5413–5415 (2007).

35. MacMillan, D. W. C. The advent and development of organocatalysis. *Nature* **455**, 304–308 (2008).

36. List, B. Proline-catalyzed asymmetric reactions. *Tetrahedron* **58**, 5573–5590 (2002).

37. Casas, J., Persson, P. V., Iversen, T. & Córdova, A. Direct Organocatalytic Ring-Opening Polymerizations of Lactones. *Adv Synth Catal* **346**, 1087–1089 (2004).

38. Hafrén, J. & Córdova, A. Direct Organocatalytic Polymerization from Cellulose Fibers. *Macromol Rapid Commun* **26**, 82–86 (2005).

39. Yorimitsu, H., Kotora, M. & Patil, N. T. Special Issue: Recent Advances in Transition-Metal Catalysis. *The Chemical Record* **21**, 3335–3337 (2021).

40. Dunn, P. J. The importance of Green Chemistry in Process Research and Development. *Chem. Soc. Rev.* **41**, 1452–1461 (2012).

41. Corma, A. & Garcia, H. Crossing the Borders Between Homogeneous and Heterogeneous Catalysis: Developing Recoverable and Reusable Catalytic Systems. *Top Catal* **48**, 8–31 (2008).

42. Rafi, A. A., Ibrahem, I. & Córdova, A. Copper nanoparticles on controlled pore glass (CPG) as highly efficient heterogeneous catalysts for "click reactions". *Sci Rep* **10**, 20547 (2020).

43. Arai, M. & Zhao, F. Metal Catalysts Recycling and Heterogeneous/Homogeneous Catalysis. *Catalysts* **5**, 868–870 (2015).

44. Deiana, L., Rafi, A. A., Tai, C., Bäckvall, J. & Córdova, A. Artificial Arthropod Exoskeletons/Fungi Cell Walls Integrating Metal and Biocatalysts for Heterogeneous Synergistic Catalysis of Asymmetric Cascade Transformations. *ChemCatChem* **15**, (2023).

45. Kaushik, M. *et al.* Cellulose Nanocrystals as Chiral Inducers: Enantioselective Catalysis and Transmission Electron Microscopy 3D Characterization. *J Am Chem Soc* **137**, 6124–6127 (2015).

46. Dong, Y., Wu, X., Chen, X. & Wei, Y. N-Methylimidazole functionalized carboxymethycellulose-supported Pd catalyst and its applications in Suzuki cross-coupling reaction. *Carbohydr Polym* **160**, 106–114 (2017).

47. Córdova, A. *et al.* A sustainable strategy for production and functionalization of nanocelluloses. *Pure and Applied Chemistry* **91**, 865–874 (2019).

48. Afewerki, S. *et al.* Sustainable Design for the Direct Fabrication and Highly Versatile Functionalization of Nanocelluloses. *Global Challenges* **1**, (2017).

49. Devaraj, N. K. & Finn, M. G. Introduction: Click Chemistry. *Chem Rev* **121**, 6697–6698 (2021).

50. Rostovtsev, V. V., Green, L. G., Fokin, V. V. & Sharpless, K. B. A Stepwise Huisgen Cycloaddition Process: Copper(I)-Catalyzed Regioselective "Ligation" of Azides and Terminal Alkynes. *Angewandte Chemie International Edition* **41**, 2596–2599 (2002).

51. Liang, L. & Astruc, D. The copper(I)-catalyzed alkyne-azide cycloaddition (CuAAC) "click" reaction and its applications. An overview. *Coord Chem Rev* **255**, 2933–2945 (2011).

52. Tornøe, C. W., Christensen, C. & Meldal, M. Peptidotriazoles on Solid Phase: [1,2,3]-Triazoles by Regiospecific Copper(I)-Catalyzed 1,3-Dipolar Cycloadditions of Terminal Alkynes to Azides. *J Org Chem* **67**, 3057–3064 (2002).

53. Lowe, A. B. Thiol-ene "click" reactions and recent applications in polymer and materials synthesis. *Polym. Chem.* **1**, 17–36 (2010).

54. Wågberg, L. *et al.* The Build-Up of Polyelectrolyte Multilayers of Microfibrillated Cellulose and Cationic Polyelectrolytes. *Langmuir* **24**, 784–795 (2008).

55. Rol, F., Belgacem, M. N., Gandini, A. & Bras, J. Recent advances in surface-modified cellulose nanofibrils. *Prog Polym Sci* **88**, 241–264 (2019).

56. Robles, E., Urruzola, I., Labidi, J. & Serrano, L. Surface-modified nano-cellulose as reinforcement in poly(lactic acid) to conform new composites. *Ind Crops Prod* **71**, 44–53 (2015).

57. Hokkanen, S. *et al.* Adsorption of Ni(II), Cu(II) and Cd(II) from aqueous solutions by amino modified nanostructured microfibrillated cellulose. *Cellulose* **21**, 1471–1487 (2014).

58. Alimohammadzadeh, R., Sanhueza, I. & Córdova, A. Design and fabrication of superhydrophobic cellulose nanocrystal films by combination of self-assembly and organocatalysis. *Sci Rep* **13**, 3157 (2023).

59. Alimohammadzadeh, R., Medina, L., Deiana, L., Berglund, L. A. & Córdova, A. Mild and Versatile Functionalization of Nacre-Mimetic Cellulose Nanofibrils/Clay Nanocomposites by Organocatalytic Surface Engineering. *ACS Omega* **5**, 19363–19370 (2020).

60. Wang, Y., Wang, X., Xie, Y. & Zhang, K. Functional nanomaterials through esterification of cellulose: a review of chemistry and application. *Cellulose* **25**, 3703–3731 (2018).

61. Córdova, A. & Hafrén, J. Direct organic acid-catalyzed polyester derivatization of lignocellulosic material. *Nord Pulp Paper Res J* **20**, 477–480 (2005).

62. Hafrén, J., Zou, W. & Córdova, A. Heterogeneous 'Organoclick' Derivatization of Polysaccharides. *Macromol Rapid Commun* **27**, 1362–1366 (2006).

63. Zhao, G., Hafrén, J., Deiana, L. & Córdova, A. Heterogeneous "Organoclick" Derivatization of Polysaccharides: Photochemical Thiol-ene Click Modification of Solid Cellulose. *Macromol Rapid Commun* **31**, 740–744 (2010).

64. Ávila Ramírez, J. A., Suriano, C. J., Cerrutti, P. & Foresti, M. L. Surface esterification of cellulose nanofibers by a simple organocatalytic methodology. *Carbohydr Polym* **114**, 416–423 (2014).

65. Ávila Ramírez, J. A., Fortunati, E., Kenny, J. M., Torre, L. & Foresti, M. L. Simple citric acid-catalyzed surface esterification of cellulose nanocrystals. *Carbohydr Polym* **157**, 1358–1364 (2017).

66. Espino-Pérez, E., Domenek, S., Belgacem, N., Sillard, C. & Bras, J. Green Process for Chemical Functionalization of Nanocellulose with Carboxylic Acids. *Biomacromolecules* **15**, 4551–4560 (2014).

67. Spinella, S. *et al.* Concurrent Cellulose Hydrolysis and Esterification to Prepare a Surface-Modified Cellulose Nanocrystal Decorated with Carboxylic Acid Moieties. *ACS Sustain Chem Eng* **4**, 1538–1550 (2016).

68. Spinella, S. *et al.* Polylactide/cellulose nanocrystal nanocomposites: Efficient routes for nanofiber modification and effects of nanofiber chemistry on PLA reinforcement. *Polymer (Guildf)* **65**, 9–17 (2015).

69. Li, D., Henschen, J. & Ek, M. Esterification and hydrolysis of cellulose using oxalic acid dihydrate in a solvent-free reaction suitable for preparation of surface-functionalised cellulose

nanocrystals with high yield. *Green Chemistry* **19**, 5564–5567 (2017).

70. Li, B. *et al.* Cellulose nanocrystals prepared via formic acid hydrolysis followed by TEMPO-mediated oxidation. *Carbohydr Polym* **133**, 605–612 (2015).

71. Braun, B. & Dorgan, J. R. Single-Step Method for the Isolation and Surface Functionalization of Cellulosic Nanowhiskers. *Biomacromolecules* **10**, 334–341 (2009).

72. Afewerki, S. *et al.* Sustainable Design for the Direct Fabrication and Highly Versatile Functionalization of Nanocelluloses. *Global Challenges* **1**, 1700045 (2017).

73. Rull-Barrull, J., d'Halluin, M., Le Grognec, E. & Felpin, F. Harnessing the Dual Properties of Thiol-Grafted Cellulose Paper for Click Reactions: A Powerful Reducing Agent and Adsorbent for Cu. *Angewandte Chemie International Edition* **55**, 13549–13552 (2016).

74. Maleki, L., Edlund, U. & Albertsson, A.-C. Thiolated Hemicellulose As a Versatile Platform for One-Pot Click-Type Hydrogel Synthesis. *Biomacromolecules* **16**, 667–674 (2015).

75. Guo, J. *et al.* Superhydrophobic and Slippery Lubricant-Infused Flexible Transparent Nanocellulose Films by Photoinduced Thiol–Ene Functionalization. *ACS Appl Mater Interfaces* **8**, 34115–34122 (2016).

76. Aalbers, G. J. W. *et al.* Post-modification of Cellulose Nanocrystal Aerogels with Thiol–Ene Click Chemistry. *Biomacromolecules* **20**, 2779–2785 (2019).

77. Navarro, J. R. G. *et al.* Surface-Initiated Controlled Radical Polymerization Approach to In Situ Cross-Link Cellulose Nanofibrils with Inorganic Nanoparticles. *Biomacromolecules* **21**, 1952–1961 (2020).

78. Navarro, J. R. G. & Edlund, U. Surface-Initiated Controlled Radical Polymerization Approach To Enhance Nanocomposite

Integration of Cellulose Nanofibrils. *Biomacromolecules* **18**, 1947–1955 (2017).

79. Georgouvelas, D., Abdelhamid, H. N., Li, J., Edlund, U. & Mathew, A. P. All-cellulose functional membranes for water treatment: Adsorption of metal ions and catalytic decolorization of dyes. *Carbohydr Polym* **264**, 118044 (2021).

80. Lehr, M., Miltner, M. & Friedl, A. Removal of wood extractives as pulp (pre-)treatment: a technological review. *SN Appl Sci* **3**, 886 (2021).

81. Björklund Jansson, M. & Nilvebrant, N.-O. 7. Wood Extractives. in *Wood Chemistry and Wood Biotechnology* 147–172 (Walter de Gruyter, 2009). doi:10.1515/9783110213409.147.

82. Kirker, G., Hassan, B., Mankowski, M. & Eller, F. Critical Review on the Use of Extractives of Naturally Durable Woods as Natural Wood Protectants. *Insects* **15**, 69 (2024).

83. Sablík, P., Giagli, K., Pařil, P., Baar, J. & Rademacher, P. Impact of extractive chemical compounds from durable wood species on fungal decay after impregnation of nondurable wood species. *European Journal of Wood and Wood Products* **74**, 231–236 (2016).

84. Demets, O. V., Takibayeva, A. T., Kassenov, R. Z. & Aliyeva, M. R. Methods of Betulin Extraction from Birch Bark. *Molecules* **27**, 3621 (2022).

85. Reunanen, M., Holmbom, B. & Edgren, T. Analysis of archaeological birch bark pitches. *Holzforschung* **47**, 175–177 (1993).

86. Krasutsky, P. A. Birch bark research and development. *Nat Prod Rep* **23**, 919 (2006).

87. Kwan, I., Huang, T., Ek, M., Seppänen, R. & Skagerlind, P. Bark from Nordic tree species – a sustainable source for amphiphilic polymers and surfactants. *Nord Pulp Paper Res J* **37**, 566–575 (2022).

88. Huang, T., Li, D. & Ek, M. Water repellency improvement of cellulosic textile fibers by betulin and a betulin-based copolymer. *Cellulose* **25**, 2115–2128 (2018).

89. Niu, X., Foster, E. J., Patrick, B. O. & Rojas, O. J. Betulin Self-Assembly: From High Axial Aspect Crystals to Hedgehog Suprastructures. *Adv Funct Mater* **32**, (2022).

90. Moriam, K. *et al.* Hydrophobization of the Man-Made Cellulosic Fibers by Incorporating Plant-Derived Hydrophobic Compounds. *ACS Sustain Chem Eng* **9**, 4915–4925 (2021).

91. Gonçalves, A. R. P., Paredes, X., Cristino, A. F., Santos, F. J. V. & Queirós, C. S. G. P. Ionic Liquids—A Review of Their Toxicity to Living Organisms. *Int J Mol Sci* **22**, 5612 (2021).

92. Parviainen, A. *et al.* Sustainability of cellulose dissolution and regeneration in 1,5-diazabicyclo[4.3.0]non-5-enium acetate: a batch simulation of the IONCELL-F process. *RSC Adv* **5**, 69728–69737 (2015).

93. Cabral, J. P., Kafle, B., Subhani, M., Reiner, J. & Ashraf, M. Densification of timber: a review on the process, material properties, and application. *Journal of Wood Science* **68**, 20 (2022).

94. Bjurhager, I., Berglund, L. A., Bardage, S. L. & Sundberg, B. Mechanical characterization of juvenile European aspen (Populus tremula) and hybrid aspen (Populus tremula × Populus tremuloides) using full-field strain measurements. *Journal of Wood Science* **54**, 349–355 (2008).

95. Charles Sears. Process of preparing wood matrices. (1900).

96. Henrik-Klemens, Å. *et al.* The glass transition temperature of isolated native, residual, and technical lignin. *Holzforschung* **78**, 216–230 (2024).

97. Jakob, M., Gaugeler, J. & Gindl-Altmutter, W. Effects of Fiber Angle on the Tensile Properties of Partially Delignified and Densified Wood. *Materials* **13**, 5405 (2020).

98. Salmen, L. Temperature and water induced softening behaviour of wood fiber based materials. (Department of Paper Technology, Royal Institute of Technology, 1982).

99. Joelsson, T. *et al.* The impact of sulphonation and hot-pressing on low-energy high-temperature chemi-thermomechanical pulp. *Holzforschung* **76**, 463–472 (2022).

100. Mastantuoni, G. G., Li, L., Chen, H., Berglund, L. A. & Zhou, Q. High-Strength and UV-Shielding Transparent Thin Films from Hot-Pressed Sulfonated Wood. *ACS Sustain Chem Eng* **11**, 12646–12655 (2023).

101. Lin, B. P., He, B. H. & Zhao, G. L. The Impact of Lignin Content on Paper Physical Strength of CTMP. *Adv Mat Res* **236–238**, 1242–1245 (2011).

102. Mason, W. H. Process of making integral insulating board with hard welded surfaces. (1931).

103. Song, J. *et al.* Processing bulk natural wood into a high-performance structural material. *Nature* **554**, 224–228 (2018).

104. Jiang, B. *et al.* Lignin as a Wood-Inspired Binder Enabled Strong, Water Stable, and Biodegradable Paper for Plastic Replacement. *Adv Funct Mater* **30**, (2020).

105. Joelsson, T. *et al.* High strength paper from high yield pulps by means of hot-pressing. *Nord Pulp Paper Res J* **35**, 195–204 (2020).

106. Li, Z. *et al.* A Strong, Tough, and Scalable Structural Material from Fast-Growing Bamboo. *Advanced Materials* **32**, 1906308 (2020).

107. Mattsson, A. *et al.* Lignin Inter-Diffusion Underlying Improved Mechanical Performance of Hot-Pressed Paper Webs. *Polymers (Basel)* **13**, 2485 (2021).

108. Neyses, B., Scharf, A. & Sandberg, D. Continuous densification of wood with a belt press: how knot features impact the densification outcome. *Wood Mater Sci Eng* **18**, 1587–1596 (2023).

109. Sadatnezhad, S. H., Khazaeian, A., Sandberg, D. & Tabarsa, T. Continuous Surface Densification of Wood: A New Concept for Large-scale Industrial Processing. *Bioresources* **12**, 3122 (2017).

110. Joelsson, T. *et al.* Unique steel belt press technology for high strength papers from high yield pulp. *SN Appl Sci* **3**, 561 (2021).

111. Neyses, B., Hagman, O., Sandberg, D. & Nilsson, A. DEVELOPMENT OF A CONTINUOUS WOOD SURFACE DENSIFICATION PROCESS – THE ROLLER PRESSING TECHNIQUE. in *Proceedings of the 59th International Convention of Society of Wood Science and Technology* (Curitiba, 2016).

112. Liu, P.-Y. *et al.* The Oxidative Damage of Plasmid DNA by Ascorbic Acid Derivativesin vitro: The First Research on the Relationship between the Structure of Ascorbic Acid and the Oxidative Damage of Plasmid DNA. *Chem Biodivers* **3**, 958–966 (2006).

113. Deiana, L. *et al.* Efficient and Highly Enantioselective Aerobic Oxidation–Michael–Carbocyclization Cascade Transformations by Integrated Pd(0)-CPG Nanoparticle/Chiral Amine Relay Catalysis. *Synthesis (Stuttg)* **46**, 1303–1310 (2014).

114. Ibrahem, I. *et al.* Copper Nanoparticles on Controlled Pore Glass and TEMPO for the Aerobic Oxidation of Alcohols. *ChemNanoMat* **4**, 71–75 (2018).

115. A Matter of Life(time) and Death. *ACS Catal* **8**, 8597–8599 (2018).

116. Ramesh Naidu, V., Rafi, A. A., Tai, C., Bäckvall, J. & Córdova, A. Regio- and Stereoselective Carbon-Boron Bond Formation via Heterogeneous Palladium-Catalyzed Hydroboration of Enallenes. *Chemistry – A European Journal* **29**, (2023).

117. Deiana, L. *et al.* Artificial plant cell walls as multi-catalyst systems for enzymatic cooperative asymmetric catalysis in non-aqueous media. *Chemical Communications* **57**, 8814–8817 (2021).

118. Li, M. *et al.* Silver-Triggered Activity of a Heterogeneous Palladium Catalyst in Oxidative Carbonylation Reactions. *Angewandte Chemie International Edition* **59**, 10391–10395 (2020).

119. Zheng, Z. *et al.* Efficient Heterogeneous Copper-Catalyzed Alder-Ene Reaction of Allenynamides to Pyrrolines. *ACS Catal* **12**, 1791–1796 (2022).

120. Wu, H. *et al.* Heterogeneous Copper-Catalyzed Cross-Coupling for Sustainable Synthesis of Chiral Allenes: Application to the Synthesis of Allenic Natural Products. *Angewandte Chemie International Edition* **62**, (2023).

121. Deiana, L. *et al.* Cellulose-Supported Heterogeneous Gold-Catalyzed Cycloisomerization Reactions of Alkynoic Acids and Allenynamides. *ACS Catal* **13**, 10418–10424 (2023).

122. Pramanik, K., Sarkar, P. & Bhattacharyay, D. 3-Mercapto-propanoic acid modified cellulose filter paper for quick removal of arsenate from drinking water. *Int J Biol Macromol* **122**, 185–194 (2019).

123. Jiang, X. *et al.* A Facial Strategy for Catalyst and Reducing Agent Synchronous Separation for AGET ATRP Using Thiol-Grafted Cellulose Paper as Reducing Agent. *Polymers (Basel)* **10**, 26 (2017).

124. Wulandari, W. T., Rochliadi, A. & Arcana, I. M. Nanocellulose prepared by acid hydrolysis of isolated cellulose from sugarcane bagasse. *IOP Conf Ser Mater Sci Eng* **107**, 012045 (2016).

125. Rafi, A. A. *et al.* A facile route for concurrent fabrication and surface selective functionalization of cellulose nanofibers by lactic acid mediated catalysis. *Sci Rep* **13**, 14730 (2023).

126. Roman. Maren & Winter, W. T. Effect of Sulfate Groups from Sulfuric Acid Hydrolysis on the Thermal Degradation Behavior of Bacterial CelluloseArticle link copied! *Biomacromolecules* **5**, 1671–1677 (2004).

127. Nielsen, L. J., Eyley, S., Thielemans, W. & Aylott, J. W. Dual fluorescent labelling of cellulose nanocrystals for pH sensing. *Chemical Communications* **46**, 8929 (2010).

128. Cai, C., Wei, B., Jin, Z. & Tian, Y. Facile Method for Fluorescent Labeling of Starch Nanocrystal. *ACS Sustain Chem Eng* **5**, 3751–3761 (2017).

129. Komesu, A., Oliveira, J. A. R. de, Martins, L. H. da S., Wolf Maciel, M. R. & Maciel Filho, R. Lactic Acid Production to Purification: A Review. *Bioresources* **12**, 4364–4383 (2017).

130. Lafia-Araga, R. A., Sabo, R., Nabinejad, O., Matuana, L. & Stark, N. Influence of Lactic Acid Surface Modification of Cellulose Nanofibrils on the Properties of Cellulose Nanofibril Films and Cellulose Nanofibril–Poly(lactic acid) Composites. *Biomolecules* **11**, 1346 (2021).

131. Sethi, J. *et al.* Water resistant nanopapers prepared by lactic acid modified cellulose nanofibers. *Cellulose* **25**, 259–268 (2018).

132. Alimohammadzadeh, R., Rafi, A. A., Goclik, L., Tai, C.-W. & Cordova, A. Direct organocatalytic thioglycolic acid esterification of cellulose nanocrystals: A simple entry to click chemistry on the surface of nanocellulose. *Carbohydrate Polymer Technologies and Applications* **3**, 100205 (2022).

133. Newman, R. H. Homogeneity in cellulose crystallinity between samples of Pinus radiata wood. *Holzforschung* **58**, 91–96 (2004).

134. Andersson, S., Wikberg, H., Pesonen, E., Maunu, S. L. & Serimaa, R. Studies of crystallinity of Scots pine and Norway spruce cellulose. *Trees - Structure and Function* **18**, 346–353 (2004).

135. Sofla, M. R. K., Brown, R. J., Tsuzuki, T. & Rainey, T. J. A comparison of cellulose nanocrystals and cellulose nanofibres extracted from bagasse using acid and ball milling methods. *Advances in Natural Sciences: Nanoscience and Nanotechnology* **7**, 035004 (2016).

136. Avella, A. *et al.* Organo-Mediated Ring-Opening Polymerization of Ethylene Brassylate from Cellulose Nanofibrils in Reactive Extrusion. *ACS Sustain Chem Eng* **12**, 10727–10738 (2024).

137. Wu, L. *et al.* Facile preparation of super durable superhydrophobic materials. *J Colloid Interface Sci* **432**, 31–42 (2014).

138. Ferrero, F. & Periolatto, M. Application of fluorinated compounds to cotton fabrics via sol–gel. *Appl Surf Sci* **275**, 201–207 (2013).

139. Krafft, M. P. & Riess, J. G. Selected physicochemical aspects of poly- and perfluoroalkylated substances relevant to performance, environment and sustainability—Part one. *Chemosphere* **129**, 4–19 (2015).

140. Francolini, I., Galantini, L., Rea, F., Di Cosimo, C. & Di Cosimo, P. Polymeric Wet-Strength Agents in the Paper Industry: An Overview of Mechanisms and Current Challenges. *Int J Mol Sci* **24**, 9268 (2023).

141. Berg, J.-E. *et al.* Refining gentleness – a key to bulky CTMP. *Nord Pulp Paper Res J* **37**, 349–355 (2022).

142. Myz, S. A., Politov, A. A., Kuznetsova, S. A. & Shakhtshneider, T. P. Morphological Changes in Betulin Particles as a Result of Polymorphic Transformations, and Formation of Co-Crystals under Heating. *Powders* **2**, 432–444 (2023).

143. Drebushchak, T. N. *et al.* CRYSTALLINE FORMS OF BETULIN: POLYMORPHISM OR PSEUDOPOLYMORPHISM? *Journal of Structural Chemistry* **61**, 1260–1266 (2020).

144. Westermark, U. & Hatakeyama, H. Physical and chemical changes in the outer cell wall layers in wood fibers during chemimechanical pulping. *Nord Pulp Paper Res J* **11**, 95–99 (1996).

145. Makarov, I. *et al.* Antifungal composite fibers based on cellulose and betulin. *Fibers* **6**, (2018).

146. Rubacha, M. Magnetically active composite cellulose fibers. *J Appl Polym Sci* **101**, 1529–1534 (2006).

147. Shi, J., Lu, Y., Zhang, Y., Cai, L. & Shi, S. Q. Effect of thermal treatment with water, H2SO4 and NaOH aqueous solution on color, cell wall and chemical structure of poplar wood. *Sci Rep* **8**, 17735 (2018).

148. Shi, J., Peng, J., Huang, Q., Cai, L. & Shi, S. Q. Fabrication of densified wood via synergy of chemical pretreatment, hot-pressing and post mechanical fixation. *Journal of Wood Science* **66**, 5 (2020).

149. Wang, Z., Winestrand, S., Gillgren, T. & Jönsson, L. J. Chemical and structural factors influencing enzymatic saccharification of wood from aspen, birch and spruce. *Biomass Bioenergy* **109**, 125–134 (2018).

150. Mastantuoni, G. G., Tran, V. C., Engquist, I., Berglund, L. A. & Zhou, Q. In Situ Lignin Sulfonation for Highly Conductive Wood/Polypyrrole Porous Composites. *Adv Mater Interfaces* **10**, 2201597 (2023).

151. Barman, D. N., Haque, Md. A., Hossain, Md. M., Paul, S. K. & Yun, H. D. Deconstruction of Pine Wood (Pinus sylvestris) Recalcitrant Structure Using Alkali Treatment for Enhancing Enzymatic Saccharification Evaluated by Congo Red. *Waste Biomass Valorization* **11**, 1755–1764 (2020).

152. Oriez, V., Peydecastaing, J. & Pontalier, P.-Y. Lignocellulosic Biomass Mild Alkaline Fractionation and Resulting Extract Purification Processes: Conditions, Yields, and Purities. *Clean Technologies* **2**, 91–115 (2020).

153. Shrestha, B. *et al.* A Multitechnique Characterization of Lignin Softening and Pyrolysis. *ACS Sustain Chem Eng* **5**, 6940–6949 (2017).

154. Li, K., Zhao, L., Ren, J. & He, B. Interpretation of Strengthening Mechanism of Densified Wood from Supramolecular Structures. *Molecules* **27**, 4167 (2022).

Appendices

Appendix 1. ^{1}HNMR (top) and ^{13}CNMR (bottom) spectra of (1-benzyl-1H-1,2,3-triazol-4-yl) methanol in $CDCl_3$.

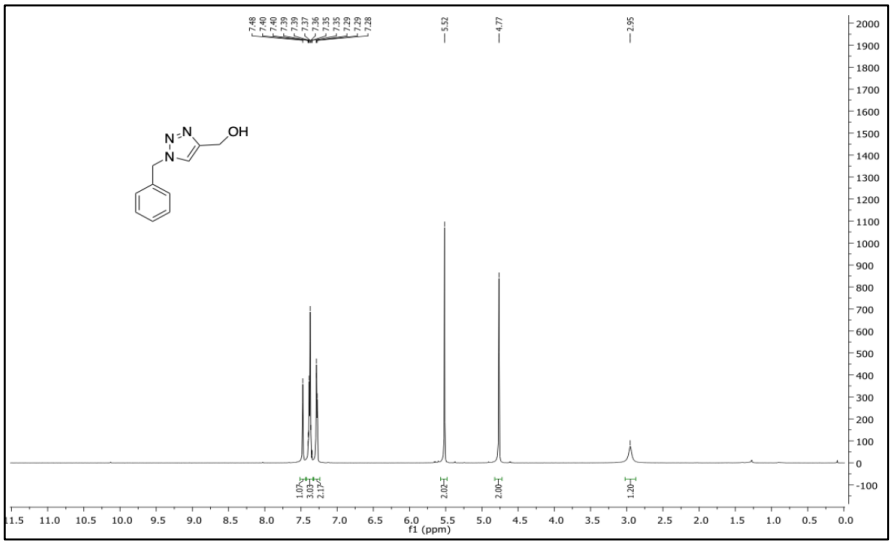

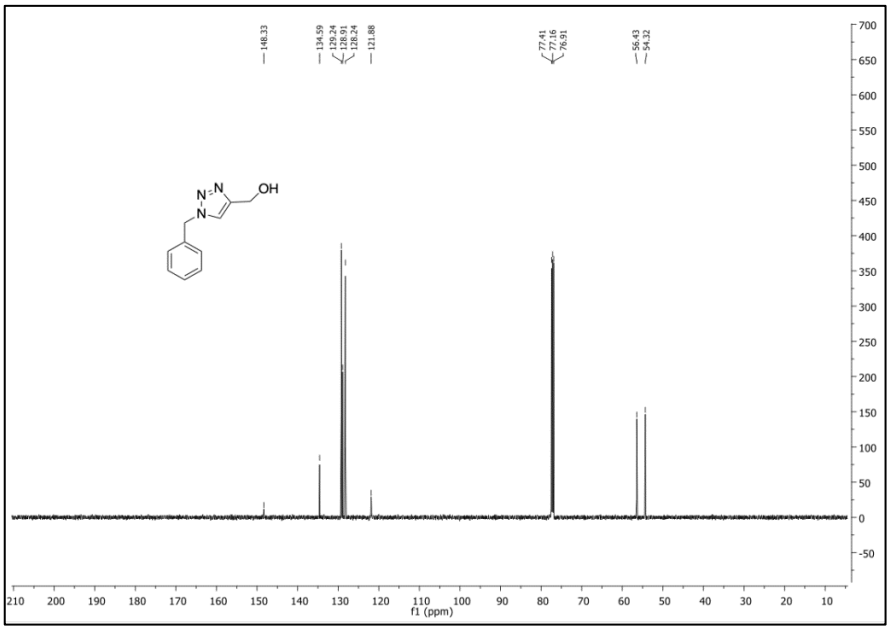

Appendix 2. Procedures for cellulose-based heterogeneous catalysts

Aminopropyl functionalized microcrystalline cellulose (MCC-AMP).
To a suspension of MCC (Avicel PH-101, 500 mg, 3.08 mmol, 1 equiv) and L-tartaric acid (73 mg, 0.46 mmol, 5 mol% of silane) in 20 mL dry toluene, was added 3-(Trimethoxysilyl)-propylamine (9.2 mmol, 3 equiv.) The mixture was stirred for 48 h at 82 ^{o}C. The obtained material was washed by acetone Soxhlet extraction and dried to give a white MCC-AMP powder (elemental analysis: C:42.4, N:0.96, Si:1.92 wt.%).

MCC-AMP-Pd^{II} preparation procedure
To a suspension of MCC-AMP (183 mg) in 5.5 mL DI water was added a solution of Li_2PdCl_4 (101 mg, 0.39 mmol) in DI water (3.7 mL, pH 9). The reaction was stirred for 24 h at RT. The mixture was centrifuged and washed with water and acetone (each 3x15 mL). The MCC-AMP-Pd^{II} was dried under vacuum giving 170 mg of brown powder.

MCC-AMP-Pd preparation procedure
To a suspension of MCC-AMP-Pd^{II} (170 mg) in 5.5 mL water was added a solution of $NaBH_4$ (170 mg, 4.50 mmol) in water (1.8 mL) and stirred for 1 h at RT. The suspension was washed with water and acetone (each 3×15 mL) and dried under vacuum (grey MCC-AMP-Pd powder). The Pd content determined by elemental analysis was 19.17 wt.%. The Pd^0/Pd^{II} ratio based on XPS analysis was 3.5:1.

MCC-AMP-Cu preparation procedure
To a suspension of MCC-AMP (400 mg) in water (10 ml, pH 9), was added a solution of $Cu(OTf)_2$ (200 mg, 0.55 mmol) in water (4 mL, pH 9) at RT. After 24 h, the mixture was washed with water and acetone. Next, MCC-AMP-Cu^{II} was suspended in 24 mL water, and $NaBH_4$ (160 mg, 4.23 mmol) in 8 mL water was added. After 1h, the mixture was washed with water and acetone (3×30 mL) and dried under vacuum giving MCC-AMP-Cu (Cu content: 8.7 wt.%; Cu^I/Cu^{II} ratio: 1.25:1.0).

Appendix 3. Preparation of PLA nano composites and the tensile strength of PLA with and without adding CNF components.

Micro-compounding and tensile tests: The fabricated CNFs materials (LA-CNF and CNF) were mixed with PLA (melt-blending) using a twin-screw micro-compounder (Xplore, 15 mL) at 190 °C, first at 10 rpm for around 11 min and then at 100 rpm and under nitrogen for 3 min.

Using Xplore IM 5.5 micro injector, dog bone shape specimens for tensile tests were made via injection molding technique, (injection temperature 195 °C, applies pressure 7 bar, and temperature of mold 50 °C). The tensile tests were carried out using Zwick Z2.5 (ZwickRoell Ltd., UK) with the rate of 2.5 mm/min.

Composition	Tensile strength [MPa]	E-modulus [GPa]	Elongation at break [%]
PLA (neat)	66	1020	9
PLA with CNF (1 %wt.)	72	1000	10
PLA+LA-CNF (1 %wt.)	69	1040	11

Appendix 4. Treatment of cellulosic materials with betulin/EtOH solution.

Betulin (375 mg, 0.85 mmol) was solved in 100 mL ethanol (8.5 mM) and used for the treatment. The cellulosic material was impregnated with the prepared betulin/EtOH solution and then air dried. The following table reports the WCAs measurements of the cellulosic materials treated with betulin/EtOH solution.

Entry	Cellulosic material	Impregnation time	WCAs (θ)[a]
1[b]	CNC film	0	45°
2	CNC film	10 min	80°
3	CNC film	4 h	83°
4	CNC film	18 h	82°
5	Filter paper	3 h	< 10°
6[c]	Filter paper	3 h	< 10°

[a] The WCAs were measured after 10 s. [b] Not impregnated with the betulin solution. [c] Hot pressed at 97 °C, 1 bar for 30 min.

Appendix 5. Preparation of aqueous betulin colloidal suspension

300 mL of deionized water was added to betulin (6 g, 13.55 mmol) and vigorously stirred at room temperature for 1 h. Next, it was sonicated at 35 °C for 90 min resulting a homogeneous milky suspension.

The prepared betulin aqueous suspension (20 mg/mL).

An average particle size of 857±16 nm and PDI of 0.31±0.06 were determined by a dynamic light scattering instrument.

Appendix 6. Impregnation treatment of cellulosic materials with betulin aqueous suspension (20 mg/mL).

The cellulosic materials were impregnated with the prepared betulin aqueous suspension (20 mg/mL) for 10 min. Next, the cellulosic material was removed from the suspension and left to air dry. The corresponding betulin-impregnated cellulosic materials were next heated in a furnace for 3 min at 280 ^{o}C. The following table shows the WCAs of the corresponding treated samples.

WCAs of the different cellulosic materials treated with the aqueous betulin suspension and heat-treated

Entry	Cellulosic material	Contact angle (θ)[a]
1	Filter paper	110 ^{o}
2	CTMP3	118 ^{o}
3	CTMP2	114 ^{o}
4	CTMP1	120 ^{o}
5	CNC coated paper	83 ^{o}
6	Cotton fabric	130 ^{o}
7[b]	Filter paper	nd
8[c]	Filter paper	< 10 ^{o}

[a] WCAs were measured after 5 min. [b] Sodium dodecyl sulfate SDS (20 mol%) was tested as a surfactant in the betulin/H_2O suspension. SDS burn at 280 ^{o}C. [c] Pluronic P-123 (1.5 mol%) was tested as a surfactant in the betulin/H_2O suspension. Nd= not determined.

Appendix 7. Materials and pulp information used in Paper IV

Betulin (98%) was obtained from Nature Science Technologies Ltd. Filter paper (>99% cellulose) was obtained from Munktell. The raw material for pulping consisted of Norway spruce chips, of which 30% was sawmill chips, from Billerud Rockhammar mill. The pulp was from the mill trials in Rockhammar 20-22nd February 2019. The samples were all CTMP with different amounts of bound sulfur (S). *CTMP1* and *CTMP2* with 28% dryness were from primary HC refiner; *CTMP1* (with bound sulfur of 2.4 (S) g/kg; refining peak temperature of 165 °C; specific refining energy of ~800 kWh/t; refining gap of 0.6 mm; *CTMP2* (with bound S of 1.0 (S) g/kg; refining peak temperature of 165 °C; specific refining energy ~800 kWh/t; refining gap of 0.6 mm). *CTMP3* with 85% dryness is form final step and the same as *CTMP2* (bound sulfur content of 1.0 (S) g/kg). The lignin contents of CTMP samples were similar and measured to be between 27.7-27.5 wt.%. More details about pulp preparation can be found in the reference literature.[141]

Making handmade papers from CTMP pulps

Handmade laboratory CTMP paper sheets were made using a Rapid-Köthen sheet former instrument (ISO 5269-2). CTMP (dry mass: 50 g) was dispersed in 2 L of hot water (stirred for 15 min and disintegrated by a disintegration machine). Next, the mixture was diluted to around 8 kg total weight and stirred for 10 min. The mixture was transferred into the Rapid-Köthen sheet former, and the resulting wet CTMP hand sheets were dried (96 kPa, at 95 °C for 10 min, grammage 140 g/m^2).

Wet and dry tensile tests

The tests were done in the standard testing environment (ISO 187, 23 °C, and 50 % RH). Grammage, density, and thickness were determined according to ISO 536 and ISO 534 and ISO 5270, respectively. Dry tensile strengths and wet strengths (after 1 min immersion in water) were determined according to ISO 1924 and ISO 3781, respectively.

Appendix 8. Hot-Pressing instrument used in Paper V

Hot pressing was performed via a planar-pressing equipment built at Mid Sweden University, and the equipment mainly consists of heating blocks, a pillar stand, and compression testing machine. The heating blocks contain three pockets where electrical heating elements (each 500 W) are located. The heating blocks, with 20 mm thermal isolating plates, are mounted in pillar rack ball brushings to ensure the best alignment between the blocks. The upper pillar rack is fixed to a hydraulic MTS™ material testing machine load cell, and the lower part to the movable hydraulic piston rod. For the control of block temperature, each has a built-in thermocouple sensor connected to Eurotherm PID-type regulators which are limited to 300 °C. To control compression loads, MTS™ MPT software is used for creating block-programmed loads vs. time sequences up to 100 kN.

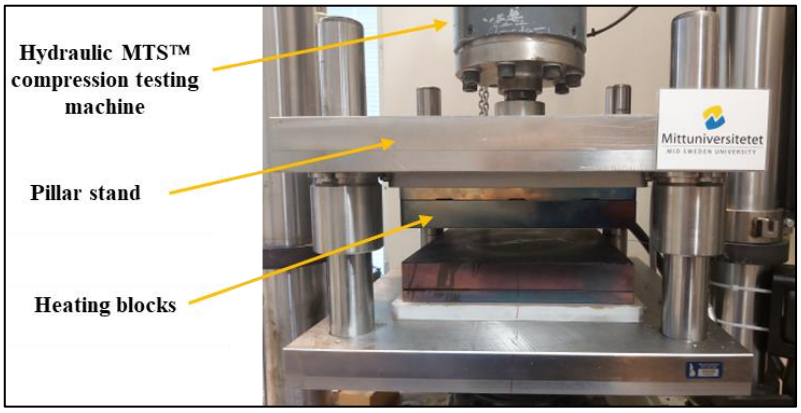

Planar hot-pressing equipment at Mid Sweden University.

Appendix 9. SEM images of filter paper, CTMP2 & CTMP3 samples.

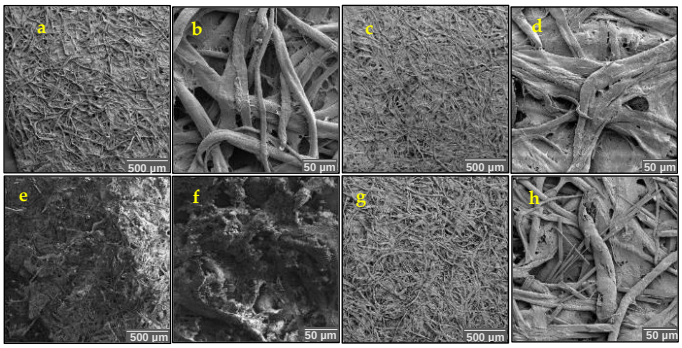

SEM images of filter paper-starting (a,b), filter paper-NoBET-HP (c,d), filter paper-BET-NoHP (e,f), and filter paper-BET-HP (g,h).

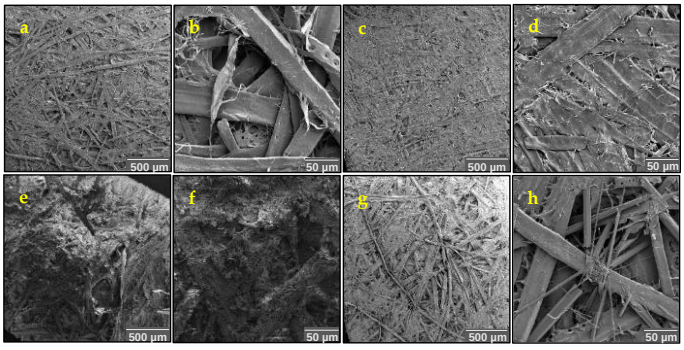

SEM images of CTMP2-starting (a,b), CTMP2-NoBET-HP (c,d), CTMP2-BET-NoHP (e,f), and CTMP2-BET-HP (g,h).

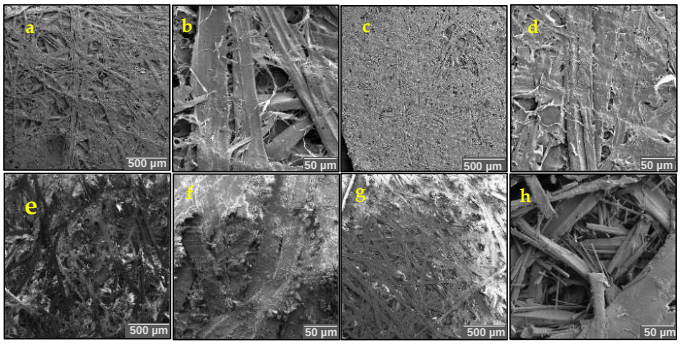

SEM images of CTMP3-starting (a,b), CTMP3-NoBET-HP (c,d), CTMP3-BET-NoHP (e,f), and CTMP3-BET-HP (g,h).

Appendix 10. The procedure and tensile strengths for the static hot-pressed samples.

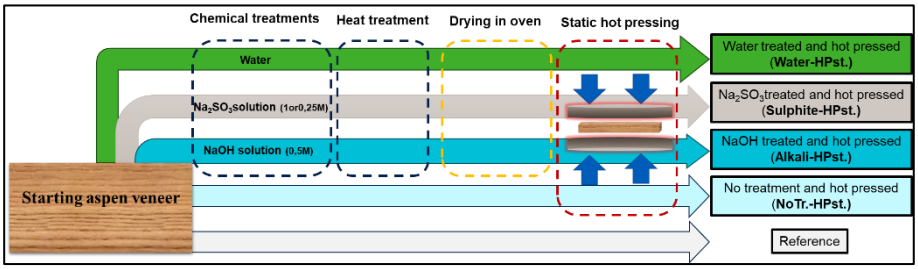

Five veneer samples with dimension of 6*20*0.15 cm^3 were put in a desiccator containing 4 L of the related solution. The desiccator was connected to a vacuum pump for 8 h then the pump was turned off and the veneer samples were left as they were for 16 h (total immersion time 24 h). After 24 h, first the vacuum of desiccator was slowly broken, then the samples were taken out, weighed, and kept in a sealed plastic bag. The samples were heat treated in the reactor at 160 °C for 10 min. Before hot pressing, the moisture content of samples was reduced to 5% by means of an oven, then hot pressed.

Entry[a]	Samples	Pressure[b] (bar)	Density[c] (kg/m^3)	Tensile strength (MPa)
1	NoTr.-HPst.	181	1183	254
2	Water-HPst.	56	1116	274
3	Alkali-HPst.	111	1393	331
4	Sulfite-HPst. (0.25M)	78	1096	280
5	Sulfite-HPst. (1M)	184	1346	325
6[d]	NoTr.-HPst.	164	1260	310
7[e]	Water-HPst.	41	1090	266
8	Reference	-	385	49

[a] Temperature for hot pressing was 190±5 °C; Moisture content before hot pressing: 5%; puls time: 60s. [b] Applied pressure in hot pressing. [c] Density of sample after hot pressing. [d] Moisture content before hot pressing: 20 wt.%; puls time: 48s, and no heat treatment in the reactor. [e] No heat treatment in the reactor.

Appendix 11. Continuous steel belt hot pressing machine at IPCO.